3rd TRIGGER
International Conference
8-10 October 2019, Zanjan, Iran

Institute for Advanced Studies
in Basic Sciences
Gava Zang, Zanjan, Iran

Book of Abstracts

سازمان زمین‌شناسی کشور
GEOLOGICAL SURVEY OF IRAN

SORBONNE UNIVERSITÉ

cnrs

Oral Presentations

EARLY JURASSIC METAMORPHISM IN CENTRAL IRAN: GEODYNAMIC IMPLICATIONS

Zanchi, A.[1], Zanchetta, S.[2], and Javadi, H.[3]

[1,3]Department of Earth and Environmental Sciences, Univ. Milano- Bicocca, Milan, Italy
[2]Geological Survey of Iran, Meraj Boulevard, Teheran, Iran
E-mail: andrea.zanchi@unimib.it

Central Iran consists of several terranes, mainly derived from Gondwana and accreted to the Eurasian margin during the Cimmerian orogeny. In its NW part, three metamorphic complexes containing dismembered "ophiolites", the Anarak, Jandaq and Posht-e-Badam, occur. The age of metamorphism, geodynamic significance, and palaeogeographic provenance of such units are largely debated. The evolution of the Anarak complex is, until now, the best understood among the others. It has been interpreted as an allochthonous crustal fragment belonging to the accretionary belt developed during Carboniferous times on the southern margin of Eurasia. The mechanisms and timing of large-scale deformation during Mesozoic and Cenozoic times that brought the Anarak unit in its present-day position are poorly understood. An undefined Precambrian to early Palaezoic age has been instead inferred for the Posht-e-Badam and Jandaq complexes.

The Jandaq complex is divided in two subunits: the Arusan ophiolitic mélange and the Jandaq metamorphic unit. To the north, the complex is in tectonic contact with the Airekan basement, mainly made of Lower Cambrian granites. The ophiolitic mélange consists of serpentinized harzburgites, metagabbros, prasinites and quartzites, the last likely representing metacherts. Minor marbles lenses also occur. The ophiolites display a predominant greenschists facies mineralogical assemblage, with only minor relicts of amphibolite-facies minerals. The surrounding basement consists of metapelites with minor amphibolites. The metamorphic peak phase assemblages in micaschists is made of garnet, kyanite, staurolite, plagioclase, biotite and muscovite. Garnet is also stable within mafic rocks of the same unit, indicating that the Jandaq metamorphics reached P-T conditions well within the garnet amphibolite facies. We provided new Norian U-Pb zircon ages for the granites that intruded the Arusan ophiolites. Peak metamorphism that affected the Jandaq metamorphics is constrained to the Early Jurassic by new Ar/Ar data on peak metamorphic minerals. Preliminary data seems also to suggest the same age for the metamorphic event that affected the Arusan ophiolites.

All these data suggest that the two subunits of the Jandaq complex experienced a significant post-Cimmerian tectonometamorphic collisional event. We notice that the same record has been recently recognized within the Mashhad metamorphic complex (Sheikholeslami et al., 2019), suggesting that this tectonic event affected several areas of central and NE Iran. The Upper Jurassic-Lower Cretaceous Chah Palang Conglomerate finally non-conformably

covered the Jandaq complex. Our new data strengthen the idea that part of Central Iran was displaced to its present-day position along the Great-Kavir - Doruneh fault system during Mesozoic and Cenozoic times. Cenozoic dextral shearing along precursors of this fault system was also identified by us within the Jandaq-Arusan area.

KEYWORDS: Central Iran, metamorphism, ophiolites, structural geology.

The Iranian Plateau at the end of the Quaternary: new synthesis of geological, archaeological and historical data

Nazari, H.[1], Ritz, JF.[2]

[1] Research Institute for Earth sciences, Geological Survey of Iran, Tehran-Iran.
[2] Laboratoire Géosciences Montpellier, Université de Montpellier – CNRS UMR 5243, Montpellier France.

From a synthesis of geological and geochronological data combined with archaeological and historical data, we show that the northern part of the central plateau of Iran corresponded to a huge lake, at least as large as the Aral Sea, at the very end of the Pleistocene-early Holocene period, there are ca 16 Ka, at the transition between marine isotope stage MIS 2 and 1.

The morphological and stratigraphic markers of this ancient lake still visible in some areas of the central plateau of Iran, especially in the Kavir desert, the Qom-Aran desert and the region of Masileh, as well as archeological and historical data allow reconstructing its evolution during the past 15 thousands years. These various data allow showing that this huge lake (which most likely also existed during the previous interglacial MIS 5e period) experienced dry periods during which it get evaporated and wet periods during which it was filled again.

Indices showing the presence of the lake around 16-14 ka, are ancient shorelines located at an altitude of ~ 1100 m found in many places around the current Great Kavir depression. Our geochronological data suggest then that between the beginning of the Holocene (~ 11.5 ka) and 8 ka, the lake level gradually decreased by 250 m, to reach the altitude of 850 m. We believe that the cause of this lowering is the evaporation due to warmer and drier climate.

Around 8200 years ago, due to a a sudden drop of the temperature, the Neolithic peoples moved from higher altitude to warmer and more fertile plains, and settled in such areas such as Sialk, Shoorabeh hill, Gharehtappeh, Qomrood, Cheshmeh Ali etc... The spatial distribution of archaeological and historical data indicates the drying up of the Masileh Basin, in a region higher than the heights of the Kavir Desert. And we think that the Masileh Basin has survived to the Sasanid Empire. The eastern part of the Kavir Basin had dried up earlier. The lake of the Masileh Basin (the Great Salt Lake Basin and the Howz-e-Sultan Basin) probably corresponds to the ancient Lake Saveh mentioned in the old myth.

The absence of archaeological remains dating back to the second millennium BC suggests that the lake rose in the late Bronze Age (NB / pre-Islamic archaeological remains are confined to the edge of the ancient lake). However, the existence of cultural remains from intermittent human settlements in the Iron Age within the area of the former lake suggests that there may have been a period of drought again.

KEYWORDS: Paleoclimatology, Paleo-lake, Saveh Lake, Iran.

Frictional behavior of carbonate fault rocks in Zagros Suture Zone

Yassaghi, A.[1], and CMarone, C.[2]

[1]Dept. of Geology, Tarbiat Modares University, 14115-175, Tehran, Iran.

[2]Dept. of Geosciences, Pennsylvania State University, University Park, 16802, Pennsylvania, USA

Email: yassaghi@modares.ac.ir

Frictional strength of carbonate fault rocks generally depends on the rock internal fabric/structures and composition. The fault rocks are frictionally strong and may have the potential for seismic slip. In this paper, we investigate frictional behavior of carbonate fault rocks from the Zagros suture zone. We present field observations along with results from friction experiments on carbonate intact and powdered fault rocks from Zagros suture zone. Due to the absence of micro-seismicity and lack of deformation out of GPS measurements, the Zagros suture zone considered as currently inactive. We measured frictional strength and rate/state dependence of the fault rocks over a range of normal stresses and shear slip velocities. They showed potentially stable, velocity-strengthening frictional behavior. Our results suggest that solution seams, cleavage processes in clay content carbonate rocks, and development of stylolite and calcite veins in pure carbonate fault rocks of the suture zone continually rejuvenate and rework shear structures that result in velocity-strengthening frictional behavior. We propose that these processes occurred in the Zagros suture zone during its exhumation to the upper crust throughout the final continental collision between the Arabia microplate and central Iran.

Low-temperature thermochronology and structural constraints on Cenozoic fault kinematic inversion in Northern Iranian Plateau margin, case of the Kushk-e-Nosrat Fault, central Iran

Khodaparast, S.[1], **Madanipour, S.**[2], **Enkelmann, E.**[2], **Nozaem, R.**[3], **Hessami, K.**[4], **and Matthews, W.**[2]

[1]Department of Geology, Tarbiat Modares University, Tehran, Iran.
[2]Department of Geoscience, University of Calgary, Alberta, Canada.
[3]School of Geology, College of science, University of Tehran, Iran.
[4]International Institute of Earthquake Engineering and Seismology, Tehran, Iran.
Email: Sedighekhodaparast@yahoo.com

Deformation reorganization in Alborz Mountains of the northern margin of the Iranian Plateau represents a Late Cenozoic slip sense inversion of major fault systems from right to left lateral strike slip motion. This late Pliocene kinematic change has been attributed to the clockwise rotation of the rigid South Caspian Basement (SCB) block. However our knowledge of the southward penetration of this kinematic change in to the central parts of the Iranian Plateau is still debated. Here we integrate detail structural kinematic data and apatite (U-Th)/He low-temperature themochronometry on the WNW-ESE trending Kushk-e- Nosrat (KN) Fault system to unravel the uplift and cooling history and regional distribution of kinematic change at the northwestern margin of the Iranian Plateau. There is a parallel fault set in the western side of KN Fault and also several different sets of strike slip related structures along KN Fault system, which are classified into three categories based on their cross-cutting relation and the superposition of kinematic indicators. Structural analysis suggests dextral, dextral transpression and sinistral kinematics. The relative timing of activity is respectively documented along KN Fault system since Miocene time. The cooling ages from a significant restraining bend on the west side of KN Fault suggest older cooling ages at the bend margin which getting younger toward the core. The cooling ages are peaking at two major cooling events including early Miocene (~20-18Ma) and early Pliocene (~6-4Ma). We associate the Miocene cooling to dextral motion and the Pliocene age to the initiation of dextral transpression on the restraining bend. This bend created a local highland region with 1000 meters local relief at the western side of KN Fault system. Our structural evidence also indicates an inversion from a dextral transpression array to a sinistral array possibly during post Pliocene time. This kinematic change is regionally due to the clockwise rotation of SCB as it also proposed for the central Alborz Mountains of northern Arabia-Eurasia collision zone. We propose here the KN Fault system in the northern margin of the Iranian Plateau as the southernmost boundary of the region experienced fault slip sense inversion due to post Pliocene shift in kinematics of SCB.

KEYWORDS: Fault slip inversion, Northern Iranian Plateau Margin, KN Fault system, South Caspian Block

Tectonic geomorphology of highlands in Tehran region

Solaymani Azad, S.[1, 2]

[1]Seismotectonics & Seismology Department of Geological Survey of Iran, P.O.Box: 13185 1494, Teheran, Iran.

[2]Université Montpellier 2, Laboratoire Géosciences Montpellier, UMR 5243, Montpellier, France.

In the central portion of the Arabia-Eurasia collision zone, Tehran domain locates in a transitional boundary between seismotectonic zones of Central Iranian lowland (to the south) and Alborz highland (to the north). Accordingly, it affects from interaction of the both of active tectonic zones. In this research, we will discuss tectonic geomorphology of the region within the mountain front of the Alborz territory on the hanging wall of the North Tehran fault. Our results highlight some prominent topographic scars as important features showing co-seismic deformation markers. Huge landslides and rockfalls, offset geomorphic surfaces etc. could be present as the main direct and indirect co-seismic deformation features. All these geomorphic markers reveal seismic potential of Tehran new capital city to experience really strong seismic events, maybe in new future. This is differ from previouse maximum credible earthquake magnitude estimated for this area. Then, the results of seismic hazard studies of Tehran City are still under estimated and a new seismic hazard assessment needs to be run for this important area.

Risk Assessment of Geo-Hazards and Post-Earthquake Fire in Tehran

Zare, M.[1], Kamranzad, F.[2], Memarian, H.[2]

[1]International Institute of Earthquake Engineering and Seismology (IIEES), Tehran, Iran.
[2]College of Engineering, University of Tehran, Iran.

Email: mzare@iiees.ac.ir

Tehran is one of the most hazardous metropolises of the world in terms of the risk of different natural disasters (e.g. earthquake, flood, subsidence, drought, landslide, fire following earthquake, etc.). On the other hand, Tehran has over 8,700,000 populations with a mixture of old non-resistant structures as well as modern high-rise buildings which affect the vulnerability of this city. Risk of natural hazards is usually defined as below:

$$\text{Risk} = \text{Hazard} * \text{Vulnerability} * \text{Exposure}$$

In which Hazard represents the probabilities and intensities of a disaster. Vulnerability can be considered in terms of technical, physical, organizational, psycho-social or economic vulnerabilities and the Exposure is the number or the amount of a target which is considered as elements at risk such as the population of a city.

In this study, for the city of Tehran, the hazard assessment of earthquake, flood, landslide and subsidence are performed to derive an overall multi-hazard map. Then, by combining the overall multi-hazard map with the distribution of non-resistant structures as the vulnerability factor and the population density as the exposure term, a risk map of the multi-hazards is prepared (Fig. 1). The risk map of the multi-hazards in Tehran indicates that the central and southern regions of the city are located at a higher risk zone than other regions, so that the central and southern regions need a closer attention in disaster risk reduction plans.

In addition, during the recent years, several researchers have attempted to model and assess the post-earthquake fire in urban areas (e.g. the studies by Cousins et al. 2002; Scawthorn 2012 and Li et al. 2014). The recent serious fire incidents in single tall buildings in 2017 such as the fire in the Plasco Building in Tehran (Fig. 2-a) and the Grenfell Tower in London (Fig. 2-b), draws our attention to the fact that how resilient will urban areas be in case of an extensive post-earthquake conflagration? Therefore, modeling of the risk of earthquakes and their subsequent fires should be regarded as an important issue in disaster risk reduction strategies in urban areas, especially in the metropolises and large developing cities like Tehran.

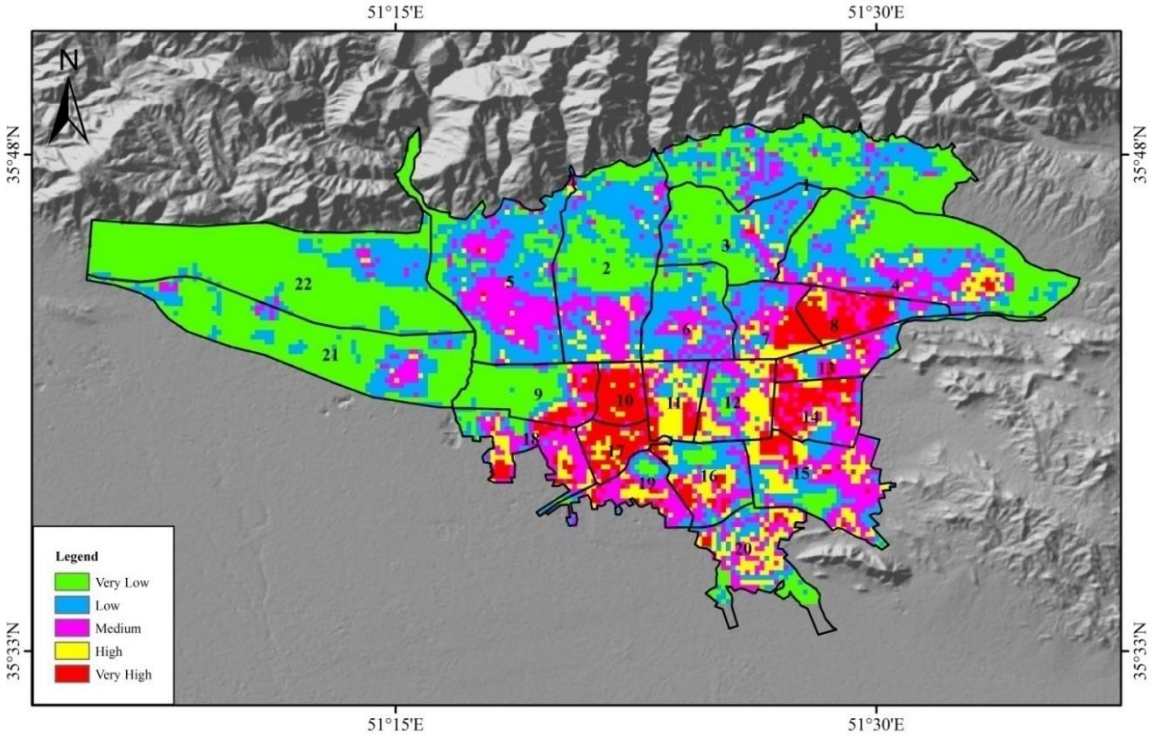

Fig. 1. Risk map of the multi geo-hazards in Tehran.

In this paper, we have attempted to model the risk of probable post-earthquake fire in Tehran. At first, the earthquake hazard map was prepared by preparation and combination of two maps: a PGA map with 475 years return period for surface deposits using the probabilistic seismic hazard analysis and fault rupture hazard map. Then, a human exposure map was provided in terms of population density according to the latest census of Iran (Statistical Center of Iran, 2017). In the next step, the raster maps of several vulnerability factors (Table 1) were depicted with the pixel sizes of 50*50 meter in the ArcGIS software, and by aggregating these maps, an overall vulnerability map was prepared. Finally, by multiplying the hazard map with the vulnerability and the exposure maps, the risk map of the post-earthquake fire was prepared for Tehran (Fig. 3) which indicates that the central and southern regions of this city are located at a higher risk zone.

(a)

(b)

Fig. 2. Two recent fire incidents in high-rise buildings in 2017: (a) The 17-storey Plasco Building in Tehran which was engulfed by a fire and fully collapsed on January 19, 2017 and (b): The 24-storey Grenfell Tower in London which was burned almost completely by a huge fire on June 14, 2017.

Table 1. Factors of risk of post-earthquake fire in Tehran

Hazard	Exposure	Vulnerability
• Surface PGA • Surface fault rupture zone	Population density	• High-rise buildings (> 10 floors) • Buildings quality (high quality, moderate, worn out or non-resistant) • Narrow paths (width<10 m) • Accessibility to main streets, freeways and highways • Bridges and tunnels • Fire hydrant valves • Accessibility to fire station • Accessibility to hospitals • Strategic facilities (oil refinery, gas and water lines, etc) • Potential flammable places (wood and textiles warehouses) • Population centers (the great bazaar, malls, stadiums, etc)

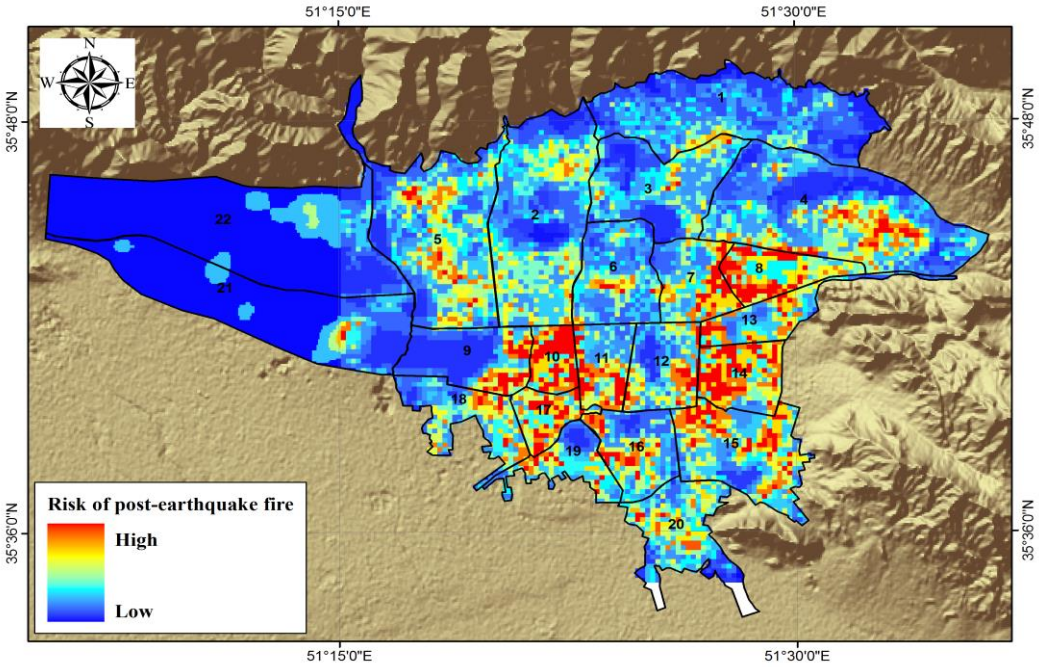

Fig. 3. Risk Map of post-earthquake fire in Tehran

References

Cousins, J., Heron, D., Mazzoni, S., Thomas, G. and Lloydd, D., (2002). Estimating Risks from Fire Following Earthquake. New Zealand Fire Service Commission, 47 pages.

Li, J., Wang, Y., Chen, H. and Lin, L., (2014), Risk assessment study of fire following an earthquake: a case study of petrochemical enterprises in China, Natural Hazards Earth Syst. Sci., 14, pp. 891–900, doi:10.5194/nhess-14-891-2014.

Scawthorn, C., Eidinger, J.M., Schiff, A.J., (2005). Fire Following Earthquake. American Society of Civil Engineering, 345 pp. ISBN: 0-7844-0739-8.

Scawthorn, C., (2012). Fire Following Earthquake: Analysis and Mitigation in North America. Proceedings of the International Symposium on Engineering Lessons Learned from the 2011 Great East Japan Earthquake, March 1-4, 2012, Tokyo, Japan.

Statistical Center of Iran, (2017). https://www.amar.org.ir/english.

Zoback, M.L., (2006). The 1906 earthquake and a century of progress in understanding earthquakes and their hazards. GSA Today, 16(4/5), 4-11. doi: 10.1130/GSAT01604.1.

QFL: Memory of Ancient Rocks

Hosseini-Barzi, M.[1], Etemad-Saeed, N.[2]

[1]Shahid Beheshti University, Tehran, Iran.
[2]Institute for Advanced Studies in Basic Sciences (IASBS), Zanjan, Iran.
E-mail: m_hosseini@sbu.ac.ir

Geoscience uses remnant information from ancient rocks and sedimentary deposits to unravel the history of our 4.6 billion years old planet. Using actualistic point of view, provenance study is a back-striping of a sedimentary cycle to develop reliable paleogeographic models of Earth for particular time and area in the past. In fact, provenance study is a special and temporal investigation of parent rock lithology, age, tectonic setting of the hinterland and of the basin, and paleoclimate. Among different methods of provenance study, we want to illuminate the outstanding importance of petrography in the framework of QFL memory and its priority. Although, in recent decades scientists emphasize on quantitative approaches, these kinds of data only are as spot and stain of reality in provenance work. In contrast, petrography as a descriptive and qualitative method, possess the real face of vanished rocks and therefore can be used as undeniable evidence for provenance. Traditionally petrographic techniques include compositional and textural analyses and can provide reliable information on origin, timing, and composition of grains of silisiclastic rocks. Although, it should be noted that some tricky points may affect validity of petrographic data. Grain identification, selective destruction of grains during sedimentary and diagenetic processes, and distinguishing intrabasinal and extrabasinal grains are the most important limitations. However, multiplicity of diagrams in provenance studies could help us for filtering the effect of different variables to illuminate the main controlling factors. Ultimately better understanding of paleogeography in provenance studies needs a close cooperation of sedimentologists, field geologists, and tectonists.

KEYWORDS: Paleogeography, Petrography, Provenance, QFL memory, Sedimentary cycle

The story of Kermanshah radiolarite basin from Early Jurassic to Late Cretaceous

Abdi, A.[1], Bádenas, B.[2], Mahmudy Gharaie, MH.[3], Gorican, N.[4], Toodekesht, S.[1], SAmini, S.[1], Mattioli, M.[5]

[1]Zamin rizkavan Co. Ltd. Tehran, Iran
[2] Department of Earth Sciences, Faculty of Sciences, University of Zaragoza, Spain
[3]Department of Geology, Faculty of Sciences, Ferdowsi University of Mashhad, Mashhad, Iran
[4]Ivan Rakovec Institute of Paleontology, Research Centre of the Slovenian Academy of Sciences and Arts, Ljubljana, Slovenia
[5] Université de Lyon, UCBL, ENSL, CNRS, LGL-TPE, F-69622 Villeurbanne, France
E-mail: Asadabdi656@gmail.com

The Kermanshah Radiolarite basin was developed at the western border of central Neo-Tethys Sea and the eastern edge of Gondwana during the Mesozoic era (Gharib and De Wever, 2010). This basin was located northeast of the Arabian continental platform and, in West Zagros, was separated from the Neotethys basin by the Bisotoun carbonate platform (Navabpour et al., 2011). During this time period, a high variety of marine sedimentary rocks, including radiolarites, pelagic limestones, pyroclastic deposits, shales and gravity deposits (internalites, turbidites, debris flows, etc.) were accumulated. These rocks are exposed in the Kermanshah area (West Iran) in the Zagros orogenic system (e.g., Wrobel-Daveau et al., 2010). The outcrops studied in this work, 5 sections, is located at the south of the Kermanshah city, between the Kuh-e-Sefid fault to the south and the Bisotoun fault to the north of the Kermanshah city.

An integrated analyses of sedimentological, paleontological and geochemical data has been performed to in order to improve the knowledge of the sedimentary evolution of the basin and the controlling factors (e.g. tectonics, climate, and volcanism). Paleontological studies (calcareous nannofossils, radiolarians and planktonic foraminifera) indicate and Early Jurassic to Late Cretaceous age for the studied sections. The Lower Jurassic (earlier than Sinemurian) succession is formed by shales with intercalations of turbidites, pyroclastic and radiolarite beds passing upwarads to pelagic limestones with intercalated internalites and pyroclastic deposits. The Upper Jurassic to Lower Cretaceous succession is characterized by chertshale alternations (radiolarites: Baumgartner, 2013) with intercalations of pyroclast layers. The lower Cretaceous deposits also include intercalations of Fe- and Mn-rich metalliferous and black chert deposits. The Upper Cretaceous succession is formed by pelagic limestone and shale layers with intercalations of gravity deposits such as turbidites, olistrostromes and debris flow. Relatively Enrichment of LREE, Zr, Nb, Hf, and Th indicate a upper continental crust source for the Early to Late Jurassic as well as Late Cretaceous deposits. However, flat to slightly light rare element-enriched (LREE) patterns and positive correlation of P, V, Zn, As with Fe, and enrichment of V, Co and Ni elements in Early Cretaceous chert and metalliferous deposits conform to those of modern mid-ocean ridge (MOR) iron-rich sediments.

It is concluded that continental break-up and initial sea-floor spreading took place probably during the earlier time of Sinemurian triggering deposition of distal turbidity deposits. Fe- and Mn-rich metalliferous sediment in Early Cretaceous indicate that further opening of the basin and creation of oceanic crust continued until this time. Lastly, occurrence of gravity flow deposits in Late cretaceous indicate basin closure and emplacement onto Arabian foreland.

KEYWORDS: South Neotethys; West of Iran; Kermanshah radiolarite basin; Sedimentology; Biostratigraphy; Geochemistry

Hormuz Formation of Jabal Sanam Salt Structure: The Oldest Rocks Outcrops in Southern Iraq

Soltan, B.[1], and Abdulnaby, W.[1]

[1]Department of Geology, College of Science, University of Basrah

Jabal Sanam structure is a salt dome located in southern Iraq near Iraq-Kuwait border. Sanam salt structure has an oval shape with 1.7 km length and 1.5 km width. The highest elevation of Jabal Sanam is about 96 km above surrounding areas and 152 km above sea level. Jabal Sanam is a salt plug of which its cap rocks crop out on the surface and compose mainly from evaporates and it has general properties similar to that of Infra-Cambrian Hormuz series.

Detailed geological field investigations were carried out at Jabal Sanam structure that has very lithological complexity and large variety in its rock components. Therefore, the reconstruction of the lithological and stratigraphical succession of the structure is difficult. The cap rocks of Jabal Sanam considered as a complex because of the significant difference in thickness and dips of beds from place to place and many parts of them disappear under the slopes of the sediments as a result of big-scale distortion by the effect of salt intrusion. Thus, the reconstruction of the lithological succession was needed to make a composite section. The detailed fieldwork and petrological properties showed that Jabal Sanam structure contains three major units: brecciated limestone unit, gypsum unit, and dolomite (dolostone) unit.

Petrological, stratigraphic and tectonic correlation were made with similar structures in Iran and the Arabian Peninsula in light of their composition, which in general consist of Infra-Cambrian evaporates of Hormuz Formation. This study shows great similarity between the rocks of Hormuz Formation complex and those of Jabal Sanam that can be considered in terms of stratigraphy and petrology as equivalent rock unit of Hormuz Formation. The development of Hormuz evaporative rocks in isolated and isochronous sedimentary basins indicates the independence of sedimentary conditions from those associated with the geneses of Jabal Sanam rocks. Therefore, the study suggests that the rocks of Jabal Sanam can be called Sanam Formation.

Paleoenvironmental and Biostratigraphy studies of the Qum Formation based on calcareous nannofossils in Shadiyan section, Central Iran

Senemari, S.[1], and Bahrammanesh Thehrani, M.[2]

[1]Imam Khomeini International University, Qazvin, Iran
[2]Geological Survey of Iran, Tehran, Iran.
Email: senemari2004@yahoo.com

One of the most extensive Tertiary deposits in central Iran, the marine sediments of the Qum Formation, the first in the area around Qum based on stratigraphy and paleontology was identified. Type section of the Qum Formation is studied around Qum (Khaksar and Maghfouri-Moghadam, 2007). The most important things that can be done given of this formation in Iran, determining the exact age of by calcareous nanofossil. In this study, the sediments of Qum Formation were investigated in Shadiyan section, southeast of Kashan. This Formation with a thickness of about 340 m consists of marl and marly limestone, and gradually covered by conglomerate of Pliocene. The study of 100 samples taken from the section led to the identification of 33 species of calcareous nannofossils. According to distribution of the index species, created several distinct biostratigraphic marker zones in this section, described as nanno floral zones NN1, NN2, NN3 and NN4. As a result of this study and based on the identified zones, the age of Qom Formation in the studied section is Late Chattian to Burdigalian/Langhian. We can also learn about the predominant conditions of the studied sedimentary basin that was in fact part of the Neo-Tethys basin with the existence of indexed species calcareous nannofossils that indicate warm climate and high water depths of the basin in low latitudes.

KEYWORDS: Qum Formation, Biostratigraphy, Calcareous nannofossils, Kashan, Chattian, environment change.

Why garnierite is absent from mineralization in the Ni-bearing laterites from Bavanat region, Fars province, Iran?

Rasti, S.[1], Rajabzadeh, M.[1], Quantin, C

[1]Department of Earth Sciences, Faculty of Sciences, Shiraz University, Shiraz 7146713565, Iran
[2]UMR 8148GEOPS, Université Paris Sud — CNRS, 91405 Orsay Cedex, France

E-mail address: mrajabzadeh@shirazu.ac.ir.

Nickel-bearing laterites in Bavanat region occur in two parallel belts between the Sedimentary Zagros Orogenic (SZO) and Metamorphic Sanandaj-Sirjan (MSS) zones in SW Iran. These belts, trending NW-SE are called Northern belt and Southern belt and extend 180 and 450 km, respectively. They are the only known Ni-bearing soft rocks in the country. These laterites are regarded as the weathering products of ultramafic rocks (mainly harzburgite) of the Neyriz ophiolite which emplaced on continental margin during collision between Afro-Arabian and Iranian micro-plate in Late Cretaceous. Lithologies of the study area include altered ultramafic plutons, marl, limestone and conglomerate overlaid by recent sediments. The weathering of ophiolite ultramafic rocks under Mediterranean climatic conditions led to the development of the iron oxide soils containing nickel rich ferruginous horizons. Vertical profile of the laterites includes protolith, hard and soft saprolite, and then oxide horizon. Protolith is the extremely serpentinized harzburgite composed of olivine and orthopyroxene with dark green color and network texture. Minerallogically, hematite, goethite, talc, dolomite and, quartz increase whereas chlorite, olivine, serpentine and, pyroxene decrease from hard saprolite to oxide horizon. Hematite and goethite are the dominant phases in the oxide horizon. The Ni concentration varies gradually from base to top of the soils, and reaches up to 12 g/kg in the oxide horizon. Iron oxide-hydroxide minerals are the major Ni-bearing phases in the studied laterites. SEM-EDS analyses showed that liberated Ni from serpentine group minerals in the parent rock was concentrated in hematite in oxide horizon. Concentration of Ca, Na, K and, Mg decrease, whereas concentrations of Fe, Mn, Ni, Cr, Co and Al increase in an upward direction along the selected profiles.

Garnierite is the main Ni-bearing mineral in Ni laterites around the world. This mineral occurs in saprolite horizon at the top of the serpentinized parent peridotites. The lack of garnierite in the studied latterites is explained by a number of geological and environmental factors. Very low Ni concentration (0.69 to 2.39 g/kg) in the protolith did not provide the abundant Ni source of formation the garnierite. High Fe concentrations (up to 9.54 wt%) of the parent serpentines and the presence of a few clasts of these phases in saprolite horizon prevent the formation of garnierite in the studied laterites. The rainforest climate condition was also unfavorable for Ni transportation and accumulation in the weathering solutions. Despite the in-situ profile thicknesses of 10-15 m in some places, the weathering intensity was low and the weathering period was relatively short. These result in little or no formation of nickel-rich secondary silicates. In addition, insufficient joints and fractures in the source rock from Bavanat region prevent fluid circulation along fractures, the process that controls the infiltration of Ni-saturated solution and the precipitation of garnierite in the lower part

(saprolite) of the laterite profile. Garnierite minerals cannot precipitate from fluids enriched in light isotopes of Ni (-0.05 to +0.15 ‰). High pH values (up to 8) of Ni-laterite samples in Bavanat region and low organic matter content as well (between 0.69 and 1.93 g/kg) also explain the absent of garnierite in these soils.

KEYWORDS: Bavanat; Garnierite; Iran; Laterite; Mineralization; Nickel.

Seismic hazard assessment for Makran from mechanical modelling

Cubas, N.[1]

[1]Sorbonne Universités, UPMC Univ Paris06, ISTEP, Institut des Sciences de la Terre de Paris, France

Recent geodetic studies have shown that some accumulation of elastic strain along the plate interface is required to explain the velocities on both western and eastern Makran. They proposed a relatively strong coupling along the eastern segment where the 1945 earthquake occurred, a decrease along the central part, and a possible increase westward. However, due to the sparsity of stations and the large trench-coast distance, these studies were unable to constrain the locked zones.

From heat flow measurements, we now know that the effective friction along megathrusts differs significantly between aseismic or seismic patches. These differences of effective friction are significant enough to produce wedge segments with varying morphologies and deformation patterns. As a consequence, studying the prism deformation can allow us to locate more precisely the locked zones. During this talk, I will show how mechanical modelling can help us to establish relationships between deformation and seismic behavior and thus improve the seismic and tsunamigenic hazard assessment. During this presentation, I will first show results obtained along the South American, Japan, Sumatra and Cascadia subduction zones. Finally, I will discuss recent results for the Makran accretionary prism.

New seismic constraints for deep structure of the western Makran subduction zone, SE Iran

Motaghi, K.[1], Meymand, R.Z.[1], Momeni, H.R.[1], Akbarzadeh, M.[1], Mokhtarzadeh, R.[1], Ghods, A.[1], Sobouti, F.[1], Priestley, K.[2]

[1]Department of Earth Sciences, Institute for Advanced Studies in Basic Sciences, Zanjan, Iran
[2]University of Cambridge, Madingley Road, Cambridge CB30EZ, UK
E-mail: kmotaghi@iasbs.ac.ir

Deep structure of the western Makran subduction zone in SE Iran has not been investigated in details so far. Shortage of seismic stations and events in the region made improper data coverage which in turn made it impossible to prepare high resolution seismic images for the region. To solve this shortage, the Institute for Advanced Studies in Basic Sciences in Zanjan, Iran, has installed a dense seismic array since May 2016 and gathered continues data in 35 seismic stations (at least one year for each station) so far. Combining these data with sparse seismic stations from Iranian national networks generated a unique chance for preparing high resolution teleseismic images for the region. The study region (25–30oN and 58–62oE) covers the accretionary prism at northern shoreline of Oman Gulf to north of Taftan volcano which is part of the Makran volcanic arc. We carried out a teleseismic P-wave travel time tomography, a teleseismic surface wave tomography and a P receiver function analysis to reveal the deep features. The obtained results show that the slab is almost flat up to ~100 km north of the northern shoreline of the Oman Gulf attesting that subduction trench is beneath Qasr-e-Qand fault. This is inconsistent with widely-accepted tectonic maps showing the subduction starts at middle of the Oman Gulf. The resolved slab bends even more beneath the Taftan volcano reaching to depth of 300 km in a high angle. This geometry has been confirmed by combining the obtained results from three different images prepared by the above mentioned seismological techniques.

KEYWORDS: Western Makran subduction zone, Surface wave tomography, Teleseismic travel time tomography, P receiver functions

Khaledzadeh, M.[1, 2], Ghods, A.[1], Zeyen, H.[2], Abbasi, M.[3]

[1]Institute for Advanced Studies in Basic Sciences (IASBS), Zanjan, Iran
[2]GEOPS, Univ. Paris-Sud, CNRS, Université Paris-Saclay, 91405 Orsay, France
[3]Surveying Engineering Department, University of Zanjan, Iran
E-mail: mkhaledzadeh@iasbs.ac.ir

Makran subduction zone extends ~1000 km between SE Iran to SW Pakistan in E-W direction and from 24°N inside the Oman Sea to the JazMurian and Mashkel depressions in N-S direction. The Makran is a unique subduction zone in terms of its very low subducting angle, wide accretionary prism, and a large distance of 400-600 km between its volcanic arc and deformational front.

In order to estimate the geometry of the subduction zone in the Iranian side of the Makran, the department of Earth Sciences of Institute for Advanced Studies in Basic Sciences (IASBS) deployed a seismic network in Makran region in June 2016. The network is consisted of 30 seismometers and will be working in the region up to the end of 2019. The network is installed along a line starting from the Iranian coasts of Oman Sea and crosses the accretionary wedge and Bazman-Taftan volcanic arcs in Central Iran. In this study, we present a new crustal and lithospheric density model for the Makran subduction zone by applying an integrated geophysical modeling method along a N-S profile centered at 60.5°E latitude. The profile starts inside the Oman Sea at 23°N and extends along the IASBS seismic profile. We model density and thermal structure of the crust and lithosphere by integrating seismological data, gravity (free-air and Bouguer), geoid, absolute topographic elevation data while assuming local isostatic equilibrium (e.g. Zeyen and Fernandez, 1994), to reduce non-uniqueness of the geophysical modeling. The calculation is performed using a finite element technique which links the different equation of states. The lithospheric density is assumed to vary linearly with temperature whereas the density of sediments is assumed to vary exponentially with depth. For the crustal parts, we defined constant densities.

We constrained the geometry of the offshore part of the model using the results of previous reflection and refraction seismic studies. Based on the previous studies, the angle of the subducting plate is very low ~1°-2° in the front of Makran wedge where the sedimentary cover is ~7 km thick and the oceanic crust has an average thickness of 9 km. We assumed a density of 2300-2450 gr/cm3 for the sedimentary cover. A phase change is considered for the oceanic crust where the basalt partially changes to eclogite at depths deeper than 40 km. The density of basalt and the partially eclogitized oceanic crust are assumed to be 3050 and 3200 gr/cm3, respectively. For the continental part, we used the result of receiver function along the IASBS seismic profile (Mokhtarzadeh et al., 2019). The receiver function analysis showed a very low angle of ~3° for the subducting Arabian plate at and north of the Iranian Oman sea coastlines, ~13° north of the Qasr_e_Qand fault, south of JazMurian depression and then a more dipping plate of ~35° for the north of the Taftan-Bazman volcanic arc. The receiver function study also showed a normal continental crust with a thickness of 40-50 km beneath JazMurian and Central Iran. We split the continental crust into upper and lower parts with a density of 2800 and 2950 gr/cm3 and average thickness of 25 and 15 km, respectively.

We defined the density for the continental sediments in the range of 2450-2600 gr/cm3 that is suitable for Eocene-Miocene Flysch and Molasses that construct the accretionary wedge and Quaternary sediments covering the JazMurian depression. Moreover, we defined a narrow ophiolite belt with an average width and density of 15 km and 2700 gr/cm3, in the south of JazMurian, similar to its surface outcrop in the geological map. The magnetic field map in JazMurian shows that there is a strong magnetic anomaly beneath the Quaternary sediments in this area. Previous studies related this positive strong magnetic anomaly to the old remnant oceanic crust that created with back-arc spreading mechanism. However, the gravity signals shows a negative anomaly above the JazMurian, very similar to the gravity signal of the continental part. If there is a back-arc related oceanic crust in JazMurian, we expect a strong Bouguer gravity anomaly above the JazMurian like the oceanic area. The rather thin (~40 km) and strongly magnetized continental crust of JazMurian suggests that the JazMurian was a passive volcanic thinned marginal basin connected to Central Iran before commencement of the subduction. Therefore, we defined a magnetized volcanic basement as a marginal basin in JazMurian to justify both gravity and magnetic signals. We considered constant values for density and temperature of the asthenosphere, 3200 gr/cm3 and 1300° C, respectively. These values are used as a reference to construct the density of lithosphere. In this way, we defined the temperature-dependent density for oceanic and continental lithosphere that varies with respect to this reference values. We determine the thickness of oceanic lithosphere from the global plate cooling model.

The proposed density model has a good fit with the observed free-air and Bouguer gravity and geoid signals. The misfit values are 16 and 11 mGal for Bouguer and free-air signals and 0.37 and 334 m for geoid and topographic elevation signals, respectively. To achieve a reasonable model, our priority is to obtain first a good fit for the gravity data, then for the geoid and finally for the topographic elevation data. This is because local isostatic equilibrium may not always be established and the crust and lithosphere may compensate some part of the topographic load with their inherent rigidity. Our density model shows a lack of isostatic equilibrium in the deformational front and in coastlines where short topography wavelengths are present. Our modeling suggests a normal continental crust for the JazMurian depression, a lithospheric thickness of 110 km for the ~90 Myr. Old subducting plate, and a partially eclogitized oceanic crust at depths deeper than 40 km.

KEYWORDS: Geoid, Gravity, Integrated Geophysical Modeling, Local Isostasy, Makran, Steady State

References

Mokhtarzadeh, R., Sobouti, F., Priestley, K., Ghods, A., Motaghi, K., 2018. Structure of the western Makran subduction zone from seismological studies. 2nd TRIGGER International Conference, Tehran.

Zeyen, H., Fernandez, M., 1994. Integrated lithospheric modeling combining thermal, gravity and local isostasy analysis: application to the NE Spanish Geotransect. J. Geophys. Res. 99, 18089–18102.

Imaging the crust and upper mantle structures in the makran subduction zone in south-east of iran

Abdollahi, S.[1], Ebrahimzadeh Ardestani, V. [1], Zeyen, H.[2], and Shomali, Z.H.[1, 3]

[1] Earth Physics Department, Institute of Geophysics, University of Tehran, Tehran, Iran

[2] CNRS/Université Paris-Saclay, Département des Sciences de la Terre, Orsay, France

[3] Department of Earth Sciences, Uppsala University, Uppsala, Sweden

E-mail: sabdollahi@ut.ac.ir

In this study, Simulated Annealing (SA) algorithm is applied to non-linear inversion of fundamental mode Rayleigh wave group dispersion curves for shear and compressional wave velocities. At first, to determine the efficiency and stability of the Simulated Annealing method, two noise-free and two noisy synthetic data sets are inverted. Then real data for Makran region are inverted to examine the usage and robustness of the proposed approach on real surface wave data. In a second step, we applied 3D Gravity Modeling based on surface wave analysis results to obtain the density structure of each layer. The reason for using both types of data sets, is that gravity anomaly has a bad vertical resolution and surface wave group velocities are good for placing layer limits at depth, but they are not very sensitive to densities. Therefore, using gravity data increases the overall resolution of density distribution.

Our results show that Moho depth increases from Oman Sea (18-28 km) and Makran fore-arc setting (35–40 km) to the Taftan-Bazman volcanic-arc (46–48 km). Also, results show a high shear and compressional velocity under the Gulf of Oman which reduce to the North of the Makran region. We find a high-velocity anomaly in the upper mantle under the Oman Sea corresponding to the subducting slab. The density image shows an average crustal density with maximum values under the Gulf of Oman decreasing northward to the Makran region. The crustal density is high in the Oman Sea as should be expected for the oceanic crust.

KEYWORDS: Gravity; Makran; Moho; Shear velocity; Simulated Annealing algorithm

A plume-ridge interaction for Neo-Tethys: Insights from various basalts of Makran accretionary complex, SE Iran"

Wan, B.[1], and Esmaeili, R.[1]

[1]State Key Laboratory of Lithospheric Evolution, Institute of Geology and Geophysics, Chinese Academy of Sciences

The Makran region in southeast Iran provides a spectacular subduction-accretionary complex to understand continental growth. In this paper, we present new major and trace element compositions of mafic volcanic blocks from the ophiolitic mélange complex exposed in the Makran area. Our aim was to assess the genesis of these rocks and discuss their implications on the evolution of the Neo-Tethys Ocean. These volcanic blocks are composed mainly of basalts with minor trachytes. Based on their geochemistry, the basalts in the ophiolitic mélange complex are divided into three groups, N- MORB, E-MORB, P--MORB and alkaline basalts. The chemistry of these rocks suggests that they were formed most likely in a plume-ridge interaction oceanic setting from partial melting of a highly heterogeneous mantle characterized by the extensive occurrence of OIB-metasomatized portions .Despite exposed as blocks or components in the wide Makran subduction-accretion complex, none of these basaltic groups exhibit geochemical evidence of subduction. These rocks are more similar to oceanic plateau and/or ridges similar to Iceland-Reykjanes Ridge before being fragmented and accreted into the Ophiolitic Mélange Complex.

Coseismic deformation and source parameters of 12 December 2017 Mw 6.2 Hojedk Iran earthquakes

Vajedian, S[1], Mousavi, Z.[2], Motagh, M.[1,3]

[1]Institute of Photogrammetry and GeoInformation, Leibniz University Hannover, 30167 Hannover, Germany; vajedian@ipi.uni-hannover
[2]Department of Earth Sciences, Institute for Advanced Studies in Basic Sciences,45137-66731 Zanjan (IASBS), Iran;
[3]GFZ German Research Centre for Geosciences (GFZ), Section of Remote Sensing, 14473 Potsdam, Germany;

On December 1st 2017 an Mw 6.1 earthquake struck a region between Central Iran and Lut block in southeastern Iran. The mainshock followed by two moderate aftershocks (Mw 5 and Mw6) occurred on 12 December positioned in close spatial proximity to each other. The area has been hit continuously by the 10 tremendous events (Mw > 5) over the eight months. This study investigates the geometric and kinematic characteristics of the seismogenic faults ruptured during the earthquakes occurred on 1st and 12th December 2017.

Monitoring the crustal deformation caused by earthquakes provides invaluable kinematic coseismic information to better understanding of tectonics processes. SAR interferometry is a popular technique to remotely detect large coverage Earth's surface deformation associated with various phenomena including earthquakes, volcanic activity and landslide movements. However in the presence of large deformation, in near-field area, InSAR observations get complex and noisy due to the image mis-registration. Retrieving near field displacement may be more of interest however, as they allow to improve constraints on fault geometry and slip distribution especially within the shallowest crust.

Here is this study, we use the available Sentinel-1 TOPS and ALOS-2 ScanSAR in both geometries of ascending and descending to retrieve LOS surface deformation. Beside LOS observations, we implement orientation correlation method to estimate sub-pixel offset over the near-field area. We then combine both observations including coseismic deformation derived from InSAR and near field offsets retrieved from orientation correlation to estimate the source model.

Combining geodetic observations acquired by independent methods, InSAR and offset tracking in this study, requires a data weighting method to balance the observed data with respect to each other. Considering data quality of the observed data in weighting approach can significantly improve resolving source model parameters. To properly combine observations, here we use noise covariance structures obtained from the observed data. We further use resolution based resampling method to downsample the continuous measurements in order to reduce the computational cost. Bayesian optimization method is implemented on the resampled data to apply coseismic joint inversion in order to solve the source model

parameters. We complement the satellite observations by additionally using of aftershock relocations and surface rupture evidence obtained from optical satellite as independent constraints to find a unique fault structure that is more consistent with the real earth. Once the unique fault is defined, we fix the fault geometry and split it to a coarse grid of dislocations. We then appropriately resize dislocations so that each discrete dislocation is robustly constrained by the observed data. Our results demonstrate earthquakes occurred in the area were caused by reactivity of Lakar Kuh fault located between north-south trending Kuhbanan and Nayband faults. The main deformation related to the 12 December earthquake occurred as a result of WNW-ESE thrusting faulting where main rupture was concentrated at a depth between 8 and 10 km, characterized by a shallow rupture reaching the surface.

KEYWORDS: InSAR, Orientation Correlation, Bayesian, Earthquake, Coseismic analysis

GPS and seismic data to highlight the interaction between deep and shallow deformation related to the 2013 Okhotsk earthquake, Kamchatka

Walpersdorf, A.[1], Titkov, N.[2], Chebrov, D.[2], Rousset, B.[1], Jara, J.[1], Campillo, M.[1], Shapiro, N.[3]

[1]ISTerre, Université Grenoble Alpes, CNRS, Grenoble, France (andrea.walpersdorf@ujf-grenoble.fr),
[2]Kamchatka Branch of the Geophysical Service, Russian Academy of Sciences, Petropavlovsk-Kamchatsky, Russia (nik@emsd.ru),
[3]Institut de Physique du Globe, Paris, France

The 24/05/2013 Okhotsk earthquake (M=8.3) took place at 600 km depth on the Kamchatka subduction zone that accommodates 8 cm/yr of westward convergence of the Pacific plate with respect to the North American plate. The Okhotsk event has been preceded by several shallow earthquake swarms that stopped instantaneously at the time of the large and deep earthquake. This work aims at investigating the interaction between shallow and deep seismicity based on a detailed earthquake catalog, and to search for related signals of transient surface displacements monitored by the Kamchatka permanent GPS network. The earthquake catalog localizes the swarms before Okhotsk in depths between 40 and 80 km, and some notable activity of aftershocks between 500 and 700 km depth, with no events in the intermediate depths. The cumulated number of earthquakes from 2004 to 2016 reflects the occurrence of the shallow swarms by an increased rate before Okhotsk, while the earthquake rate of deep events (500-700 km) decreases simultaneously. Furthermore, an increase of earthquake rate is observed in 2009 in both depths. While it is difficult to extract a clear signal of surface deformation comparing the period before and after 2009 in the GPS data, the shallow swarms do have a surface expression, indicating purely co-seismic release of constraints during the last swarm just before Okhotsk, and co- and a-seismic release for the most energetic swarm with a cumulated magnitude of 7.1. In particular, during this swarm, a large-scale transient motion is observed of ~5mm toward the SE, covering the whole peninsula. Investigations are ongoing to identify possible sources, like hydrological loading (using GRACE data), stress transfer following the 2011 Tohoku event, or following the 2007 Kuril earthquakes that created large scale a-seismic creep over several years. Eventually, this transient is a first observation of a loading and unloading mechanism of the deep slab that could explain the simultaneous increase and decrease of seismic activity in shallow and large depths, respectively, before the Okhotsk event.

Aquifer storativity and hydraulic head estimation from InSAR

Rezaei, R. [1, 2], Mousavi, Z. [1,3]

[1] Department of Earth Sciences, Institute for Advanced Studies in Basic Sciences (IASBS), 444 Prof. Sobouti Blvd., Zanjan 45137–66731, Iran.

[2] Center for Research in Climate Change and Global Warming (CRCC), Institute for Advanced Studies in Basic Sciences (IASBS), 444 Prof. Sobouti Blvd., Zanjan 45137–66731, Iran.

[3] Earth System Physics Section, Abdus Salam International Centre for Theoretical Physics, Trieste, Italy.

E-mail: (arezaei@iasbs.ac.ir)

This study uses Interferometric Synthetic Aperture Radar (InSAR) to quantify the land deformation across the Gorgan confined aquifer system (GCAS), Iran, susceptible to significant subsidence imposed by aquifer storage depletion. Analysis of TOPS S1 month-scaled images from 2014 to 2016 reveals that significant inelastic (70 mm/yr on average) and periodic elastic (ranging from about 20 to 132 mm) deformations based on the decomposed vertical displacement map have occurred in GCAS. It is also observed that a high cross-correlation coefficient exists between the seasonal (de-trended) components of head and land deformation time series (ranging from 0.60 to 0.93; ~0.78 on average). From a joint well-InSAR data analysis, we estimate bulk aquifer parameters of the elastic skeletal storativity (0.0035 to 0.0142; 0.0085 on average), specific storage (1.54×10^{-5} to $7.68\times10^{-5}\ m^{-1}$; $4.35\times10^{-5}\ m^{-1}$ on average), and compressibility (1.50×10^{-10} to $7.40\times10^{-10}\ N/m^2$; $4.20\times10^{-10}\ N/m^2$ on average) at 14 piezometer locations. InSAR-derived aquifer storage parameters are reasonably correlated with the hydrogeological setting of GCAS. Further, the elastic land deformation data are acceptably converted to head fluctuations at 14 piezometers where the heads reconstructed from InSAR and measured in piezometers are consistent over a broad portion of GCAS. Finally, the confining degree map across GCAS is extracted from seasonal elastic land deformations that occurred between wet and dry seasons in 2015. The higher confining degrees are observed in those areas of higher subsidence signatures, implying that the subsidence potential in confined aquifers is higher compared to unconfined aquifers. In this study, we have demonstrated more benefits of the InSAR observations in estimating aquifer storage properties and reconstructing head in confined aquifers of significant subsidence signatures with better temporal and spatial resolution than that can retrieve from hydrogeological data alone.

KEYWORDS: Aquifer confining degree; Aquifer storage parameters; Gorgan Plain of Iran; Inelastic and elastic land deformation; InSAR deformation map

Characterizing surface deformation in the 1990 Rudbar earthquake (Iran) using optical image correlation

Ajorlou, N.[1], Hollingsworth, J.[2], Mousavi, Z.[1], Ghods, A.[1], Masoumi, Z.[1]

[1] Institute for Advanced Studies in Basic Sciences, Zanjan, Iran

[2] ISTerre, Univ. Grenoble Alpes, Grenoble, France

E-mail: (n.ajorlou@iasbs.ac.ir)

The 1990 June 20th Rudbar earthquake (7.3 Mw) was a catastrophic event that killed ~40,000 people, made ~500,000 people homeless, and destroyed three cities and 700 villages in Northern Iran. The earthquake ruptured a previously unknown left-lateral strike slip fault over a distance of 80 km (Fig. 1a) in the western Alborz Mountain belt. The field study indicated a maximum horizontal displacement of ~60 cm and a vertical displacement of ~95 cm [Berberian et al., 1992; Berberian and walker, 2010]. The main shock was followed by several aftershocks, with many striking north of the fault plane, and displaying strike-slip or reverse focal mechanisms (Fig. 1a). The reported surface slip displacements are surprisingly low given the relatively shallow and high moment release in this event, coupled with the pure nearly vertical left-lateral fault (e.g. ~2.5 m of slip would be expected from a Mw 7.3 event with a fault surface of 15 in depth and 80 km in length). The Rudbar earthquake occurred before InSAR and GPS eras, thus we re-examine the surface displacement field using optical image correlation to better understand the faulting associated with the Rudbar earthquake. This method allows the retrieval of near-field fault displacements by cross-correlation of pre- and post-earthquake satellite and aerial images [Leprince et al., 2007; Avouac et al., 2015]. We use SPOT images from before (1989) and after (1994) the earthquake to document the horizontal deformation produced by the Rudbar earthquake. We find much larger surface slip (~1 to 5 m, Fig. 1b) than those reported by field measurements (~60 cm, Berberian et al., [1992]). To study the surface rupture in more detailes, we correlat aerial photos of 1955-2003 and 1968-2003. We use Ames Stereo Pipeline to bundle adjust all our photos together to make a seamless DEM and ortho-photo mosaic, which we then correlate [Shean et al., 2016] applying COSI-corr [Leprince et al., 2007]. The disparity between the two measurments is related to a distributed deformation occurring in a volume around the fault. We found that the horizontal displacement happened within an average width of ~770 m centered on the Rudbar fault. Furthermore, we identify a newly mapped surface rupture with lenght of 23 km in the eastern end of the Rudbar fault.

KEYWORDS: Optical image correlation, aerial photo, Rudabr fault, COSI-corr, Ames Stereo Pipeline

a **b**

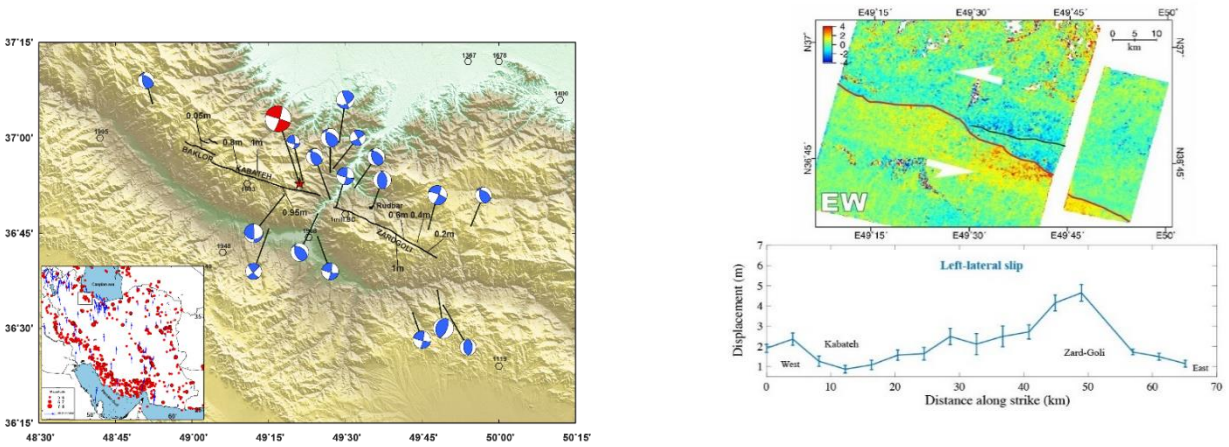

Figure 1. (a) The black solid lines present the Rudbar fault trace mapped by Berberian et al., [1992]. The horizontal displacements, reported by Berberian and Walker, [2010]. The red and blue beach balls represent the focal mechanisms of mainshock and aftershocks, respectively [Gao and Wallence, 1995, Jozi 2014]. The location of the mainshock is marked by a red star. (b) Correlation map in east-west direction of SPOT images. The red line shows the surface trace of Rudbar fault as mapped by our method. The black line shows a new surface rupture for the Rudbar event. The lower panel show the horizontal displacement along the Rudbar fault (solid red lines) strike. The vertical lines show error for each measurement.

References

Avouac, J.-P., Leprince, S. (2015). Geodetic Imaging Using Optical Systems, in Treatise on Geophysics, G. Schubert, Ed. Elsevier, Oxford, ed. 2, (2015), vol. 3, pp. 387-424.

Berberian, M., Qorashi, M., Jackson, J. A., Priestley, K., & Wallace, T. (1992). The Rudbar-Tarom earthquake of 20 June 1990 in NW Persia: preliminary field and seismological observations, and its tectonic significance. Bulletin of the Seismological Society of America, 82(4), 1726-1755.

Berberian, M. and Walker, R. (2010), The Rudbār Mw 7.3 earthquake of 1990 June 20; seismotectonics, coseismic and geomorphic displacements, and historic earthquakes of the western 'High-Alborz', Iran, Geophysical Journal International, Volume 182, Issue 3, 1 September 2010, Pages 1577–1602.

Jozi, A., Ghods, A., Rezaeian, M., 2014. Seismotectonics of northern Iran using local network data, Master thesis, Institute for Advanced Studies in Basic Sciences, Zanjan, Iran.

Investigating the Signature of the Offsets on Wavelet Rough Sets in GPS Experiment

Moghtased-Azar, K.[1], Safari, A.[2], and Tehranchi, R.[2]

[1]Department of Surveying & Engineering, Faculty of Civil Engineering, University of Tabriz, Tabriz, Iran
[2]School of Surveying and Geospatial Engineering, Research Institute of Geoinformation Technology (RIGT), College of Engineering, University of Tehran, Tehran, Iran
E-mail: moghtased@tabrizu.ac.ir

The GPS position time series can be contaminated by the presence of probable offsets. An offset is defined as a sharp change of the mean caused by known or unknown reasons. In order to estimate the unknown parameters and their uncertainties accurately, the locations of probable offsets have to be detected. The problem of the allocation methods of the offsets in GPS time series based on the least squares principle, such as Detection, Identification and Adaptation (DIA) procedure, is that they depend not only on the correct structure of the design matrix, but also on the covariance matrix of the observations. Hence, the objective of this study was to use wavelet rough sets of Maximal Overlap Discrete Wavelet Transform (MODWT) to address the location of the offsets in continuous GPS (CGPS) time series without apriori information of the functional or stochastic models. The performance of the proposed method was tested against The Detection of Offsets in GPS Experiment (DOGEx) database. These time series consist of an intercept, linear trend, two trigonometric functions for the annual and semi-annual signals, offsets, and white and flicker noises composed in an additive model. The results of the proposed method were compared to those of other methods using three different metrics including (i) fifth percentile ranges in velocity biases, (ii) sensitivity versus specificity and (iii) TP (true positive), FP (false positive) and FN (false negative) ratios. The results indicated that the method had an equivalent offset detection threshold of 5.7 mm and fifth percentile range (5% to 95%) in velocity biases were equal to 1.24 mm/year. Meanwhile, the sensitivity and 1-specificity values were 0.54 and 0.28, respectively. Furthermore, the offsets detected by this method were split into 34.3% of TP, 36.5% of FP and 29.2% of FN. Consequently, based on these metrics, the proposed method offered the best results among all tested solutions.

KEYWORDS: Discrete wavelet transform, GPS time-series, Maximal overlap discrete wavelet transform, Offset detection

Regional gravity-field modeling combining terrestrial and SGG-derived surface residual gravity disturbances based on least-squares collocation

Saadat, S.A.[1], Safari, A.[2], Pitoňák, M.[3], Moritz Rexer[4], Cheraghi, H.[1], Djamour, Y.[1], Arabi, S.[1], Nankali, H.[1] and Tavakoli, F.[1]

[1]National Cartographic Center (NCC), Meraj Avenue, Azadi Square, Tehran, Iran
[2]School of Surveying and Geospatial Engineering, College of Engineering, University of Tehran, Tehran, Iran
[3]NTIS - New Technologies for the Information Society, Faculty of Applied Sciences, University of West Bohemia, Technická 8, 306 14 Plzeň, Czech Republic
[4]Institute for Astronomical and Physical Geodesy, Institute for Advanced Study, Technische Universität München, Arcisstrasse 21, 80333 Munich, Germany

Gravity of the Earth has main role in many geosciences such as geodesy and geophysics. Gravity field recovery of the void areas, where the terrestrial gravity data are not available is very important, because gravity surveys are difficult in some regions like inaccessible deserts or mountainous areas. In this study the regional gravity field modelling of the Earth is done by combining surface gravity disturbances and satellite gravity gradiometry (SGG) data based on the least-squares collocation (LSC) over the void areas in Iran, where the existing gravity data are not intensified or available. The gravity disturbances are obtained at minimum geocentric sphere, which is inside the topographic masses by joint inversion of the four high-accuracy components (Vxx, Vyy, Vzz, Vxz) of the GOCE SGG data using second derivatives of the Hotine integral. The GOCE-only global geopotential model (GGM) GO_CONS_GCF_2_TIM_R5 up to degree and order 60 is applied to reduce the effect of the omitted distant-zone, which is restored after calculation. The residual terrain model (RTM) is removed to estimate the effect of omission error of the GGM and provide mass-free space outside the boundary surface. The GOCE-based gravity disturbances at minimum geocentric sphere are continued upward on the Earth's surface based on planar approximation of the Poisson integral and subtracted from terrestrial gravity measurements to compute the residual gravity disturbances. The surface residual gravity disturbances are gridded in different cell-sizes according to the distribution of input gravity data and the locations of the empty cells that represent the void areas are determined. The height-uncorrelated residual values are applied to predict the residual gravity disturbance for every empty cell based on the LSC method using analytical local covariance function. The calculated results yielded an improvement of about 18.1% to 24.6% in gravity field recovery compared to the only RTM-corrected GGM-based solutions for two selected test areas in Iran.

KEYWORDS: Gravity field recovery, GOCE gradiometry data, Hotine integral, void area, Iran

Geochemical Multivariate Outlier Detection in Compositional Data

Simin Saadati[1], Omid Asghari[1], Mohammad Fahimi Nia[1]

[1]Faculty of Mining Engineering, University of Tehran, Tehran, Iran
E-mail: simin.saadati@ut.ac.ir

Compositional data and mostly geochemical data have the kind of information that is relatively connected rather than being absolute. Multivariate outlier detection methods indicate the benefits of transformation in data to distinguish potential outliers more efficiently. In this article, we use isometric log-ratio (ilr) transformation, which seems to be the most effective method to result in reasonable outcome practically and theoretically. Interpretation of distant elements and also deciding on their outlyingness is complex; therefore, methods suggested in this case consider residential data in multivariate database using single variable scatter plots, maps, and plots. Considering three methods, outlier detection is one of the principles in multivariate data analysis. Compositional data or multivariate data sets are positive values which are constant in the sum. In practice, standard statistical methods can be obscure if applied directly to the original data. Therefore, the isometric logratio (ilr) is introduced for its one-to-one transformations of compositional data into the real space. Three methods of detecting outliers are applied to the data. First, we tried using a method from PCA family called Sign function, which stands for Modified Principal Component Analysis. In this method, the data is modified by the statistical mean of the data. In the second method, the estimated covariance of the data is used to allocate a distance to each observation demonstrating how far the observation is from the center of the data cloud. This distance measure is called robust Mahalanobis distance (MCD) in which robust distance is used as the estimator. The third method is the robust Mahalanobis distance which is applied to transformed data by isometric logratio (ilr). The data used in this case is Sarigunay epithermal gold deposit which is analyzed using these three methods. It is located within a mildly alkaline latitic to trachytic volcanic complex in central-northwest Iran. Including 1054 observation in 15 different variables and mainly focusing on Au paragenesis, it shows various outlier portions. Using Sign function 55% of whole observations are indicated as outliers, which is 53% for robust Mahalanobis distance before transformation and 6% for robust Mahalanobis distance after transformation in compositional data.

KEYWORDS: Compositiona data; Mahalanobis; Multivariate analysis; Sarigunay

The Morphology of transported gold grains, Case Study: Razligh Stream, Sarab, NW of Iran

Khan Mohammadi, A.[1], Mirmohammadi, M.[1] and Meshkani, A.[1]

[1] University of Tehran, School of Mining Engineering

E-mail: Abolfazl97khan@ut.ac.ir

Placer is first used as a place where gold can be extracted from sand. Now, the term placer is a deposit made from sand and other clastic sediments that contain valuable mineral or minerals, which are collected by weathering or mechanical processes. The necessary conditions for formation of placer deposits are existence of valuable mineral in source areas, which is relatively heavy and it's resistant to weathering and abrasion. Second, separation of minerals from gangue and third is ore concentration in local areas. Since gold is a heavy mineral and it's also resistant to weathering, the study of gold deposits can yield results. The studied area is located between 37°56'55"N- 47°33'37"E and 38°00'13"N- 47°30'30"E coordinates. Based on geological studies and maps, Neogene volcanic rocks include andesite, trachyte, and dacite and also Eocene shale and ignimbrite are most important rock types at Sarab area. There are two main faults that divide north part of Sarab into gold-bearing and without gold placers. In this study, totally 44 samples were taken along Razligh Stream that surprisingly 34 samples of them had gold grains. The total number of gold grains are 210 and among all of them the largest of grains was 1284 microns and smallest was 49 microns in size. Morphological Study on recovered gold grains shows that sphericity (Krumbein Index) and roundness are functions of transported istance from source and generally they have direct relationship with each other. Relationship between minimum krumbein index of gold grains and transported distance from source along Razligh stream is defined in the equation (1); Pearson correlation between them is 0.493 and p-value or Sig is 0.004.

Which X is distance from sample with maximum elevation on Razligh stream profile, Relationship between minimum roundness of gold grains and transported distance from source is defined in the equation (2) along Razligh stream; Pearson correlation between them is 0.469 and pvalue or Sig is 0.007.

(1) Min Sphericity = 1 - 1 / (X ^ 0.167765)

(2) Min Roundness = 6.76883e-009 × X ^ 2 +0.592372

Which X is distance from sample with maximum elevation on Razligh stream profile, Mean and median roundness of gold grains are 0.71 and 0.73 respectively. The result of this study based on roundness index and krumbein index of sphericity and their relationships with transported distance shows that studied gold grains may originated from one or more gold deposits located at radius of about 5km. According to previous morphological studies on Razligh stream gold grains particularly flatness index of grains confirms this allegation.

KEYWORDS: Gold grains; Morphology; Placer gold deposit; Roundness; Sarab; Sphericity

Geochemical modeling and hydrothermal alteration mapping in Sonajil Cu-Au alkaline porphyry prospect area, NW Iran

Safari, M.[1], Hezarkhani, A.[1], Esmaeillzadeh, N.[2]

[1]Department of Mining and Metallurgical Engineering, Amirkabir University of Technology.

[2]Department of Mining Engineering, Sahand University of Technology

E-mail: Mortezasafarisss@aut.ac.ir

The Sonajil porphyry, in the Ahar-Arasbaran volcanic belt which is the most potential metallogenic province in NW of Iran for porphyry and epithermal gold and copper mineralization. The oldest rocks exposed in the Sonajil area are a sequence of Eocene tuffs with intercalations of andesite and andesitic breccia. The Sonajil porphyritic stock with a variant composition from quartz-monzonite to granodiorite due to different intrusive phases has been emplaced within the Eocene andesitic sequence and followed by the Incheh Oligocene granitoid emplacement in the north of Sonajil stock. Several dykes and veins of Incheh have penetrated into the Sonajil porphyry subsequently. The youngest rock units in the study area are the recent terraces and river deposits and a thick basaltic lava flow erupted at the center of porphyry system and covered a significant area. Rocks in the study area were subjected to intense hydrothermal alteration due to several intrusion phases. Potassic alteration is presented at the surface as small patches traced to 100m depth in the drilling core logs. Phyllic alteration is widespread in the surface and it is the prominent type of alteration in the borehole. Propylitic alteration is almost absent at surface and in depth has small footprints; and finally, argillic alteration have been recognized almost in all the area especially near the potassic outcrops. Argillic alteration shows hypogene origin rather than supergene since montmorionite is a widespread mineral in argillic alteration within the study area and jarosite is absent.

The current study investigates the petrochemistry and Cu mineralization in the Sonajil porphyry based on the drilling core samples. Statistical analysis approach (fractal modeling and element chemical behavior modeling) have been carried out to delineate the anomal subpopulation in the drilling core samples. According to results, a set of criteria is defined for mineralized samples population in the study area. In purpose of mapping hydrothermally altered zones in the study area and defining targets for further exploration, a remote sensing study based on ASTER remotely sensed data carried out. Conventional mapping techniques such as band ratioing, principle component analysis and matched filtering are used to map clay minerals and separate the different alteration zones. Based on the field surveys alterations in the study area are classified to three types (intense, intermediate and weak) with respect to presence of clay minerals then the average spectra for each of the alteration classes are calculated. The average spectra of these three classes were used to find the minerals presented in each of the classes, then the detected minerals were used as endmembers to map the study area.

Geochemical studies demonstrate that Cu mineralization in depth occurs from 50m to 200m and mostly hosted by andesitic and quartz dioritic rocks which are subjected to potassic alteration. The main mineralization is the chalcopyrite veins and veinlets that are accompanied by bornite, covellite and chalcocite ore minerals. Lower Cu grades are observed in the phyllic alteration and a small number of high grade Cu samples are in andesitic tuffs with propylitic alteration. The Sonajil Porphyry lacks a considerable supergene zone because of a wide impenetrable basaltic lava cap which inhibits circulation of meteoritic water beneath and low sulfide-bearing minerals such as pyrite in hypogene zone and subsequently low acid production to leach the Cu in the supergene zone. The petrological composition and mineralization style in hypogene zone indicates that the Sonajil is an alkaline Cu-Au porphyry system with sub-economic Cu grade due to lack of initial Cu concentration in the magmatic fluids and latterly intruding Incheh dykes into the Sonajil stock which prevented hydrothermal ore-bearing fluids to circulate in adjacent rocks and depositing Cu.

KEYWORDS: Sonajil, Porphyry System, ASTER, Hydrothermal Alteration, Gold Vein

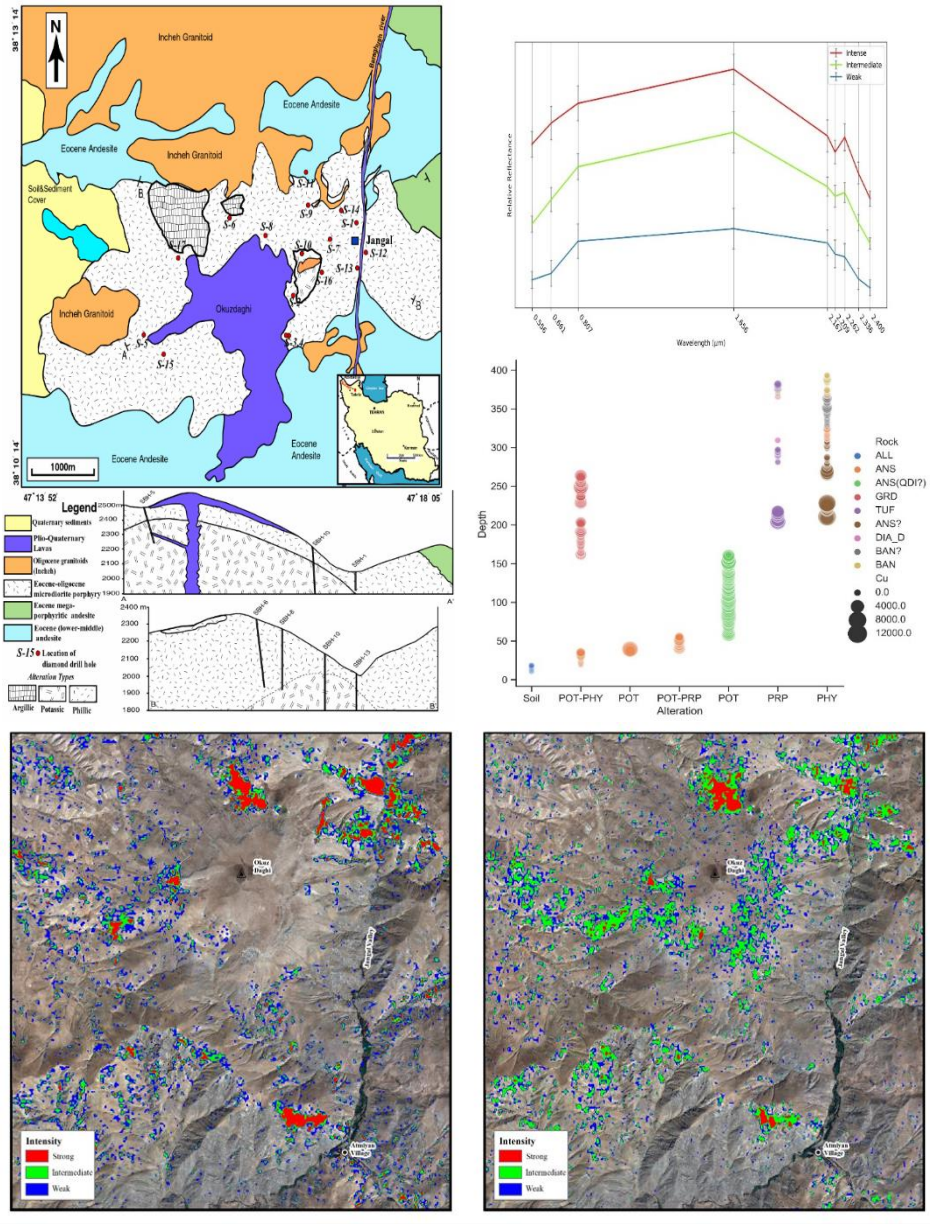

Detecting rare earth elements using reflectance spectroscopy; a case study of esfordi phosphate deposit, central Iran

Karimzadeh, Z.[1*], Tangestani, M. H.[1] and Modabberi, S.[2]

[1]Department of Earth Sciences, Faculty of Sciences, Shiraz University, Shiraz, Iran

[2]Department of Economic Geology, School of Geology, University of Tehran, Tehran, Iran

E-mail: Karimzadeh-shu@shirazu.ac.ir

Modern-day devices, transport, computer, and telecommunication technologies require increasing supply of rare earth elements (REEs). As a consequence, adequate and robust detection methods become essential for exploration and discovery of new deposits of REEs, the improved characterization of existing deposits, and the future recycling of today's high-tech products. REEs display diagnostic absorption features in visible to shortwave infrared (VNIR-SWIR) reflectance spectra. Neodymium (Nd) has the most prominent absorption features in VNIR region and, as a whole, could be a key pathfinder for REEs. This study is an effort to detect REEs in Esfordi phosphate deposit, 36 Km northeast of Bafgh, Iran, by using hyperspectral spectroscopy. This deposit is hosted in Precambrian-Cambrian volcano-sedimentary rocks with 16.5 million tones of phosphate minerals and avarage grade of 13.9% P2O5. The litratures show that the avarage grade of total rare earth oxides in this deposit is 1.2%. Among the 60 field samples of surface outcrops, 10 samples were collected from rhyolitic and dioritic rocks, altered zones consisting of actinolite, epidote, kaolinite and limonite, veins of chalky white, maroon-red and yellowish green phosphate minerals and fine grain apatite hosted in green metasomatite zone for petrographic studies and laboratory spectroscopy. Spectral analysis of chalky white, maroon-red and yellowish green apatite, and fine grain apatite indicated the Nd absorption features centered near 583, 744, 802, and 871 nm. To evaluate these findings, the selected samples were analyzed by inductively coupled plasma-mass spectrometry (ICP-MS) technique for rare earth elements. The concentrations of Nd were 92 to 1677.14 ppm and for ∑REE, it was 188.26 to 9521.82 ppm. The Nd absorption features correlate positively with whole-rock Nd contents. It was demonstrated that Nd absorption features were only detected in samples with Nd concentrations >1,000 ppm. The result of this study was a qualitative outcrop map that highlights enriched zones of neodymium. It was concluded that reflectance spectroscopy is a nondestructive, time and cost-saving method for determining neodymium at outcrops, and could be conducted in the field and drill core libraries as well.

KEYWORDS: Rare earth elements; Reflectance spectroscopy; Neodymium; Esfordi phosphate deposit.

Processing of ASTER satellite imagery for detecting iron oxides in Almobolagh Mountain, West Hamadan, Iran

Moradpour, H.[1], Rostami Paydar, G.[2], Valizadeh Kamran, K.[3], and Bakhtiar Feizizadeh.[3]

[1]Faculty of Planning and Environmental Sciences, Tabriz University, Iran.
[2] Department of geology, Ahvaz Branch, Islamic Azad University, Ahvaz, Iran.
[3] Department of Remote Sensing and Geographical Information Systems, Faculty of Planning and Environmental Sciences, Tabriz University, Iran.
E-mail: moradpourhooman@gmail.com

The provinces of Hamedan, Kurdistan, and Kermanshah in western Iran contain more than 10 iron ore deposits, which some of them are in operation. These reserves are largely different from other sources of iron in other regions of Iran, especially in central Iran. The Babali iron deposit is located about 60 km west, Southwest of Hamedan and near the Almobolagh Mountain. This range is located in the Sanandaj-Sirjan (SSZ) dynamic geologic zone, which has occurred due to the history and events of tectono-magmatism, in which extensive alterations have occurred along with iron mineralization. The data of these studies belong to the terrestrial satellite ASTER sensor, which has been processed by the integration of bands (VNIR + SWIR) and utilizing the software ENVI 5.3. This study aims to investigate various measuring techniques on ASTER image sensors which are intended to represent images for the exploration of iron ore deposits of this region. The method of false-color combination (FCC), relative absorption band imaging (RBD) and Matched Filtering (MF) method was used to determine alteration mapping, mineralogical and geological evidence. The alteration types exist in volcanic-sedimentary units as well as around the semi-deep igneous bodies. Propyilitic alteration is the most characteristic alteration. This phenomenon is widely observed in the diorite, granitic and kalaoinite rocks of the Almobolagh Mountain and Babali mine region. Argillic alteration is often in the outbreak of some rhyolitic masses and acidic Tuffs. In the RBD method, argillic alteration from the band (4+7)/5, propylitic (6+9)/8 and Philic (5+7)/6 were used. In the FCC method for the identification of the gossan, the alteration and the host rock from the combination R:4/2 G:4/5 B:5/6 and for the silica and Fe2+ of the combination R:14/12, G:(1/2)+(5/3), B:MNF band 1 and for the alteration zone in the area of the combination was R:9/8, G:4/3, R:2/1. In the MF method, minerals with iron oxide compounds such as hematite, magnetite, Jarosite, goethite, and siderite were used to investigate iron oxide. Finally, the southern and southwestern parts of the Almobolagh Mountain are recommended for priority exploration in the region.

KEYWORDS: Almobolagh Mountain, iron oxide, ASTER data, FCC, RBD, MF

Towards a comprehensive geodynamic evolution of Northern Sistan (E. Iran)

Agard, P.[1], Jentzer, M.[1], Whitechurch, H.[2], Fournier, M.[1], Omrani, J.[3], Bonnet, G.[4], Zarrinkoub, MH.[5], Mahdi Khatib, MM.[5]

[1]Sorbonne Universités, UPMC Univ Paris06, ISTEP, Institut des Sciences de la Terre de Paris, France
[2]Ecole et observatoire des sciences de la Terre (EOST), University of Strasbourg, France
[3]Geological Survey of Iran
[4]Dept. of Geology, Faculty of Sciences, University of Birjand, Birjand, Iran
[5]Dept. of Earth Science, University of California, Santa Barbara, USA

The diachronous closure of the Neotethyan realm, from the Alps to the Himalayas, led to the formation of numerous mountain belts. The Sistan belt, which stretches N-S across ~700 km, preserves extensive ophiolite fragments, is still poorly documented and is oriented at odds with respect to the other major adjacent structures like Zagros, Makran or Alborz. Five mains domains have been recognized in Sistan in the early 1980s: the Afghan and Lut continental blocks, the Neh and Ratuk ophiolitic complexes (respectively slightly and highly metamorphosed, the latter at high pressure low temperature conditions) and the overlying Sefidabeh basin. Currently, only local petrological and stratigraphic studies exist but the overall structure is still elusive and its geodynamic history is largely debated. In order to refine the tectonic style of each domain and their mutual relationships, detailed field investigations were performed in the northern part of the Sistan belt.

Eleven representative cross sections, from the km to 10 km-scale, are combined into two largescale (~200 km long) comprehensive sections across Northern Sistan. These notably indicate that (1) the main vergence concords with a north-east dipping subduction polarity, (2) the Neh complex is a large-scale obducted ophiolite thrust onto the Lut block and (3) the migration of the deformation is essentially *en sequence*.

Metamorphic investigations (1) reveal for the first time the existence of a metamorphic sole in Sistan in support of intra-oceanic subduction (with P-T conditions around 700°C-0.7 GPa) and evidence for subordinate intra-oceanic slicing, (2) constrain the extent of burial in sedimentary basins through estimation of their maximum temperatures (~250°C, via RAMAN spectroscopy on organic matter)and (3) document an older, much higher temperature event affecting former sediments of the Lut block (which we tentatively relate to the rifting stage). Petrological investigations on magmatic rocks reveal that (1) the ophiolite structure is that of an ultra-low spreading ocean and that (2) Upper Cretaceous magmatic rocks located on the Afghan block correspond to a calc-alkaline low-K magmatic arc associated with north-east dipping subduction.

These structural and petrological data, together with those of previous studies, allow to propose a refined geodynamic evolution for Northern Sistan, whose main stages are: a rifting stage prior to the Barremian, active spreading during the Aptian-Albian, onset of NE-dipping subduction during the Turonian, intra-oceanic subduction and inception of obduction during the late Campanian to Maastrichtien and onset of 'soft' collision during the early Eocene. Soft collision, together with ongoing mostly strike-slip deformation since the mid-Miocene,

make Northern Sistan a key, well preserved, ‘frozen-in’ example of the progressive evolution from subduction to collision.

The Eocene to Oligocene High-K intrusions in Lut block-East of Iran: implication of Eastern Iran Magmatic Belt's tectonomagmatic evolution

Omidianfar, S.[1], Monsef, I.[2], Rahgoshay, M.[1], Zheng, J.[3] and Cousens, B.[4]

[1]Faculty of Earth Sciences, Shahid Beheshti University, Tehran, Iran
[2]Department of Earth Sciences, Institute for Advanced Studies in Basic Sciences (IASBS), Zanjan 45137-66731, Iran
[3]State Key Laboratory of Geological Processes and Mineral Resources, School of Earth Sciences, China University of Geoscience, Wuhan, China
[4]Ottawa-Carleton Geoscience Centre, Department of Earth Sciences, Carleton University, 1125 Colonel By Drive, Ottawa, ON., K1S 5B6,Canada

The studying intrusion is well-exposed in the south Birjand around the Koudakan which herein compared to previously studied outcrops along the Eastern Iran Magmatic Belt. This pluton is composed mainly of diorite, monzodiorite, tonalite, granodiorite, and granite with high-K calcalkaline to shoshonitic affinities. The U-Pb zircon geochronology from monzodiorite and tonalite rocks reveals the crystallization ages of 41.7 ± 3.4 to 37.88 ± 0.77 Ma (Bartonian). The chondrite and primitive mantle normalized rare earth and trace elements patterns show enrichment in the light rare earth elements, K, Rb, Cs, Pb, Th, and U and depletion in heavy rare earth elements, Nb, Zr, and Ti. The studying samples have low values of εNd(i) (+1.32 to +1.68), and high 87Sr/86Sr(i) ratios (0.7044 to 0.7047) indicating mantle derived melts isotopically similar to the Island Arc Basalts (IAB). These isotopic and geochemical signatures indicate an enriched mantle source for these rocks and thus indicate a contribution of subducted slab component to their mantle source. Additionally, the Nd-Sr isotopic modeling suggests less assimilation (~ 5 to 10%) of upper continental crust by juvenile mantle melts. Our new geochemical, isotopic, and geochronological studies plus taking into account other regional geological evidence indicate that the Koudakan intrusion like other Eocene to Oligocene granitoids in Lut block formed in a post-collisional tectonic environment. We suggest northeastward subduction of the Neo-Tethys Ocean beneath the Lut block caused the mantle wedge to be enriched by the slab components. At a later stage, a collision between the Lut and Afghan blocks was accompanied by lithospheric delamination, and subsequent asthenospheric upwelling led to melting of metasomatized mantle and generation of Eocene to Oligocene intrusive bodies in the Eastern Iran Magmatic Belt.

Middle Jurassic compressional to extensional tectonics of the Sanandaj-Sirjan magmatic arc revealed by S-type granites

Maghdour-Mashhour, R.[1] & Ali Tabbakh Shabani, A.[2]

[1]School of Geosciences, Faculty of Science, University of the Witwatersrand, Johannesburg, South Africa
[2]Faculty of Earth Sciences, Kharazmi University, Tehran, Iran
E-mail: samer.mashour@gmail.com

The Sanandaj-Sirjan Magmatic Arc (SSMA) of Iran is situated in the southwestern margin of Eurasia. It is a NW trending orogenic belt mainly of Mesozoic age. Subduction initiation beneath the SSMA and consequent arc magmatism occurs in Jurassic. The first half of Jurassic is a time during which thick sequences ranging from continental to marine deposits and volcanic rich flysch are accommodated on the SSMA (Hassanzadeh and Wernicke, 2016). The mid-Jurassic is, on the other hand, represented by a peak in calc-alkaline arc magmatism which accompanies with polyphase metamorphism of magmatic and sedimentary succession in deep basins. The Jurassic deposits are reported to be overlain unconformably by unmetamorphosed Cretaceous limestones. In spite of a plethora of studies for almost half a century, the state of stress within the SSMA during the Jurassic has still remained elusive (Hassanzadeh and Wernicke, 2016) and no explanatory picture, to best of our knowledge, is available to our geological society. S-type granites in orogenic belts could be regarded as paleo-geodynamic black-boxes of the continental lithosphere. S-type granites herald the initiation of slab roll-back phase and subsequent extensional backarc systems. On the other hand, thickening of a preexisting, sediment-dominated backarc basin is a prerequisite for their generation (Collins and Richards, 2008). In this study, petrogenesis of two S-type granitoids from the peak magmatic phase (i.e. mid-Jurassic Kolah-Ghazi and Shir-Kuh S-type granitoids; KGG and SKG hereafter) are revisited to deduce the geodynamic evolution of the SSMA during the Jurassic. Both KGG and SKG consist of a complete compositional spectrum of typical S-type granitoids: granodiorite, monzogranite and syenogranite. It is interpreted by previous researchers (Bayati et al. 2017; Sheibi et al., 2010) that the leucocratic rocks evolved from more mafic parental magma through fractional crystallization. However, our detailed inspection on the trace element concentrations of these S-type granites exhibits positive correlation with maficity index (atomic Fe+Mg). This evidence along with the presence of the peritectic garnet and cordierite in mafic rocks (e.g. granodiorite) indicate that the leucocratic portions (syenogranite) of these plutons have not arisen through fractional crystallization of mantle-derived mafic magmas, as the syenogranite would have inherited the zircon-saturated character of the hypothetical earlier mafic magma (e.g. Villaros et al., 2009). In fact, the peraluminous, S-type KGG and SKG are the product of biotite incongruent melting of a metasedimentary crustal source. Syenogranites represent melts from the anatectic source and more mafic varieties such as granodiorites and monzogranites are typically saturated with regard to zircon and represent mixtures of melt and peritectic phase such as garnet. Disequilibrium melting and accessory phase entrainment in the source is a process that requires a metasedimentary source buried deep enough in the crust before anatexis. Flat subduction, subsequent backarc compression and structural thickening of previously formed back-arc turbidite deposits on the over-riding plate are envisaged to

provide an optimum depth for anatexis in arc environments. Therefore, we suggest that Jurassic evolution history of the SSMA had been dominated by extensional arc environment which interrupted by a compressional regime during the late mid-Jurassic.

KEYWORDS: S-type granite; Sanandaj-Sirjan Magmatic Arc; Iran

A new magmatic map of Iranian plateau as constrained by susceptibility map of Iran

Ghods, A.[1], Teknik, V.[1], and Monsef, I.[1]

[1]Department of Earth Sciences, Institute for Advanced Studies in Basic Sciences (IASBS), Zanjan, Iran

The Iranian plateau is one of the most complex geodynamic setting within the Alpine-Zagros-Himalayan orogenic belt. The subduction of Neo-Tethys Ocean is responsible for the formation of the Late Cretaceous Neo-Tethyan ophiolites and Cenozoic magmatic belts within the Iranian plateau. In this paper, we report a new method to track the Cenozoic magmatic flare-ups and Neo-Tethyan ophiolites by aeromagnetic data. We present a new map of crustal susceptibility calculated by a radially averaged power spectrum method. High susceptibility regions correlate with the outcrops of magmatic and ophiolitic rocks, and low susceptibility regions coincide with the sedimentary basins. Although, sedimentary cover impedes visual identification of the Northeast Iran Magmatic Belt and Eastern Iran Magmatic Belt, but we could trace these belts southwestward into the Great Kavir plain and southward into the Lut plain, respectively. We could also show that the trend of the Urumieh-Dokhtar Magmatic Belt does not continue directly towards its northern part and this trend jumps in arc-trench distance towards Alborz-Azerbaijan Magmatic Belt. The narrower width of the Urumieh-Dokhtar Magmatic Belt implies a steeper dip of the subducted slab (~ 60º dip) during Eocene to Oligocene time. By contrast, the wider width of the Alborz-Azerbaijan Magmatic Belt suggests a gentler dip of the subducted slab (~ 35º dip). Additionally, we can identify hitherto unknown two parallel arc-shaped magmatic and ophiolitic belts in eastern Iran named as the Southern and Northern Sistan Magmatic Belts.

Uncertainties in seismic sources and their effects of seismic hazard Analysis

Talebian, M.[1]

[1]Research Institute for Earth Sciences, Geological Survey of Iran

Uncertainties are unavoidable in design and planning of an engineering system. Therefore, the tools of engineering analysis often include methods and concepts for evaluating the significant of uncertainty on system performance. Probability is the conceptual and theoretical basis for modelling and analysing such uncertainties. A significant role of Probabilistic Seismic Hazard Analysis (PSHA) method lies in its unified framework for quantitative analysis of theoretical uncertainty and assessment of associated risk. However, less attention often paid to epistemic uncertainties associated with seismic sources. A simple way of taking into account such uncertainties is to define logic trees and quantify the uncertainty associated with the inputs to PSHA. However, there are many potential threats in setting up a logic tree, mainly related to the fact that in practice the weight associated with each branch is questionable.

Special care has to be taken to protect results from being biased by unreliable information. Unfortunately, it is very common to rely of earthquake catalogues for defining seismicity parameters. An incomplete catalogue, which covers short period of time comparing to return period of earthquakes, could highly mislead especially on defining frequency of larger events or the maximum expected magnitude. An example of such inconsistency is the north Tabriz fault which has no instrumental record of major activity despite showing high rate of slip. There are many statistical methods for evaluating maximum expected magnitude of earthquake. Output of such calculations may vary by about one unite depending on assumptions and quality of inputs. In addition, errors in locations of 30 kilometres or more are very common for earlier period of instrumental records, leading to misevaluation of seismicity parameters.

Geometry of both exposed and hidden faults have great effects on PSHA results. A structure located on hanging wall of a fault receive higher ground acceleration by factor of up to 2, comparing to those on footwall. Damage due to activation of a blind fault can occur in wider region (2-3 times) depending on depth and slop of the buried fault.

A very crucial character of an active fault is its slip rate. It is essential to define slip rate of the faults by geological and geodetic studies. Space based geodetic observations have potential to provide general pattern of movements, while Paleseismological studies often concentrate on more detailed activity of individual faults. It is important to accompany these studies with geomorphologic observations which present longer history of deformation.

Finally, in order to obtain a reliable seismic hazard analysis, it is important to exclude unreliable source of information from PSHA analysis and perform comprehensive multi discipline study of active sources.

Synthetic earthquake catalogs simulating seismic activity in NW Iran fault system

Rastbood, A.[1], Bulghar, R.[2], Ghanouni, B.[3] and Ghasemzadeh, A.[4]

[1]Assistant Professor, Tabriz University, Tabriz, Iran
[2]MsC Student, Tabriz University, Tabriz, Iran
[3] MsC Student, Tabriz University, Tabriz, Iran
[4] BsC Student, Tabriz University, Tabriz, Iran
E-mail: arastbood@tabrizu.ac.ir

The characteristic earthquake hypothesis is the basis of time-dependent modeling of earthquake recurrence on major faults. However, the characteristic earthquake hypothesis is not strongly supported by observational data. Few fault segments have long historical or paleo-seismic records of individually dated ruptures, and when data and parameter uncertainties are allowed for, the form of the recurrence distribution is difficult to establish. This is the case, for instance, of the North Tabriz Fault System, for which only few characteristic earthquakes are reported for individual fault segments. The use of a physics-based earthquake simulator has allowed the production of catalogs lasting 100,000 years and containing more than 500,000 events of magnitudes ≥ 4.0. The main features of our simulation algorithm are (1) an average slip rate released by earthquakes for every single segment in the investigated fault system, (2) heuristic procedures for rupture growth and stop, leading to a self-organized earthquake magnitude distribution, (3) the interaction between earthquake sources, and (4) the effect of minor earthquakes in redistributing stress. The application of our simulation algorithm to the NTF has shown realistic features in time, space, and magnitude behavior of the seismicity. These features include long-term periodicity of strong earthquakes, short-term clustering of both strong and smaller events, and a realistic earthquake magnitude distribution departing from the Gutenberg-Richter distribution in the higher-magnitude range. One of the main ingredients of our simulation algorithm is the imposition of an average slip rate released by earthquakes to each one of the segments recognized in the investigated fault system. This slip rate is derived from a combination of geological and geodetic observations, and in particular comparison of GPS measurements with old triangulations. Although no constraint is made to the propagation of the fracture across different segments during an earthquake, the result of the longterm slip released by the simulated seismic activity matches the imposed slip rate quite well. There are no intrinsic limitations in the model to adopt a continuous slip rate distribution instead of introducing discontinuities imposed by the fault system segmentation. The frequency-magnitude distribution of the earthquakes reported in our synthetic catalogs is consistent with the frequencymagnitude distribution obtained from real observations.

KEYWORDS: Earthquake Simulator Algorithm; Synthetic Catalogs

Slip distribution of two moderate earthquakes occurred in Iran from finite fault modeling

Bazargan, S.[1], Shomali, Z.H.[2,3], and Rezapour, M.[2]

[1]University of Zanjan, Department of Physics

[2]University of Tehran, Institute of Geophysics

[3]Uppsala University, Department of Earth Science

E-mail: bazargan.s@alumni.ut.ac.ir

The slip distribution of two moderate earthquakes occurred in Iran, the 2007 June 18 M_w 5.5 Kahak and 2010 September 27 M_w 5.9 Kazerun earthquakes, were estimated from regional broadband seismic data using constrained non-negative least squares linear slip inversion method. A rupture velocity of 2.8 km/s and rise time of 1.4 sec were utilized for the first event, and 2.5 km/s and 2.2 sec were used for the second one. Results show a rupture with peak slip of 8.0 and 35.0 cm for the Kahak and the Kazerun earthquakes, respectively. Because of the non-uniqueness of the inversion problem, a set of solutions was acquired for both events. To the best of our knowledge, this is the first time to consider linear finite-fault inversion procedure for moderate earthquakes of Iran to model a set of slip histories at regional distances.

KEYWORDS: finite-fault modeling, seismic data, slip inversion, the 2007 Kahak earthquake, the 2010 Kazerun earthquake

Introduction

The tectonic of Iran is governed by convergent plate collisions along the Alpine-Himalayan active belt (Berberian, 1981; Mirzaei et al. 1998). In this study, two earthquakes were chosen from the two main seismotectonic provinces of Iran. The first event is the 2007 June 18 Mw 5.5 Kahak earthquake, which occurred in the Central-East Iran seismotectonic province, in the vicinity of the Kahak district of Qom province. The other is the 2010 September 27 Mw 5.9 Kazerun earthquake situated in the Zagros seismotectonic province, near the Kazerun County. The purpose of this study is to acquire finite-fault modeling of the broadband three-component displacement waveforms of these earthquakes through a least-squares inversion method for the spatial and temporal slip distribution.

Data

The data used in this study obtained from the national broadband seismic network operated by the International Institute of Earthquake Engineering and Seismology of Iran (IIEES). These data consist of 21 waveforms for the Kahak earthquake and 23 waveforms for the Kazerun earthquake. The aftershocks of the corresponding earthquakes were taken from the catalog of the Iranian Seismological Center (IRSC). The observed waveforms were filtered

and decimated from the original 50 to 10 samples per second. The instrument responses were removed, and the data were then converted to displacement. A band-pass filter of 0.03-0.15 Hz for the first event and 0.05-0.07 Hz for the second one were applied to the displacement waveforms.

Model Parameterization

Green's functions were computed using the frequency-wavenumber integration code (FKRPROG) developed by Saikia (1994). Also, the inversion algorithm applied to the observed data is based on a stabilized constrained non-negative least-squares method introduced by Hartzell and Heaton (1983).

Fault and subfault sizes are the first parameters constructing our parameterization. We found that the equal-sized 1 km × 1 km subfaults for the first event and 2 km × 2 km subfaults for the second one accommodate all of the slip distribution inside the given fault plane. Also, different hypocenters reported by several seismological agencies, i.e., ISC, GCMT, USGS, and EMSC were tested. If one nodal plane generates a better fit to the data, then it can be construed as the fault plane (Abercrombie et al. 2001). With this in mind, the focal mechanism (strike, dip, and rake) of faults estimated by USGS and GCMT were tested to find the nodal plane with the best fit. The measure to choose the optimal result in all runs has been total variance reduction demonstrating the fit between observed and synthetic data as well as the final variance of the data misfit. For all hypocentral parameters of the Kahak earthquake, the inversion found better fits with strike equals to 266˚ nodal plane of GCMT; thus, this plane is the fault plane. For the Kazerun earthquake, GCMT focal mechanism having a fault plane (strike, dip, rake: 301˚, 6˚, 100˚) provides the maximum fitting percentage. Therefore, we used these nodal planes for the rest of the investigation.

The next important parameter is rupture velocity. The rupture velocity was assumed to be a constant fraction of the shear wave velocity at the source area, and we tested different values of this parameter in a range of 0.7 to 0.9 of the shear wave velocity. Stabilization constraints i.e. moment minimization and smooth weight are other parameters in the inversion that reduce instability or extreme complexity. To choose the optimal results, we tested different amounts of these constraints to find the best values that yield a smooth slip model with the minimum seismic moment (Hartzell and Heaton 1983).

The results for 2007 Kahak earthquake

The Kahak earthquake was chosen to be studied because there had not been any similar earthquakes bigger than that (Mw 5.5) in a distance less than 140 kilometers, affecting Tehran, the capital of Iran. The velocity model based on the study of Ashtari et al. (2005) was used for this event. ISC hypocenter provided the best fit to the observed data with a maximum total variance reduction of about 35 % for spatial and 54 % for spatiotemporal distribution (not shown here). Hence, it was chosen as the preferred slip model of the Kahak earthquake (Figure 1, top). Also, the rupture velocity of 2.8 km/s (78 percent of shear wave velocity at the source area) provided the best fit to the data. According to different inversion trials, optimum rise time was also chosen to be 1.4 sec.

The results for 2010 Kazerun earthquake

The 2010 Kazerun earthquake (Mw 5.9) has been the largest recorded earthquake in the Kazerun region since 2000, and its aftershocks did not exceed the magnitude 4.3. The best fit to the observed data (not shown here), with a maximum total variance reduction of about 52% was obtained with ISC hypocenter. The optimum rise time of 2.2 sec yielded the best fit to the data with maximum total variance reduction and minimum variance. Velocity structure based on the study of Hatzfeld et al. (2003) has been used for this earthquake and led to 2.5 km/s as the optimum rupture velocity.

Conclusion

This study presents a set of solutions for the Kahak and Kazerun earthquakes, and among them, the ISC hypocenter and GCMT focal mechanism give the best spatial and spatiotemporal distribution with maximum total variance reduction of 35% and 54%, respectively, for the first event (Figure 1, top) and 52.2% for the spatial distribution of the second event (Figure 1, bottom). According to the lots of inversion trials, rupture velocity plays an indispensable role in the slip inversion. The observed data were re-inverted for different rupture velocities. Figure 1 (right) shows analogies between the projected final spatial distributions on the Earth's surface with the aftershock distribution. The squares depict the whole region of the fault plane. Aftershocks are a phase of relaxing stress concentrations result from the mainshock (Scholz 1990), and occurred near the western end of the slip distribution for the Kahak event. There is also a predominance of aftershocks that surrounds the majority of the slip for the Kazerun earthquake. As a whole, for both events, the aftershocks distribute mostly outside of the asperity zone. Identical results have been acquired in a good many studies such as Reasenberg and Ellsworth (1982) and Doser and Kanamori (1986).

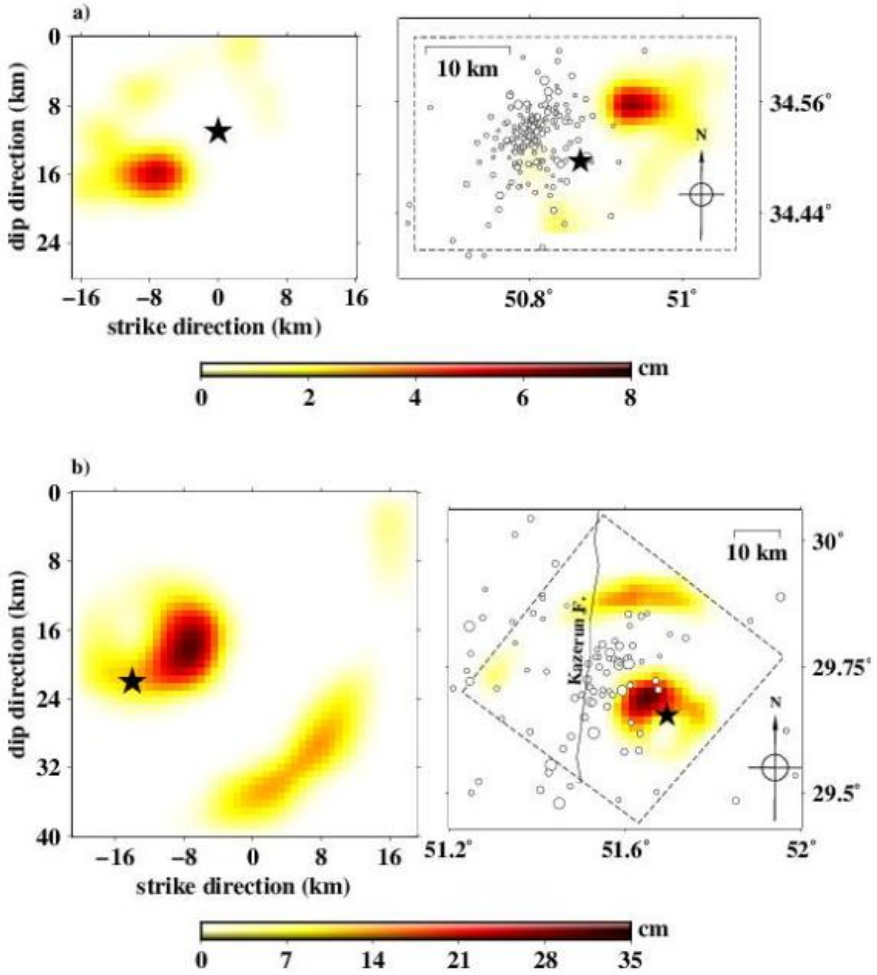

Figure 1. Slip distributions for the preferred finite-fault models for the a) Kahak and b) Kazerun earthquake in the latitude-longitude coordinate (right) and along strike-dip directions (left). Dashed squares (right) are presented the fault planes on the earth. Black stars show ISC hypocenters for both events. The white circles refer to the aftershocks which occurred during the three months after the mainshock. Generally, the aftershocks distribute outside of the asperity zone for both earthquakes. The peak slip value of the first and second event are 8.0 and 35.0 cm, respectively.

References

Abercrombie, R.E., Bannister, S., Pancha, A., Webb, T.H. and Mori, J.J. [2001] Determination of fault planes in a complex aftershock sequence using two-dimensional slip inversion. Geophysical Journal International, 146, 134-142.

Ashtari, M., Hatzfeld, D. and Kamalian, N. [2005] Microseismicity in the region of Tehran.

Tectonophysics, 395, 193-208.

Berberian, M. [1981] Active faulting and tectonics of Iran. Zagros Hindu Kush Himalaya Geodynamic Evolution, 33-69.

Doser, D.I., and Kanamori, H. [1986] Depth of seismicity in the Imperial Valley region (1977-1983) and its relationship to heatflow, crustal structure, and the October 15, 1979 earthquake. Journal of Geophysical Research: Solid Earth, 91(B1), 675-688.

Hartzell, S.H. and Heaton, T.H. [1983] Inversion of strong ground motion and teleseismic waveform data for the fault rupture history of the 1979 Imperial Valley, California, earthquake. Bulletin of the Seismological Society of America, 73, 1553-1583.

Hatzfeld, D., Tatar, M., Priestly, K., and Ghafory-Ashtiany, M. [2003] Seismological constraints on the crustal structure beneath the Zagros Mountain belt (Iran). Geophysical Journal International, 155, 403- 410.

Mirzaei, N., Mengtan, G., and Yuntai, C. [1998] Seismic source regionalization for seismic zoning of Iran: major seismotectonic provinces. Journal of Earthquake Prediction Research, 7, 465-495.

Reasenberg, P., and Ellsworth, W.L. [1982] Aftershocks of the Coyote Lake, California, earthquake of August 6, 1979: A detailed study. Journal of Geophysical Research, 87(B13), 10637-10655.

Saikia, C.K. [1994] Modified frequency-wave-number algorithm for regional seismograms using

Filon's quadrature–modeling of L(g) waves in eastern North America. Geophysical Journal

International, 118, 142–158.

Scholz, C.H. [1990] The mechanics of earthquakes and faulting. Cambridge University Press,

Cambridge.

Seismic imaging of the upper-mantle beneath the Zagros collision zone

Mahmoodabadi, M.[1], Yaminifard, F.[1,*], Tatar, M.[1], Kaviani, A.[2], Rümpker, G.[2], Motaghi, K.[3]

[1]Seismological Research Center, International Institute of Earthquake Engineering and Seismology, Iran.
[2]Institute of Geosciences, Goethe University, Frankfurt, Germany.
[3]Department of Earth Sciences, Institute for Advanced Studies in Basic Sciences, Iran.
*E-mail: faryam@iiees.ac.ir

One of the youngest orogenic belts, the Zagros orogeny in the northern margin of the Arabian plate is formed during Arabia-Eurasia collision. Despite a number of studies, many questions still remain open about the deep structure and dynamics of the collision zone. To figure out the dynamics of the collision, we have used different seismological methods to investigate the deep structure of the Zagros and its surrounding regions. First, to investigate upper mantle processes related to the collision, a proper dataset consisting of 32738 *P*-wave and 4629 *S*-wave relative arrival time residuals have been picked from distant earthquakes recorded in 129 seismic stations. The residual patterns are mapped as 3-D perturbations in *P*-wave (Mahmoodabadi et al. 2019) and *S*-wave velocity using a nonlinear teleseismic tomography method (Rawlinson et al. 2006). Then the lithospheric and uppermost mantle absolute *S*-wave velocity structure beneath the northern Zagros and western Central Iran is estimated by jointly inverting high frequency scattered wavefield observed in *P*-wave coda, together with long period surface wave phase and group velocity dispersion data (Rahimi et al. 2014) using a trans-dimensional Bayesian Markov Chain Monte Carlo approach (Bodin et al. 2012, 2014). To unravel the dynamical processes in the continental collision, it is important to figure out the accommodation of convergence and the flow behaviors in the upper mantle. We used an unprecedented dataset, consisted of 3260 core-refracted shear phases to probe the fast polarization directions and delay times of shear waves propagating through anisotropic structures beneath each seismic station using energy minimization of transverse components.
The absolute *S*-wave and relative *P* and *S*-wave velocity models, obtained by different data sets and methods, show a thick (>150 km) high-velocity anomaly beneath the northern part of the collision zone, which could be the thickened Zagros lithosphere that probably is responsible for active continental shortening. A relatively thin lithosphere (~80 km) and lower seismic velocity beneath the UDMA further NE may suggest that the lithospheric mantle of Central Iran and Alborz has been weakened by upwelling of the hot asthenosphere associated with slab break-off. Besides, the cumulative processes of Neotethyan flat-slab subduction in the middle of Cretaceous, mantle preconditioning by dehydration of subducted plate, slab roll back in the Eocene and tectonic erosion, driven by convective flow before the collision, are partially responsible for the weakened mantle lithosphere beneath the Alborz and Central Iran. The Quaternary volcanic activities in the Alborz could be the result of these processes. We observe a segment of Neotethyan oceanic slab, which is detached from the continental leading edge.
Our results suggest that the Arabian mantle lithosphere plays an important role in accommodating the convergence between the Arabian and Eurasian plates. High seismic activity to the west of the suture and lack of seismic activity to the east may support this hypothesis. Besides, the presence of a narrow low-velocity anomaly between the Zagros and

SSZ lithosphere may suggest that the mantle lithosphere lid of the Zagros is delaminating from the lower crust which prohibits transferring stress to the SSZ lithosphere causing lack of tectonic activities in the edge of the overriding plate. Shear wave splitting observations suggest that both lithosphere and asthenosphere have a contribution to the mantle anisotropy over the plateau. A simple asthenospheric flow cannot justify the mantle anisotropy data in the region. These observations show the possibility of a rotational flow around the Zagros lithosphere which may confirm its thickening and deformation. Our observations suggest that both simple-shear and pure-shear processes deform upper mantle beneath the Iranian plateau, and in some areas, crust and mantle are deformed coherently through these processes.

KEYWORDS: Continental collision, Joint inversion, Mantle dynamics, Seismic tomography, Shear-wave splitting, Zagros.

References

Bodin, T., Sambridge, M., Tkalčíc, H., Arroucau, P., Gallagher, K. & Rawlinson, N., 2012. Transdimensional inversion of receiver functions and surface wave dispersion. *J. Geophys. Res.***117**(B02), 301.doi:10.1029/2011JB008560.

Bodin, T., Yuan, H. & Romanowicz, B., 2014. Inversion of receiver functions without deconvolution. *Geophys. J. Int.*,**196**(2), 1025–1033, doi:10.1093/gji/ggt431.

Mahmoodabadi, M., Yaminifard, F., Tatar, M., Kaviani, A. & Motaghi, K., 2019. Upper mantle velocity structure beneath the Zagros collision zone, Central Iran and Alborz from nonlinear teleseismic tomography, *Geophys. J. Int.*, **218**(1), 414-428, doi:10.1093/gji/ggz160.

Rahimi, H., Hamzehloo, H., Vaccari, F. & Panza, G.F., 2014. Shear wave velocity tomography of the lithosphere–asthenosphere system beneath the Iranian Plateau, *Bull. seism. Soc. Am.*, **104**(6), 2782–2798.

Rawlinson, N., Reading, A.M. & Kennett, B.L.N., 2006. Lithospheric structure of Tasmania from a novel formof teleseismic tomography, *J. geophys. Res.*, **111**(B2), doi:10.1029/2005JB003803.

High resolution tomographic images of the lithospheric structure of the Iranian plateau

Irandoust, M.[1, 2], Priestley, K.[2], and Sobouti, F.[1]

[1]Department of Earth Sciences, Institute for Advanced Studies in Basic Sciences, Zanjan, Iran
[2]Bullard Laboratories, Department of Earth Sciences, University of Cambridge, Cambridge, UK
E-mail: m.ahmadzadeh@iasbs.acir

The Arabian-Eurasian collision is similar to the Indo-Eurasian collision which has formed the Himalayas and the Tibet, but the Arabian-Eurasian collisionis much younger, and studies of the Zagros Mountains and the Iranian Plateau can provide clues to understanding the earlier stages of continent-continent collision processes. We have studied the lithospheric structure of the collision zone in Iran and obtained a high-resolution 3D shear wave velocity (Vs) structure of the crust and uppermost mantleby joint inversion of fundamental mode Rayleigh wave group velocity and P receiver functions (PRF). The surface wave measurements for the periods range 5-70 s were extracted from two seismic data sets: ambient noise cross-correlations and regional earthquakes recorded on 109 and 156 broadband stations, respectively. From these measurements, we built Rayleigh wave tomographic maps including both isotropic and azimuthal anisotropic terms for fundamental mode group velocity. Then, PRFs calculated at 256 seismic stations were interpolated for a grid of 0.5° cell size, to conduct ajoint receiver function/surface wave dispersioninversion for a uniform distribution of nodes across Iran. The short period (<20 s) Rayleigh wave tomograms do not show aclear anisortopic pattern, but at longer periods, the southern Zagros, central and eastern Iran, and Kopeh-dagh show almost NE-SW anisotropictrends, while the northern part of Zagros shows a NW-SE trend and anE-W orientation is dominant in the Alborz and NW Iran. The low Vs anomalies of the upper crust correspond to regions ofthick sediments such as theZagros fold-thrust belt, theMakran accretionary wedge, the South Caspian Basin, and the central desert of Iran. The velocity structure of southernZagros is almost homogeneous atall levels of the crust, but the low Vs anomaly beneath theLurestan separates the central Zagros from the northernmost Zagros. The underplating of the Arabian Plate below the main faults of theZagros (MRF and MZT) causing exhumation of crystalline rocks of the Sanandaj-Sirjan Zone (SSZ), is one of the visible geodynamic structures of ourmodel. The high-velocity structures of Central Alborz and Kopeh-Dagh area testament to their thickened crystalline crust. From the strong gradients of the Vs at the crust-mantle boundary, we determine a new Moho map for Iran (Fig. 1). There are strong correlations between thevariationsof topography, crustal thickness, Bouguergravity anomaly, and the distribution of the major fault systems across the Iranian Plateau. While the thickest parts of the crust are located under the collisional belts of the Iranian plateau comprising the high Zagros, SSZ, Talesh, Alborz, and Kopeh-dagh (>55 km), the regions of low deformationsuch as the Central Iran and the Lut block, and also the regions of younger and active deformation such as the Makran wedge and the simply folded belt of Zagros show the crustal thickness less than 45 km.

KEYWORDS: Iranian Plateau; Receiver function; Shear wave; Surface wave; Tomography; Moho depth.

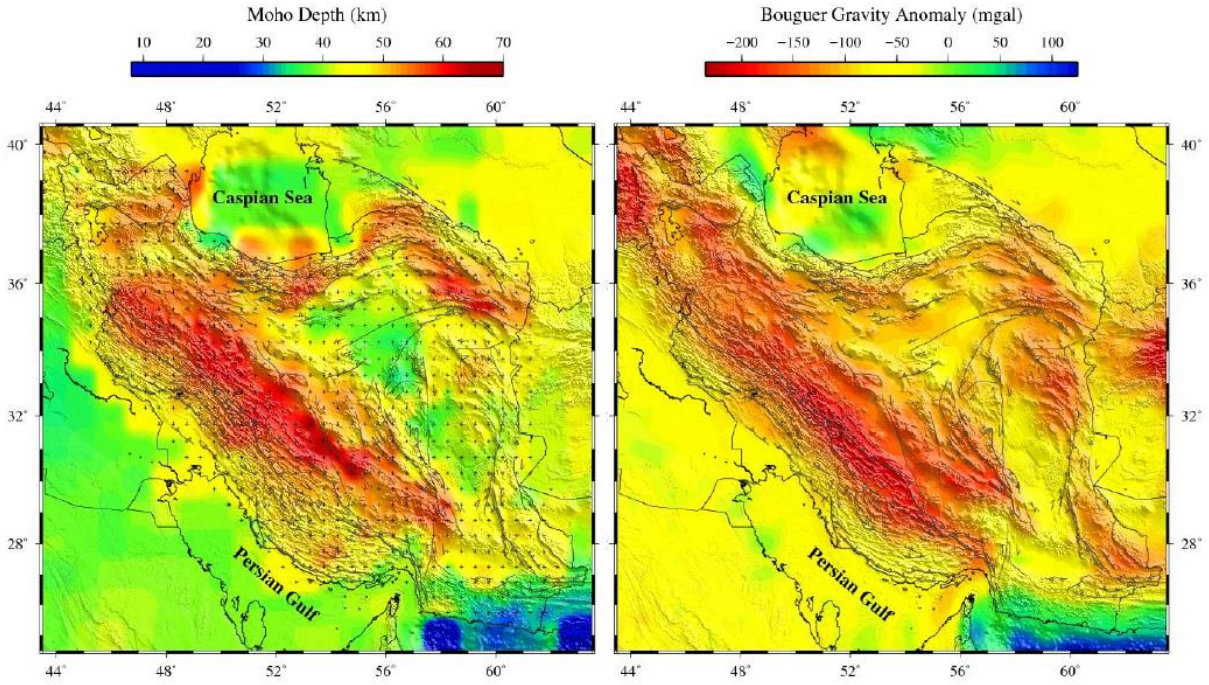

Figure 1) Left panel: Variations of the Moho depth across the Iranian plateau. The plus signs indicate the points at which we measured the Moho depths in this study. The values of the surrounding area are from the Crust1.0 model (Laske et al 2013). Right panel: Variations of Bouguer gravity anomaly (Zingerle et al 2019) in Iran.

References

Laske, G., Masters., G., Ma, Z., and Pasyanos, M., 2013, *Update on CRUST1.0 -A 1-degree Global Model of Earth's Crust*, Geophys. Res. Abstracts, 15, Abstract EGU2013-2658.
Zingerle, P., Brockmann, J.M., Pail, R.; Gruber, T., and Willberg, M., 2019, *The polar extended gravity field model TIM_R6*,doi: 10.5880/ICGEM.2019.005.

Surface wave tomography of Rayleigh waves using the STP method in Iranian Plateau

Mohammadi, N.[1, 2], Gholami, A.[1], Rahimi, H.[1], and Aoudia, A.[2]

[1]Institute of Geophysics, University of Tehran, Tehran, Iran

[2]Earth System Physics Section, Abdus Salam International Centre for Theoretical Physics, Trieste, Italy.

E-mail: rahimih@ut.ac.ir

Two dimensional surface wave travel time tomography is one of the most practical methods to image the lateral variation of phase/group velocity. Although 2-D inversion is numerically efficient, it does not consider the temporal dependency between periods and thus can lead to a suboptimal phase/group velocity. To address this issue, we propose Simultaneous Tomography of all Periods (STP) method. We consider the model parameters as a 3-D volume of dimensions x, y and T, where the first two parameters are related to spatial location of cells and T denotes period. Therefore the minimization problem is written as:

$$\min\|\mathbf{d}-\mathbf{G}\mathbf{m}\|_2^2+\lambda\mathrm{Reg}(\mathbf{m}) \tag{1}$$

Where $\mathbf{d}\,\epsilon\,\mathbb{R}^M$ includes the data corresponding to all periods and is obtained by concatenating travel times related to all periods one after another. Similarly, the model vector $\mathbf{m}$ is formed by concatenation of $\mathbf{m}_j$ associated with each period and $\mathbf{G}$ is the total sensitivity matrix corresponding to all periods:

$$\mathbf{d}=\begin{bmatrix}\mathbf{d}_1\\ \mathbf{d}_2\\ \vdots\\ \mathbf{d}_j\end{bmatrix}\epsilon\,\mathbb{R}^N,\qquad \mathbf{m}=\begin{bmatrix}\mathbf{m}_1\\ \mathbf{m}_2\\ \vdots\\ \mathbf{m}_j\end{bmatrix}\epsilon\,\mathbb{R}^N,\qquad \mathbf{G}=\begin{bmatrix}\mathbf{G_1} & 0 & 0 & \cdots & 0\\ 0 & \mathbf{G}_2 & 0 & \cdots & 0\\ 0 & 0 & \mathbf{G}_3 & \cdots & 0\\ \vdots & \vdots & \vdots & \ddots & \vdots\\ 0 & 0 & 0 & \cdots & \mathbf{G}_j\end{bmatrix}$$

In Eq. (1), Reg is the regularization functional and which plays a key role in this paper because it is responsible for coupling the model parameters along the period. We consider two types of the regularization in this paper: the traditional Tikhonov regularization (Tikhonov & Arsenin 1977) and sparsity-promoting regularization. The former is used to generate a flat model by minimizing the squared l2-norm of the model gradient while the latter is used to force the sparsity of the model in the discrete cosine transform (DCT)

domain. Furthermore, we employ the split Bregman technique (Goldstein & Osher 2009) to solve the minimization problem described by eq. (1) with the l1-norm regularization. The performance of the proposed tomography methods is shown by applying it on both synthetic and real group travel time data and then the results are compared with those obtained from the 2-D tomography method. Figure 1 shows the synthetic group velocity tomography results obtained from all tomography methods used in this study at period 30 s at noise level 10%. It can be seen that the results of STP methods, particularly the sparse STP, are more similar to the main model in comparison to the 2-D tomography. We also tested the proposed method on real data including group velocity dispersion curves extracted from the local earthquakes distributed inside Iran in the period of 2005-2016 and (Ms) range of $5 \leq Ms \leq 6.5$ recorded by the 19 broad-band stations of IIEES. Our results show that at periods less than 40 s with sufficient ray path number, there are trivial differences between tomography images obtained from the 2-D tomography and the smooth STP, while the tomography results of the spars STP reveals more details and localizes similar features better. At longer periods, generally, STP using DCT-sparsity regularization method resolves finer structures in a larger velocity variation.

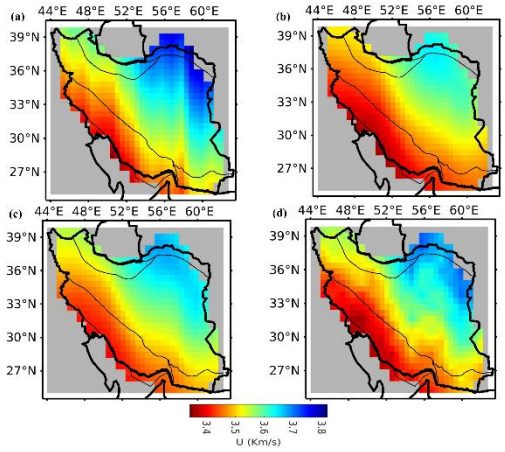

Figure 1. Synthetic group velocity tomography maps for period 30 s and noise level of 10%. (a) The main synthetic group velocity model. (b) Tomography map obtained by the 2-D tomography. (c) Tomography map obtained by the smooth STP method. (d) Tomography map obtained by the sparse STP method.

In order to show how much each method affects the shear wave velocity model, using a non-linear inversion based on Monte carlo search, we inverted local disperion curves estimated by the all methods along a pofile studied by Motaghi et al., 2015 and compared the results with their shear wave velocit model. They reported two low velocity anomalies beneath Cental Iran that these are also visible in the shear velocity model obtained from local dispersion curves calcultaed from the 2-D tomography with much more absolute values. However, shear wave velocity models extracted by the STP methods show that they, particularly the sparse one, are more able to reveal these low velocity anomalies.

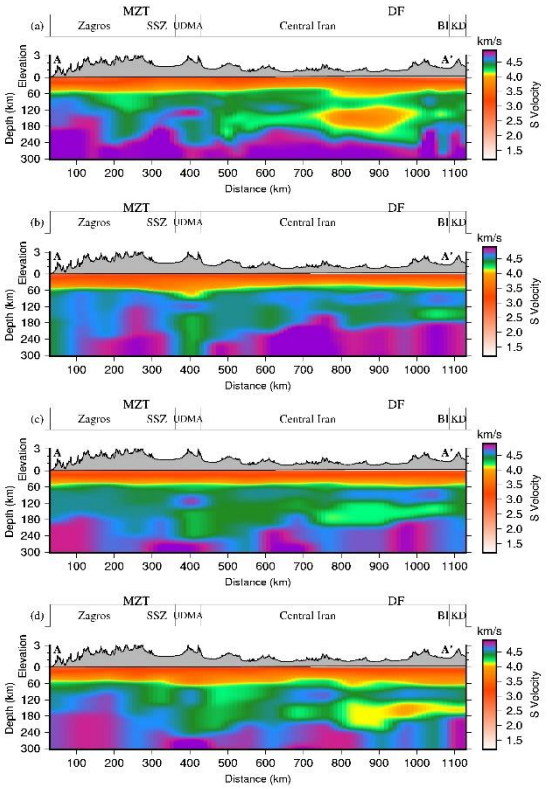

Figure 2. The lithosphere-asthenosphere beneath profile AA' (a) the result presented by Motaghi et al. 2015, (b-d) shear wave velocity models obtained from 1-D inversion of dispersion curves estimated by the 2-D tomography, the smooth STP and the sparse STP, respectively.

KEYWORDS: Inverse theory, Seismic tomography, Surface waves and free oscillations.

3-d modeling of the Tehran alluvial deposits using Active and Passive Measurments: Premilinary results of Tehran experiments

Soltani, S.[1, 2], Haghshenas, E.[1], Guillier, B.[2] and Cornou, C.[2]

[1]International Institute of Earthquake Engineering and Seisomlogy, Tehran, Iran
[2]ISTERRE, Grenoble, France
E-mail: s.soltani@iiees.ac.ir

Tehran is located in the Southern part of the central Alborz, the region with very high seismicity due to the existence of several large active faults. On the other hand, the city is built on a very thick alluvial deposits coming from the Alborz Mountains Range.

Large thickness of quaternary alluviums alongside with lateral discontinuities caused by faulting and folding in the alluvial units increases the possibility of multidimensional effects.

Haghshenas (2002), by using the data of a temporary seismologic network and applying experimental methods, showed a significant amplification of ground motion for Tehran alluvial deposits in a wide frequency range. Moreover the multidimensional effects are indirectly supported by the significant difference observed between the SSR and the HVSR results. With these conditions it is necessary to define the geometry and properties of the Tahran alluvial basin in order to predict a more realistic surface ground motion for future earthquakes.

Since the impact of an earthquake is strongly linked to the shear waves velocity in the subsurface structure we started to evaluate 3-d shear wave velocity model of the Tehran‘s alluvial deposits using Active and Passive measurements. The large number of datasets and different methods used in this study will enable us to develop this model. We deployed 22 small to medium arrays to define locally the velocity profiles as well as numerous HVSR measurements. We also measured seismic surface waves generated from active source (MASW method) to provide an experimental dispersion curve over a broad frequency band from surface to maximum reached depth.

The preliminary results confirmed the gradient increase in shear wave velocity in depth that could be explain the failure of the HVSR method in Tehran (figure 1).

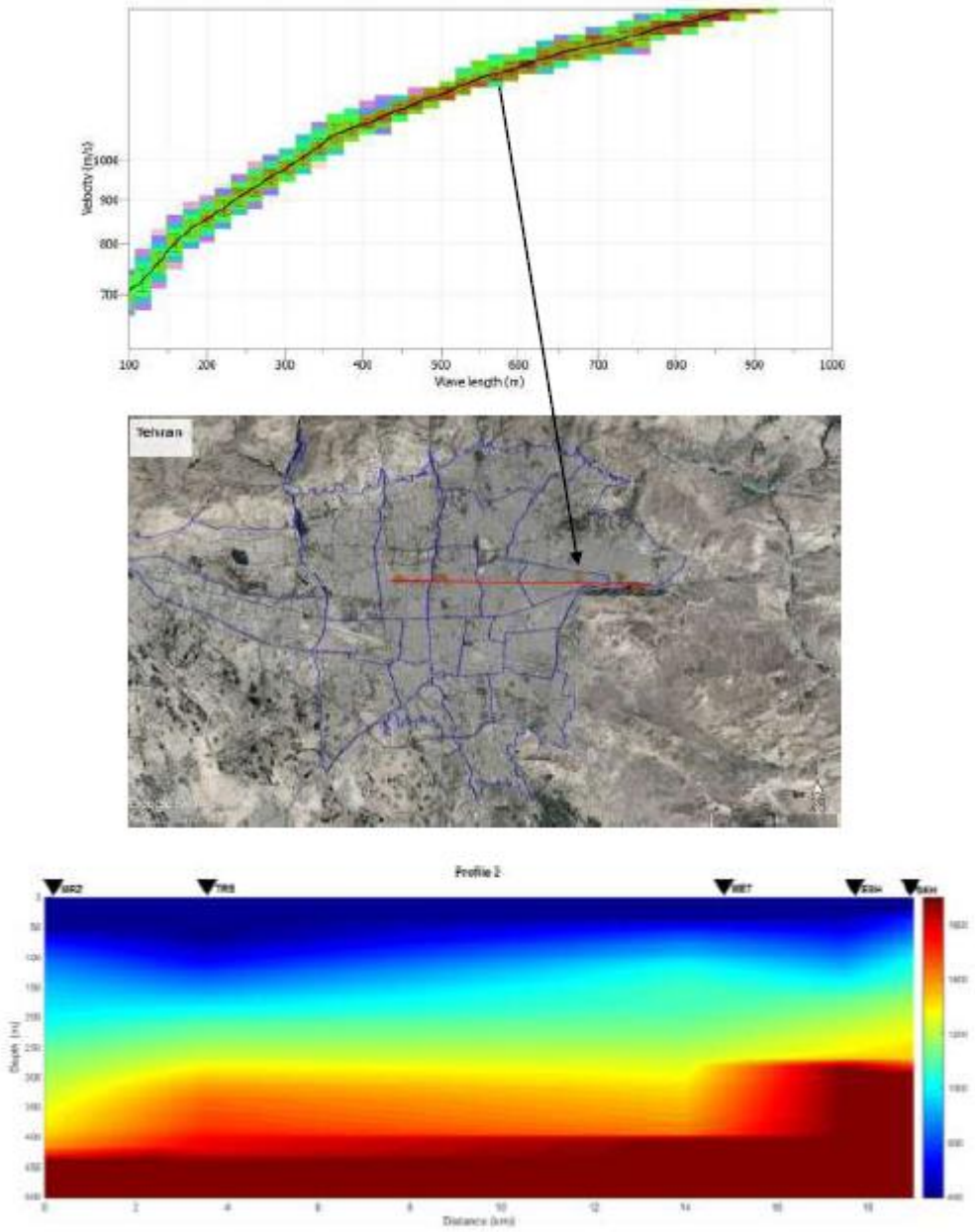

Figure 1: Up- Velocity – wavelength dispersion curve for MET Station. Middle - 2D arrays section. Bottom - an example of 2D velocity – wavelength profile (west east profile)

Institute for Advanced Studies
in Basic Sciences
Gava Zang, Zanjan, Iran

Poster Presentations

سازمان زمین‌شناسی کشور
GEOLOGICAL SURVEY OF IRAN
SORBONNE UNIVERSITÉ
cnrs

Paleoenvironments and chronology of the late Miocene Maragheh Formation, northwest Iran

Kaakinen, A.[1], Salminen, J.[1], Sakai, T.[2], Mirzaie Ataabadi, M.[3*], and Paknia, M.[4]

[1]Department of Geosciences and Geography, University of Helsinki, Finland
[2]Department of Geoscience, Shimane University, Matsue 690-8504, Japan
[3]Department of Geology, Faculty of Science, University of Zanjan, Iran
[4]Department of Science, University of Roma Tre, Rome, Italy
*Email: majid.mirzaie@znu.ac.ir

The terrestrial sequence in Maragheh (NW Iran) is a world-famous source of late Miocene fossil mammals, critical to our understanding of the late Miocene faunal and environmental evolution and dispersal patterns. While the sequence has been collected and studied sporadically over the last 150 years, the ages of the Maragheh faunas remain controversial. We present new high-resolution magnetostratigraphic records from the Dareh Gorg section, east of Maragheh town, which provide age constraints for the mammal assemblages in the middle Maragheh Formation. The correlation to the geomagnetic polarity time scale (GPTS) is based on the succession of magnetozones, paleontological constraints and recent K-Ar age determinations from this sequence, enabling a fairly unambiguous correlation of the local magnetozones to the GPTS. As a result, the recently discovered and preserved locality (field museum) is correlated to the upper part of the normal polarity chron C4n.2n (7.695–8.108 Ma). Based on the detailed sedimentological investigations, nine lithofacies are identified. The lithofacies associations are interpreted as emerging from a fluvial depositional system with occasional hyperconcentrated floods. Lithologically, the formation is dominated by fine-grained over bank deposits, including paleosols and laminated lake/pond sediments. Combined evidence from sedimentology and faunal studies suggest a seasonal climate and a mosaic vegetational habitat.

KEYWORDS: Maragheh Formation, late Miocene, mammals, magnetostratigraphy, Sedimentology

A tide-dominated delta from the upper Jurassic/lower Cretaceous of Central Iran

Sharafi, M.[1], Janocko, J.[2], Prekopova, M.[2], and Mirzaie Ataabadi, M.[3*]

[1]Research Institute of Petroleum industry, Tehran, Iran
[2]Institute of Geosciences, Faculty BERG, Technical University in Košice, Slovakia
[3]Department of Geology, Faculty of Science, University of Zanjan, Znjan, Iran
* Email: majid.mirzaie@znu.ac.ir

The upper Jurassic-lower Cretaceous Bidu Formation (also known as red beds or red series) deposits are distributed substantially in Kerman (and Tabas) basins of central Iran. In the Ab Bid area of the northern Kerman (south of Ravar), a ca. 400m thick section of this formation has been studied. It consists mainly of alternation of thick red shales and thick bedded sandstone units that display thickening and coarsening up-ward cycles. Detailed sedimentological and ichnological analysis allows recognition of four facies associations including playa (FA), delta plain (FB), upper distributary channels (FC), and delta front (FD). Playa facies association consists of evaporite layers and thin-bedded sandstone and siltstone. Delta plain facies association consists of the thick red shale intercalated with current and climbing ripple sandstone (Scr), trough cross bedded sandstone (St) and horizontal laminated sandstone (Shl), as well as *Ophiomorpha nodosa* and *Taenidium barrette* ichnofossils. Distributary channel associations include channel shape, thick sandstone units with trough and planar cross bed (St and Sp) and ichnofossils such as *Taenidium barretti*, *Ophiomorpha nodosa* and *Arenicolites*. Delta front association consists of the amalgamated sandstone unites with trough and planar cross bed (St and Sp), herring bone and tide bundles, as well as *Taenidium barretti*, *Ophiomorpha nodosa*, *Arenicolites* and *Skolithos* ichnofossils.

KEYWORDS: Red series, Bidu Formation, Central Iran, Kerman, tide-dominated delta, trace fossils

Kinematic analysis of the Qolqoleh-Kesnezan shear zone using shear indicators

Heydari, M.[1], and Behyari, M.[2]

[1]MSc student in Tectonics, Geology Department of Urmia University, Iran
[2]Assistant Professor of Geology Department of Urmia University, Iran
Email: mheydari3312@gmail.com

Qolqoleh-Kesnezan area is located in the NW Sanandaj-Sirjan zone. The Sanandaj-Sirjan zone is structurally active and is considered as an active margin and part of the Alpine-Himalayan orogenic belt. Also, this zone has high potential for gold mineralization which is of the type of shear zones. In this geological setting, two types of ductile and brittle mineralization have been identified according to geological and structural studies. Shear zones affect most of the rocks in the area. The brittle structures are comparable in scale from the fault to the joint and fractures studied and have affected the structures formed during the previous plastic deformation. The shear zones with ductile structural changes contain microstructures that show the bearing and direction of the mesoscopic and microscopic scales. Severs indicator of shear zones such as shear-band geometry (S-C fabric), porphyroclast tails and folding (kink band and chevron folds) have been identified at various points and used in kinematic analysis of these zones. These indicators show the direction of left-lateral shear in the region, which is along the main fracture trend in the region. Also, these areas are prone to mineralization, and geological structures must be considered for mineral exploration.

KEYWORDS: Qolqoleh-Kesnezan shear zone; Sanandaj-Sirjan zone; shear indicators; kinematic analysis.

Cyclostratigraphy and the effect of sequence stratigraphy on reservoir quality of the Kangan formation in the gas field of the Tabnak anticline, SW Iran

Nikbin, M.[1], Khanehbad, M.[1], Mussavi-Harami, R. [1], Mahboubi, A.[1], Khoddami, M.[2]

[1] Department of Geology, Faculty of Science, Ferdowsi University of Mashhad, Mashhad, Iran
[2] Iranian Central Oil Fields Company, Tehran, Iran
E-mail: (Mohammad.Nikbin@mail.um.ac.ir)

The Kangan Formation (Early Triassic) is one of the most important gas reservoirs in the Zagros fold-thrust belt. The study area is located in the west of the Hormozgan Province and on the Gavbandi highland. This field is one of the important gas production anticlines in the SW Iran. The sequence stratigraphy studies are based on seismic data segregation, outcrop observation, and study of thin sections related to cores and cuttings and study of petrophysical logs. The sequence stratigraphy studies in subsurface sections to identify sedimentary sequences of a well is not easy always, because many wells do not have core or are not continuously extracted from them. It is also difficult to study of cutting, especially when samples intervals are high, but well logs are available for almost all wells. In the absence of core and cutting data, these graphs (well logs) are useful tools for investigating sequences. One of these logs is the gamma ray log that petroleum geologists use to differentiate reservoir zones as well as adaptation between different wells in a field. The cyclolog software to use of gamma ray log and analyze it, providing a log that the sequence surface are completely separated and easy to identify, as well as easy matching of identified surfaces. Input data are cyclolog software, raw data of resistivity, gamma ray, neutron, density and son ic logs. But since diagenesis has less effect on the gamma log, it is used more frequently. The cyclolog software creates a log to called INPEFA (Integrate Predicate Error Filter Analysis). The basis of this log is that wavelet analysis is performed in a window of specified length specified by the user. Then, based on the results, the trend of the log is then aggregated into the next predicted stage and their trend is shown as a graph. According to the general principles and methods of sequence stratigraphy, the Kangan Formation using facies features and their equivalence with petrophysical logs, especially gamma ray log, the parasequenes accumulation pattern, sequence boundaries and their relationship with surface fluctuations seawater has led to the identification of two third-order sedimentary sequences (at the time of the formation of the third-order cycles, sea-level changes are global and not dependent on local variations) with type-II sequence boundaries. The basis for the determination of sedimentary sequences in this study is the INPEFA log obtained from the cyclolog software. Considering the trend of the curve in the wells of the gas field studied and changing the range of this curve, positive and negative trends and according to which stratigraphic boundaries (sequence boundaries and maximum flooding surface) are identified. Each sequence consisted of one positive boundary surface (match to the sequence boundary) and one negative boundary surface (match to the maximum flooding surface) and in total two wells (wells "A" and "B") was identified six positive boundary surface and four negative boundary surface. By integrating relatively more complete data from the petrographic study of well-B, the classification of each system tract was accurately verified.
As in this well, each sequence has been identified from the transgressive system tract (often

Including tidal flat and lagoon facies) and the highstand system tract (often including shoal facies) in the studied sedimentary system. However, due to the lack of complete access to all the thin sections of well-A only with the trend of the INPEFA log and gamma ray matching with well-B, the system tract and sedimentary sequences of the Kangan Formation in this section of the field have been studied and adapted. The sequences studied usually begin with transgressive system tract (TST), followed by transitional surfaces of maximum flooding surface (mfs), and finally to highstand system tract (HST). Generally, according to the thin-sections from the two wells studied and the software output well data, the sequences identified were from bottom (border with the Dalan Formation), upwards (border with the Aghar-shale member of the Dashtak Formation) are named "Sq-I" and "Sq-II", respectively.
The relationship of sequence stratigraphy with reservoir properties is investigated in relation to two main processes controlling; the porosity and permeability, namely facies distribution in sedimentary and diagenesis environments. The sequence stratigraphy emphasizes the role of sedimentary environment conditions in reservoir quality control and assesses the conditions for the development of reservoir-prone sediments regardless of the changes that the facies undergoes after deposition. Investigating the relationship between the reservoir quality of a Formation and the distribution of sedimentary facies using sequence stratigraphy concepts helps to understand the relationship between relative fluctuations in seawater in the Formation of reservoir-prone and non-prone facies, and therefore, these studies are essential for hydrocarbon reservoirs. In the Kangan Formation, highenergy facies of grain-supported (peloid and ooid grainstone) are more abundant than facies of lowenergy environmets of mud-supported (mudstone and bioclast wackestone), resulting in the formation of high-expansion reservoirs and high reservoir quality in this formation. In the two wells studied, especially well-B, according to petrophysical graphs, especially the effective porosity curve incremental trend, high reservoir horizon is located at the end of the transgressive system tract and the lower part of the highstand system tract is "Sq-II" sequence, which according to the above, it is fully compatible with the high quality grain-supported facies of the shoal environment. In these sequences, the quality of the reservoir is largely dependent on the pattern of distribution of facies and sedimentary texture created, and good reservoir units are due to the expansion of high porosity grainstone units. The mud-supported facies due to lack of porosity and high permeability, either lack reservoir quality or have low reservoir quality. These facies are related to low-energy environments and are formed in two positions; either at sea-level drop which reduces the accumulation space of the sediment or at high sea-level rise which results in excessive accumulation space and it forms the facies of deep areas. In the first sequence of well B, the transgressive system tract is related to garin-supported facies of shoal, but probably due to the influence of diagenesis processes, especially cementation and compaction, causes horizontal formation of undesirable reservoir quality. Considering the similarity of the separation parasequence of the two wells and considering the difference in thickness, the above points can be applied to well-A based on its output data

KEYWORDS: Cyclolog, Kangan Formation, Reservoir quality, Sequence stratigraphy, Tabnak Anticline.

Provenance and Tectonic Setting of the Oligocene–Lower Miocene Syntectonic Deposits in the Mahneshan Area, Central Iranian Basin

Alimola, Z.[1*], Etemad-Saeed, N.[2], Najafi, M.[2], Karimi, S.[3]

[1]Master of Tectonics of Institute for Advanced Studies in Basic Sciences (IASBS)
[2]Assistant Professor of Institute for Advanced Studies in Basic Sciences (IASBS)
[3]Bachelor science student, University of Zanjan (ZNU)
E-mail: zainab.alimoula@yahoo.com

The Mahneshan Basin is one of the Cenozoic syntectonic sedimentary basins in the north west of the Central Iran, which is located between the western Alborz Mountains and the Takab Complex (Fig. 1A; 1B). The aim of this study is to constrain the provenance and tectonic setting of the Oligocene-Miocene clastic sediments comprising the Lower Red (Orb and Org Members) and Qom formations in the Mahneshan Basin (Fig. 1c).

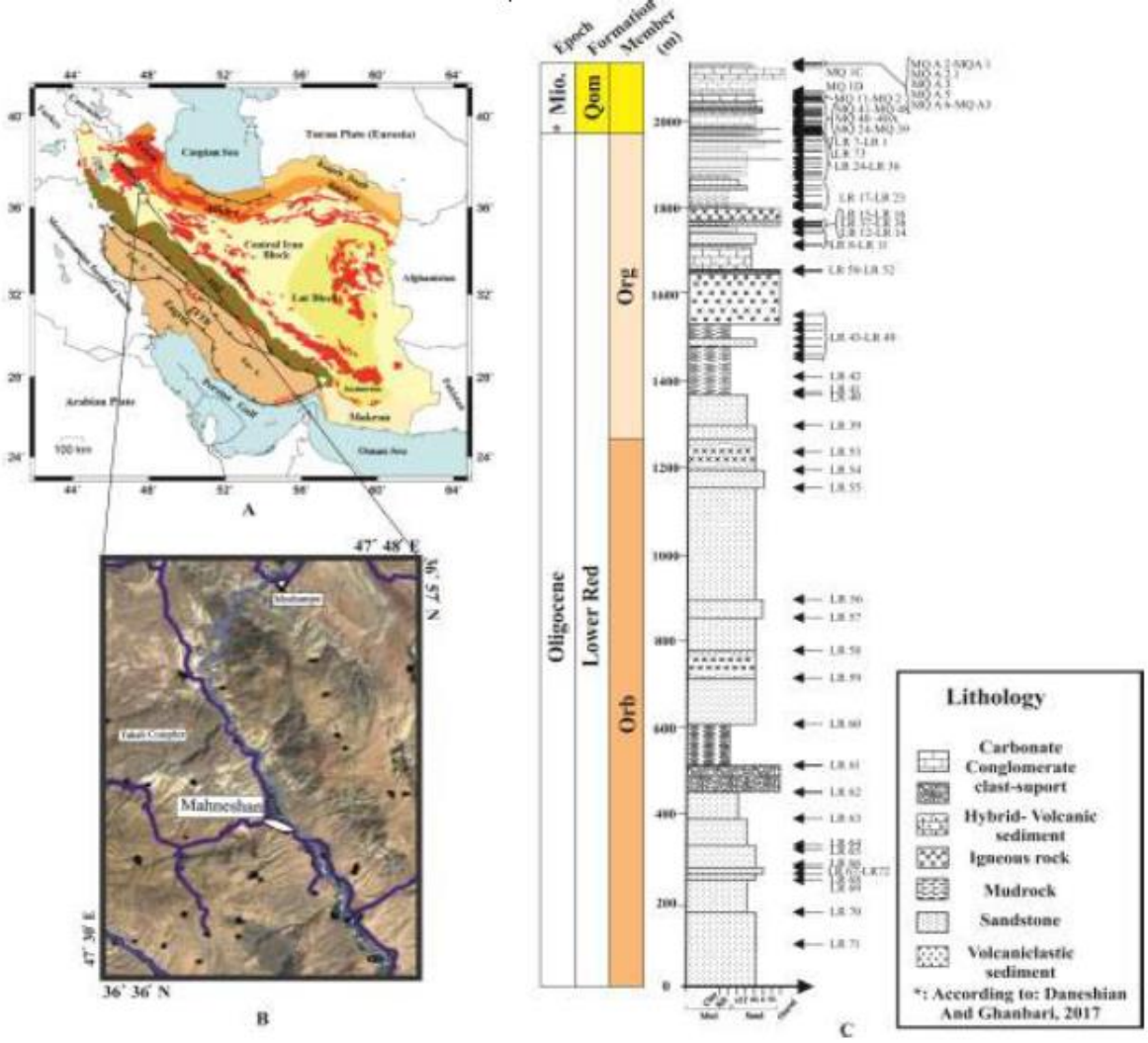

Fig. 1. (A) geological map of the Iran (Afsari et al., 2012) and (B) google earth Image from study area; (C) Stratigraphic column of the Cenozoic sedimentary basins in the north west of the Mahneshan

This well-preserved sedimentary archive provides an opportunity to examine tectono-sedimentary evolution of the Arabian-Euarasian collision zone. A combination of remote-sensing and field mapping of fault kinematics, fold geometries, growth strata patterns and unconformities allowed us to construct a structural cross-section across the Mahneshan Basin and the Takab Complex. The studied succession is composed of about 2.5-km-thick of predominantly sandstone, hybrid carbonate-volcaniclastic, volcaniclastic, and minor carbonate rocks. About 160 samples were collected from the Lower Red (Orb and Org units) and the Qom formations in this section. Standard microscopic thin sections were prepared from all samples and polarized microscopic petrography studies were performed at Institute for Advanced Studies in Basic Sciences. The modal analysis was performed by counting 300 points on 49 thin sections using the Gazzi-Dickinson method (Ingersoll et al., 1984).

In addition, petrography and modal analysis of sandstones were combined with Paleocurrent directions to define the exhumation history of source regions. Petrographically, the sandstones are poorly to well sorted lithic arkose to feldspathic volcanic arenite with average compositions of Q10F52RF38, Q8F46RF46, and Q5F35RF60 in the Orb and Org members and Qom Formation, respectively. Point-counting modal analysis and framework composition of these sandstones suggest that the Orb and lower part of the Org were derived from felsitic-metamorphic dissected/transitional arc sources which were uplifted in the west-southwest of the depositional basin, in accordance to published thermochronologic data indicating that this source may have been situated within the Takab Range Complex. Towards the Qom Formation, andesitic-basaltic sources are the main contributors to the sediments. These arc-related volcanic rocks were exposed in the north-northeast of the depositional basin. In addition, the occurrence of interbedded volcaniclastic and hybrid carbonate-volcaniclastic rocks in the Qom Formation indicate that clasts derived from contemporaneous volcanic activity.

The NW-trending Mahneshan fault zone show an almost pure reverse mechanism and aligned parallel to the Takab dextral Fault System. This implies a strain partitioning in a transpressional deformation in the Mahneshan Basin. This folding and faulting started atleast in the middle Oligocene. The exhumation of the Takab Complex occurred during the two main phases, coeval with the deposition of the middle part of Lower Red Formation (middle Oligocene), and also close to the Lower Red-Qom contact (late Oligocene).

KEYWORDS: Lower Red Formation, Qom Formation, Mahneshan Basin, Mahneshan Fault, Paleocurrent, Sediment Provenance, Strain partitioning

References

Afsari, N., Sodoudi, F., Farahmand, F.T. and Ghassemi, M.R., 2011. Crustal structure of northwest Zagros (Kermanshah) and Central Iran (Yazd and Isfahan) using teleseismic PS converted phases. Journal of Seismology, 15(2), pp.341-353.

Daneshian, J. and Ghanbari, M., 2017. Stratigraphic distribution of planktonic foraminifera from the Qom
Formation: A case study from the Zanjan area (NW Central Iran). Neues Jahrbuch für Geologie und Paläontologie-Abhandlungen, 283(3), pp.239-254.

Occurrence of Fe-Mg cordierite in contact aureole of the late Precambrian granite Doran, SW Zanjan, Iran

Haji-Abolfath, A.[1], and Izadyar, J.[1]

[1]Department of Geology, University of Zanjan, Iran
E-mail: aliabolfath@znu.ac.ir

The granite of *Doran* is the oldest known intrusive rock in Iran. The type locality of this granite crops out in south of Zanjan. The latest dating studies suggest an age of 567 Mio. years for this granite around the Chavarzagh village in western Zanjan (Hassanzadeh et al., 2008). In southwestern Zanjan, the late Neoproterozoic slates and schists of the *Kahar* Formation are metamorphosed into hornfels by the intrusion of the Granite of *Doran*.

The hornfels shows porphyroblastic texture in which porphyroblasts of quartz, alkali-feldspar and cordierite are present in cryptocrystalline matrix of a very fine muscovite-sericitic material. In addition, the accessory minerals are sphen, andalusite, zircon and opac minerals. Usually cordierite porphyroblasts are oval to ellipsoid in shape and some of them show hexagonal form with sector trilling. They are also changed to pinite. The microprobe analysis of a oval shaped cordierite blast revealed chemical composition of a Fe-Mg cordierite in which XFe and XMg are 0.616, 0.384, also an iron-rich cordierite. The existence of Fe cordierite is restricted to low pressures; with increasing XMg the stability limit of cordierite is shifted to higher pressures and also to higher temperatures. In addition, the channel volatile content of cordierite also affects its stability (Schreyer, 1986).

However by considering of diagram for the stability of Mg- and Fe-cordierite (Schreyer, 1986) the max. Pressure and temperature formation of observed cordierite could be 3 Kbar and 600 °C which reflects nearly the emplacement conditions of the Doran granite into slates and schists of the *Kahar* Formation.

KEYWORDS: Contact aureole; cordierite; granite Doran; Kahar Formation; Zanjan; Iran

Metamorphism changes and estimates of thermodynamic conditions section of metamorphic mylonite massif Ali abad-e damaq

Aghayari, F.[1] and Mahmoudi, Sh.[1]

1Geology Department, Kharazmi University, 31979-37551 Tehran, I.R of IRAN
E-mail: Farzaneh.aghayari@yahoo.com

Structural-metamorphic zone of Sanandaj-Sirjan in western Iran has experienced numerous magmatism-metamorphic history in this area, occurrence of several metamorphic phases, intrusions of igneous masses and pegmatite veins, as well as influence of tectonic forces on area, has created a complex.

Ali abad-e Damaq region consists of units of Alvand intrusive rocks, contact metamorphic rocks and ragional in which pegmatite veins and quartz veins are scattered in it.The rocks of this zone have been metamorphosed by low-grade metamorphism in green schist facies and amphibolite.

In the northern part of the region, sedimentary rocks are also exposed and some parts of the area are covered by present-day sediments. And according to Mohajjel., 1997, the study area is subdivided into complex deformations Other minor minerals that can be observed locally in zicroscopic thin sections include tourmaline, zircon, epidote, microcline, and sphene The main texture of these rocks is lipidogranoblast, which indicates the alteration and magmatic nature of this rock mass.On the other hand, these rocks have a weak S-C fabric parallel to the shear, indicating a gradual evolution of magmatism to metamorphism.Based on the ratio of porphyroclasts Stone Crumbs,in the masses of the tissues vary from ultramylonite to proteomilonite. Lithologically, the diversity of the main minerals in the main mass is relatively low. The major constituent minerals of this rock mass are quartz and feldspar (alkaline, plagioclase, perthite and feldspars). Foliation is formed by the orientation of these crystals and the accumulation of sub-minerals such as biotite, phengite muscovite, along this orientation.

According to the evidence presented in the study of microscopic thin sections, including the type and percentage of Producing minerals, the studied rock masses are in the range of granites (syenogranite and monzogranite). As well as the dominant lipidogranoblast texture of the rocks indicates the magmatic and metamorphic maior of Ali Abad-e Damaq mass.

Based on microscopic studies and determination of suitable paragenesis to estimate the temperature and pressure of the specimens purposefully for evaluation of selected chemical analysis and the results after the analysis are as follows based on the Ti and Mg thermometry method found in the structure of the biotite Henry and Guidotti (2002) and Henry et al. (2005) Ali-Abad-e Damaq rocks show a temperature range of 540 to 570 ° C.

The three feldspar Thermobarometrys available in the SOLVECALC program show that the Aliabad deep granite is formed at a pressure of 1.80 ± 0.05 Kb and a final temperature of 550 at 580 ° C. The calculated temperatures in the thermobarometry of the three feldspars are lower than that of the sub-salidos granites, indicating that the feldspars have undergone

changes in sub-salidus conditions. And these changes could be the same pressure that led to the formation of mylonites in the Ali Abad-e Damaq granite massif.

The thermometry of the Or - Ab feldspars of Ali Abad-e Damaq granite is based on the graph of the two - feldspar granite at a pressure of 1.8 kbar and a temperature of 490 to 540 ° C.Also based on Al2O3 vs. MgO, Al2O3 vs. FeO, MgO-Al2O3-FeO and MgO vs. FeO plots to determine the tectonic setting of biotites.

The magmatic tectonic setting of the studied biotites in the Ali Abad-e Damaq Mylonite granite is in the calc-alkaline and peraluminous range. According to the thermobarometric results, the metamorphic rocks of Ali Abad Damagh massif have been metamorphosed into green schist facies.

KEYWORDS: Thermobarometry, Metamorphism, Mylonite, Sanandaj-Sirjan Granite, Ali abad-e Damaq

Oligo-Miocene basaltic magmatism of Urmieh-Dokhtar magmatic belt: transitional geochemical signature between arcs to OIB sources

Ghorbani, K.[1], Morteza Delavari, M.[*, 1], Shabani, A.[1]

[1]Department of Geochemistry, Faculty of Earth Sciences, Kharazmi University, Tehran, Iran.

E-Mail*: Delavarimza@gmail.co

The Urmieh- Dokhtar magmatic belt lying parallel to the Zagros suture zone is commonly considered as the result of subduction of Neotethyan oceanic lithosphere beneath southwestern margin of Central Iranian continental terrane (Omrani et al., 2008; Chiu et al., 2013; Kananian et al., 2014). So, it provides a unique opportunity to evaluate spatial and temporal magmatic variation along a segment of Neotethyan arc. Based on earlier research (Verdel et al., 2011), the chemical characteristics and genesis of Urmieh- Dokhtar magmatism display evolution from Eocene to Oligocene. Here, we aim to put some new constraints on the genesis and tectonic environment of basaltic suites in part of Urmieh-Dokhtar magmatic belt. The study area is located to the northeast of Razan city, Hamadan Province. The western- southwestern border of the area with Sanandaj-Sirjan zone and north-northeastern border with Alborz zone are characterized by Avaj and Zanjan-Takestan- Boein Zahra Faults, respectively (Bolourchi, 1978). In the study area, basaltic units are intercalated with limestone and marls of Qom Formation suggesting that the volcanism is Oligo-Miocene in age. The basalts appear as both massive and pillowed units. Microscopically, the samples display porphyritic textures with intersertal to intergranular groundmass. The main phenocrysts are plagioclase, olivine and clinopyroxene. In some samples plagioclase forms more than 50% whereas clinopyroxene is less than 10% of mode. In olivine basalt, olivine is modally up to 20%.

The major and trace element contents of whole rock samples have been obtained by XRF (ARL Advant XP automated X-ray) and ICP-MS (Thermo Series X-I) at Ferrara University, Italy. The SiO_2 value ranges between 50 to 53.3 wt.% and total alkalis ($Na_2O+ K_2O$) is from 4.7 to 6.8 wt.%. In Nb/Y vs. Zr/TiO_2 diagram (Winchester and Floyd, 1977) all the samples plot within alkali basalt field. Moreover, TiO_2 content varies from 1.07 to 1.5 wt.% and Mg# [$MgO*100/(MgO+FeO_T)$] show relatively wide ranges of variation (49- 71.3). Low Ni values (5 to 56 ppm) displays important role of olivine fractionation in melt differentiation process. Primitive mantle- normalized multielement patterns are characterized by LILE enrichment and HFSE depletion. Furthermore, the chondrite- normalized REE patterns show LREE/HREE enricment (La/Yb= 8-13). Compared to OIB, the samples display lower LREE-MREE and higher LILE contents. The abundances of trace elements e.g. Nb, Zr values and Sm/Yb and La/Yb ratios indicate that the melt originated from a relatively enriched astenospheric mantle with low partial melting percent (< 20 %). Also, trace element ratios e.g. Zr/Nb, Nb/Th, Nb/Y, Zr/Y indicates that the tectonomagmatic setting of magma formation is transitional between arc and within-plate environment. Therefore, we interprete alkaline nature and trace element chemical signatures of studied samples as a result of low degree partial melting of deep astenospheric mantle above a subduction zone. In fact, after Eocene magmatic flare-up in central iran which triggered by Neotethyan subduction, later

magmatic activity (Oligo-Miocene) is related to the partial melting of upwelling astenospheric mantle in renewed extensional regime which is documented by formation of sedimentary basin of Qom Formation (Morley et al., 2009). Compared to the the mantle source of Eocene magmatism, that of Oligo-Miocene magmatism is relatively less affected by subduction components.

KEYWORDS: Alkaline basalt, Oligo-Miocene, Tectonic setting, Urmieh-Dokhtar magmatic belt.

Subduction-unrelated magmatism of southern periphery of Paleotethys: constraints from Late Paleozoic magmatism from the south of Masuleh, western Alborz

Sehhat, K.[1], Delavari, M.[*, 1], Saccani, E.[2], Barbero, E.[2], Hossein Mosaddegh, H.[1]

[1]Department of Geochemistry, Faculty of Earth Sciences, Kharazmi University, Tehran, Iran.
[2]Department of Physics and Earth Sciences, University of Ferrara, 44122 Ferrara, Italy
E-Mail*: Delavarimza@gmail.com

The Alborz Mountains in north of Iran correlates with the Paleotethyan Suture so preserves valuable clues for geodynamic clarifications and paleotectonic reconstructions. During life span of Paleotethys from Early Paleozoic to Late Triassic, major parts of Alborz appear as a continental margin in southern border of the oceanic basin. To test paleotectonic setting of Alborz during Late Paleozoic and its passive or active condition, geochemical data of magmatic rocks can provide useful clues. The Masuleh area (western Alborz) involves important exposures of Late Paleozoic volcanic associations. These volcanics are poorly studied and understood, so we intend to present new geochemical data about them. Field studies characterize various lithological units in tectonic and stratigraphic contact with volcanic units including Late Paleozoic low-grade metamorphics (slate-phyllite) and calcareous units of upper Devonian, Carboniferous to Permian. The whole rock geochemical data has been obtained by XRF and ICP-MS at Ferrara University, Italy. The volcanics mainly comprise basaltic to trachy-basaltic compositions. They show moderate to high alteration reflected in their LOI content (2.2 to 7.8 wt.%). Thus, for major element we used recalculated anhydrous values. The SiO2 abundances of 45.3 to 50.7 wt.% display basic nature of the studied rocks. Other major element components such as TiO2, Al2O3, CaO and MgO are in the ranges of 1-4.4, 13.7-18.3, 5-10.7 and 2.5-14.9 wt.%, respectively. Moreover, Mg# [MgO*100/(MgO+FeO*)] varies from 19-71. Wide range of major element variations likely corresponds to different modal mineralogy and also various extent of melt evolution and fractionation processes. Total alkali element abundance (Na2O+K2O) displays elevated values (1.95-7.9 wt.%) reflecting alkaline composition of the samples. Compatible elements such as Ni (2.2-213.7 ppm) and Cr (17-739 ppm) indicate highly varied amounts, as well, suggesting nearly primitive to extremely fractionated nature. In La/Sm vs. La plot, the compositional trend is consistent with fractional crystallization process. Chondrite-normalized REE patterns and primitive mantle -normalized spider diagrams are characterized by similar patterns suggesting genetic relationships of different samples. The spider diagrams display humped-shaped patterns in which the LILEs (Rb, Ba, Sr and K) and HFSEs (e.g. Th, Ta, Nb, Zr and REEs) show enrichment with increasing incompatibility and a slightly negative Nb anomaly. These patterns are consistent with typical intraplate alkaline magmatism (OIBs). REE patterns are characterized by pronounced negative slope reflecting high LREE/HREE enrichment ((La/Yb) N= 5-17). Moreover, La and Yb represent enrichment of 47-248 and 6.5-22 times chondrite abundances, respectively. Immobile trace elements (e.g. La, Y, Zr and Nb) discrimination diagrams suggest subduction unrelated within-plate mantle origin similar to OIB source. Furthermore, the mantle source nature and

partial melting degrees are inferred from modeling based on incompatible element ratios (Sm/Yb vs. La/Yb plot) suggesting that parental melt derived from garnet-bearing lherzolite and partial melting of <15%. Finally, we conclude that the area located to the southern margin of Paleotethys during Late Paleozoic was a passive margin (Gondwanian affinity) and the magmatic activity was related to thermal perturbation of mantle via hot spot/plume effects in an extensional tectonic regime.

KEYWORDS: basalt, within-plate, Late- Paleozoic, Alborz

Petrography and geochemistry of the Late Campanian siliciclastic rocks in the Kopet-Dagh basin NE Iran; implication for provenance and paleoclimate condition

Keshmiri, M.[1], Mahmudy Gharaie, M.H.*[1], Moussavi Harami, R.[1], Mahboubi, A.[1]

[1]Department of geology, Faculty of science, Ferdowsi University of Mashhad, Iran.
E mail: mhmgharaie@um.ac.ir

The Kopet-Dagh Sedimentary basin extends from the eastern part of the Caspian Sea to the northeastern part of Iran as well as into Turkmenistan and North Afghanistan. Following the collision of the Iran and Turan plates, the Kopet- Dagh Basin was formed on the southern margin of the Eurasian Plate from the Jurassic to the Neogene. Neyzar Formation is mainly composed of shales, marl, sandstone and sandy limestone. Two stratigraphic sections of Neyzar Formation (Late Campanian) near Tang-e-Neyzar and padelli village were documented by measuring and sampling in eastern part of the Kopet-Dagh basin. In this study, petrographic and geochemical parameters of shales and sandstone rocks of the Neyzar Formation in the eastern part of Kopet-Dagh basin have been analyzed to reveal their provenance such as parent rock composition, tectonic setting and source area paleoweathering indicating the paleoclimate condition. Petrographic studies showed that the sandstones are mostly classified as subliharenite and litharenite. Geochemical data revealed that the CIA values of Neyzar siliciclastic rocks confirm a medium to high weathering that could be due to warm and humid climate condition in the source area. Felsic to intermediate igneous composition of parent rocks and quatzolithic lithofacies of the Neyzar Formation sandstones and their constituents such as: Qm, Qp, Ls, Lm, and F show that these sediments may have derived from uplifted and trusted belt of sedimentary-metamorphic rocks of Binalood region in the south. In addition, geochemical and petrographic analyses suggest that Neyzar sediments are deposited in a continental rifting and recycled sedimentary orogeny's system.

KEYWORDS: Neyzar Formation, Paleoclimate, Provenance, Tectonic setting, Weathering

Petrology and Geochemistry of the intrusive units in Chahargonbad, Northeastern of Sirjan- Kerman

Saffar Heidari, M.[1*], Ghorbani, M.[2], Sheikh Fakhradini, S.[3]

[1*]M. Sc., Department of Geology, Shahid Beheshti University, Tehran, Iran
[2]Prof. , Department of Geology, Shahid Beheshti University, Tehran, Iran
[3]Ph.D. , Department of Geology, Shiraz University, Shiraz, Iran
E-mail: msaffarheidari@yahoo.com

The study area is located in southeastern Iran, about 110 Km southwest of Kerman. It is southeast of Urumieh- Dokhtar Magmatic Assemblage (UDMA). A part in UMDA called Dehaj-Sarduieh volcano-plutonic belt in Kerman province. Is specified by the occurrences of numerous felsic plutons of Oligocene-Miocene age famous for world-class porphyry copper deposits .The UDMA contains Eocene- Quaternary intrusive and extrusive rocks. The magmatic activity climax accurred in Eocene period. Geologically the area is composed of ophiolitic rocks, volcanic rocks, intrusive bodies and sedimentary rocks. The Dehaj-Sarduieh volcanic belt contains a broad range of Eocene volcano-sedimentary rocks, intruded by the so-called Jabale-Barez type granitoides with crystalline texture. Most of granitoids is composed of granite to granodiorite at south west of Kerman and they are Metaluminous and calc-alkaline. The UDMA includes alkaline and calc-alkaline volcanic rocks and the related plutonic I-type, mode by subduction of the Arabian plate beneath central Iran during Alpian orogeny. Chahargonbad granitoids are known as the Jabale-Barez type granitoids which intruded into the Eocene volcanic rocks consist of different andesite, dacite, pyroclastic and sedimentary rocks. Chahargonbad plutonic rocks contain quartzdiorite porphyry to granitoid. Garnite and quartzdiorite are mianly composed of plagioclase, alkali feldspar, quartz, amphibole, pyroxene and biotite. These rocks display granular texture. Anhedral quartz with embayed margins is as phenocrysts and inclusion in biotite, plagioclase and orthose. They are also of they are characterized by 25-40% plagioclase phenocryst with disequilibrium evidence of magma they show zoning. Based on the scheme, the analysed samples from the Chahargonbad plutons consist granite and granodiorite or quartzdiorite.

Considering K2O vs SiO2 discrimination diagram by Peccerillo and Taylor all rocks plot in the high K calc-alkaline and shoshonite field. The plutonic rocks of the chahargonbad are I-type metaluminous to slightly peraluminous. Primitive mantle-normalized trace element spider diagrams belonging to the chahargonbad intrusive show strong enrichments regarding large-ion lithophile elements (LILE) and those incompatible elements that behave as LILE. The most characteristic high-field strength elements (HFSE) and HREE have Cleary lower normalized values compared to LILE. Nb, Ti and P show negative anomalies. The flat HREE patterns of these rocks exclude garnet or spinel as a refractory phase while melting. In continental subduction zones, magma can be the result of two main origins: the upper crust and lower crust-upper mantle and a composite origin: crust mantle (mix), caused by fluids of the subducted plate. Partial melting of subducted sediments and fluids originated from the subducted slab metasomatize or enrich the origin of magma in subducted zones. Petrological evidence show that fractional crystallization from quartzdiorite to granite had main role in genesis of these rocks enrichment in LILE and depletion in high-field strength elements

(HFSE) in rare earth element distribution patterns of spider diagrams, indicate a subduction – related environment for formation of these rocks. Also, they are enriched in LREE rather than HREE. The characteristics, which are usually observed in the rock from subduction environments and active continental margins. Chemical and petrological studies indicate a common source for these igneous rocks and the main role of fractional crystallization in the evolution of magma although, minor amounts of assimilation and contamination of magma by crustal rocks occurred. The alkaline magma formed by low degree partial melting of an enriched sub-continental lithospheric garnet-lherzolite mantle. The high content of Sr, LREE enrichment, absente of Eu anomaly, HREE depletion pattern suggest the existence of garnet, amphibole and absence of plagioclase in the source rocks. Our data suggest that the plutons produced by partial melting of amphibole- eclogite or garnet- amphibolite, due to the subduction of Neotethys oceanic slab Central Iran Plate (CIP). Oblique subduction created appropriate spaces in the edge of the CIP. Hence, partial melting occurred due to decompression in the mantle wedge or base of the lower crust. The melts, which were quartz diorite to granite in composition, were injected into these spaces. In addition to mineral chemistry of some minerals, petrographic and geochemistry of special trace and rare elements can be used to distinguish the tectonic setting of the granitic rocks. All of the studied intrusive rocks on Nb versus Y and Ta versus Yb diagram are classified as volcanic arc granites and on La/Yb versus Th/ Yb diagram fall in the continental margin arc (volcanic arc) domain.

KEYWORDS: Petrology, Geochemistry, Magmatic rocks, Subduction, Calc-alkaline, Chahargonbad

Metamorphism of sedimentary rocks in the southern Sanandaj-Sirjan zone Determined from RSCM method

Gharibnejad, P.[1], Rosenberg, C.[2], Omrani, J.[3], Agard, P.[2] and Kananian, A.[1]

[1]University of Tehran, School of Geology, College of Science
[2]ISTeP, Institut des Sciences de la Terre de Paris, Sorbonne Université, 4 Place Jussieu 75252 Paris cedex, France
[3]Geological Survey of Iran
E-mail: (ParisaGharibnezhad@gmail.com)

The Sanandaj-Sirjan Zone (SSZ) played the role of active margin during the Afro-Arabian and Central Iranian continental collision. The southern part of this zone, mainly consists of Precambrian and Paleozoic metamorphic rocks, mostly characterized by Barrovian type metamorphism that formed under Amphibolite to Greenschist facies conditions. The convergence history can be traced through the subduction/obduction processes that are recorded within the geodynamic evolution of Zagros orogeny. Therefore, to reconstruct the geodynamic evolution of southern SSZ, metamorphic and structural investigations are very crucial. In south of SSZ, metamorphic conditions were documented in a few studies; but, only on the local scale. In this study we provide a temperature map, based on a data set obtained using Raman Spectroscopy of Carbonaceous Material (RSCM) of 28 peak-temperature estimates. The collected meta-sedimentary samples consist of calcareous (limestone, marble, dolomitic-marble and dolostone) and non-calcareous (phyllite and different type of schists) rocks. The obtained results indicate that older samples have higher temperature than the younger ones; hence, the samples can be classified into two groups: those with temperature between 500°C to 600°C (Precambrian and lower Paleozoic) and those with temperature ≤ 400°C (upper Paleozoic to pre-upper Mesozoic). The tectonic events that can explain burial and metamorphism of these samples probably are the Pan-African (Hercynian) and early Alpine orogeny (Cimmerian episodes and after) which were active during Precambrian and upper Paleozoic onwards. The alternative possibility is the exhumation and erosion of deep seated metamorphic rocks along the thrusts of suture zone (mainly MZT) which have been activate at least since the Eocene.

KEYWORDS: Alpine orogeny; Exhumation; Neo-Tethys; Pan-African orogeny; peak temperature; Raman Spectroscopy of Carbonaceous Material; Sanandaj-Sirjan Zone; Zagros orogeny

Mineralogical and Geochemical study of Shirkooh granitoid, Yazd

Ghanzavi, P.1, Khatami, M.1, pourfarzi, H.2

[1]School of Geology, College of Science, University of Tehran, Tehran, Iran
[2]Geological Survey & Mineral Explorations of Iran (GSI)
E-mail: pghaznavi@ut.ac.ir

Shirkouh Batholithic located 30 km southwest of Yazd in terms of structural zone in central Iran. This mass is greater than 550 square kilometers. This area, located in the Nayband Formation, and belongs to the Upper Jurassic. The coordinates of the study area are 31 degrees 23 minutes to 31 degrees 45 minutes' north latitude and 53 degrees 50 minutes 54 degrees 20 minutes east of Yazd province. Microscopic studies of 50 thin sections reveal the petrological and mineralogical information of the above specimens. In this study, GCDKIT Microsoft office excel software was used. The nature of the mass is in the range of alkalic acid in terms of the amount of alumina, peralumin. The samples in the diagrams illustrate the nature of calc-alkaline. According to lithological studies the main composition of the massive is granite- granodiorite. Field studies indicate a batholithic mass consisting of hornblende-rich granite type I as the main mineral, magnetite and rarely apatite and s-type granite inclusions containing almandine-rich garnet metamorphic enclaves that are chemically intrusive with intrusive garnets. Peralumines have similarities, cordierite, primary and secondary muscovites, and biotite and felsic microgranular with pegmatite veins. This granite (type S) is more precisely comprised of monzogranite, granite and granodiorite rocks. The main minerals forming the Shirkuh granitoid massif including biotite, cordierite, andalusite-sillimanite, zircon and apatite and ilmenite minerals are visible as minor-minerals in some samples. From the tectonic point of view, the Shirkuh batholith lies within the continental arc granite (VAG).

KEYWORDS: Geochemistry, Mineralogy, Granitoid, Shirkooh, Yazd

Coesite in the eclogite of the Sulabestarea, southeast of Birjand in Sistansuturezone, Iran: Evidence from textural and Raman studies \

Nasihatsheno, N.1, and Izadyar, J.1*

[1]Department of Geology, Zanjan University, Zanjan, Iran1
Email: Izadyar@znu.ac.ir
Email: nazila_nsh@yahoo.com

Petrographic and Raman microprobe spectroscopy were carried out for the metamorphic rocks from the Sulabest area, in the Sistan suture zone, eastern Iran, and coesite was recognized in the eclogitic rocks. The coesite-bearing eclogite consists mainly of garnet, omphacite, gloucophane and white mica. The coesite occurs as inclusion surrounding by albite within porphyroblast garnet. Eclogites in the Sulabest area form topographically prominent lenses several metres across, embedded in the schistose mélange matrix.

Microstructural investigations and mineral chemistry results indicate that eclogites in the Sulabest area recorded two events of metamorphism. The first or peak metamorphic stage (M1) is characterized by mineral assemblage of garnet, omphacite, sodic amphibole, phengite, coesite, quartz and water that indicated eclogitefacies. Phases of Peak stage contain undecomposed minerals and middle parts of minerals which have zoning and formed in early stages ofmetamorphic. The second or retrograde metamorphic stage (M2) can be recognized by mineral assemblage like; garnet, sodic-calcic amphibole, muscovite, chlorite, epidote, quartz, albite and water that indicated epidote- amphibolite facies. Phases of retrograde stage contain decomposed minerals and rim parts of minerals which have zoning and formed in future stages of metamorphic.

This finding represents a first piece of evidence for ultrahigh-pressure metamorphism in Sistan suture zone of eastern Iran. The Sistan Suture Zone of eastern Iran is a Cretaceous to Tertiary orogenic belt that formed by closure of a north wards projecting arm of the Neo-Tethys ocean. Disrupted ophiolitic rocks within the subduction complex include a tectonic mélange of metamorphic rocks. The metabasite lenses include variably overprinted eclogites, epidote–amphibolites and greenschists.

KEYWORDS: coesite, eclogite, Raman spectroscopy, Sistan suture zone, Iran.

Petrography, mineralogy and Texture of chondrule from the Sarpol Zahab H chondrite

Ghanzavi, P.[1], and Kamali, H.[2]

[1]School of Geology, College of Science, University of Tehran, Tehran, Iran
[2]Management of Iran meteorite museum
E-mail: pghaznavi@ut.ac.ir

Stony meteorites consist predominantly of the silicate minerals olivine, pyroxene, and feldspar. They may also contain metallic iron and iron sulfide, but always in lesser amounts. The stony meteorites are further divided into chondrites and achondrites. The characteristic components (40 to 90%) of chondrites are the chondrules or small spheres, ranging in diameter from 0.2 to 1 mm. On a broken surface they catch the eye because they protrude as hemispheres or because their color differentiates them from the fine-grained groundmass. Chondrules are easily removed from some chondrites, while in others they are firmly incorporated into their surroundings. They consist chiefly of olivine and pyroxene, with a small amount of feldspar that is generally found as a binding agent filling the spaces between the olivine and pyroxene crystals. Their structure becomes clear when examined in thin section under the microscope. Chondrules are a major component of chondritic meteorites. Understanding their formation conditions provides fundamental insights about how the early solar system formed and evolved. Chondrules represent a significant evolutionary step in planet formation. We studied the textures of ~20 chondrules from one groups (H) of ordinary chondrites that is a new H chondrite fell near Sarpol Zahab, Kermanshah, Iran on August 10 at 7:55 AM. The fall was observed by local villager. We also describe mineralogical and petrologic information for a selected subset of the same suite of chondrules. The data investigate the relationships between chondrule mineralogy and texture.

KEYWORDS: Chondrite, Chondrule, Meteorite, Mineralogy, Petrology

Study of Granit types and alterations of Shirkooh granitoids, Yazd

Khatami, M.[1], Ghanzavi, P.[1], pourfarzi, H.[2]

[1]School of Geology, College of Science, University of Tehran, Tehran, Iran
[2]Geological Survey & Mineral Explorations of Iran (GSI)
E-mail: maryam_khatami@ut.ac.ir

Shirkouh granitoid batholith, over 1000 square kilometers, is located in the coordinates of 31 degrees 23 minutes to 31 degrees 45minutes north latitude and 53 degrees 50 minutes 54 degrees 20 minutes east of Yazd province. The study area of Shirkouh granitoid is located 30 km southwest of Yazd in Nayband Formation and Structural Zone of Central Iran. Fifty samples of granitoid masses were subjected to XRF and ICP analyzes. Microscopic studies of 50 thin sections reveal the petrological and mineralogical information of the above specimens. In this study, GCDKIT and Microsoft office excel software were used. The studied batholithic mass can be studied in three categories: The first group is granodiorite that, have plagioclase-rich mineralogy of plagioclase-rich mineralogy in the center, quartz, potassium feldspar, and biotite that encompasses the hearing margin of the mass. The second group of monzogranites, which are the largest of the batholithic, are separated from the granodioritic melt. Cordierite mafic rocks and differentiated types of muscovite give rise to Shirkuh batholithic. The third group is leucogranite and their color is clearly shown due to the absence of dark minerals on the western margin of this batholithic mass is light, which are the result of late melt. As a result of contact metamorphism, alteration hydrothermal alteration is visible in the host rocks. According to studies of altered types of propolytic, quartz-sericite, which is the most extensive zone in the study area, advanced argillic including APS (aluminum phosphate sulphate) minerals (jarocyte minerals, alunite). Examination of trace elements indicates that the Shirkuh batholith is a type of tectonic source granite. The mentioned granite is derived from upper crust anatexy and biotite mineralization failure reactions. These granites ,Due to the high amount of aluminum are peraluminous.

KEYWORDS: Geochemistry, Alteration, Granit types, Shirkooh granitoid, Yazd

Chemical constraints on the genesis and geodynamic setting of Late Cretaceous magmatism in northeast of Tehran, Central Alborz

Namvar, R.[1], Delavari, M*,[1], Saccani, E.[2], Barbero, E.[2], Karimi, B.[3]

[1]Department of Geochemistry, Faculty of Earth Sciences, Kharazmi University, Tehran, Iran.
[2]Department of Physics and Earth Sciences, University of Ferrara, 44122 Ferrara, Italy
[3]Iran Mineral Processing Research Center, IMPRC- Kavosh Research Twon, Karaj, Iran.
E-Mail*: Delavarimza@gmail.com

The Alborz range is part of Alpine- Himalayan orogenic system which preserved important magmatic features related to the evolution of Gondwana-Eurasia junction realm. Several well-developed sub-marine Cretaceous volcanic units are exposed in Central to Northern Alborz e.g. in Marzan-Abad and Lahijan areas. The volcanics display mainly basaltic composition. Study of chemical signatures of these rocks is a key issue to constrain the tectonomagmatic environment of melt formation and paleogeographic reconstructions. In this research we aim to study the volcanic outcrops located to the northeast of Tehran (south of Amol), Central Alborz. Stratigraphic relationships show that the volcanics are interlayered with marly limestone, limestone and marls of Late Cretaceous. Here, we present new geochemical data on these rocks to identify the origin and condition of magma genesis which helps to infer paleotectonic setting of Alborz magmatism during Late Cretaceous. The major and trace element contents of whole rock samples have been obtained by XRF and ICP-MS at Ferrara University, Italy. Using recalculated anhydrous major elements, the samples display wide range of variation in SiO_2 (42-68 wt.%), TiO_2 (0.45- 4.7 wt.%), Al_2O_3 (12.6-18.8 wt.%), Mg# (17.8-49) and $Na_2O + K_2O$ (2.9-11.7 wt.%), likely reflecting various mineralogy and different degrees of fractionation. Based on Nb/Y (1.8-3.4) and Zr/Ti (0.01-0.29) ratios the rocks plot within alkali basalt, trachy-andesite and trachyte fields. High Zr (83-738 ppm) and Nb (43-111 ppm) contents is also consistent with alkaline nature of the samples. Other incompatible element values shown by normalized multi-element patterns are enriched as well, which is similar to typical within-plate alkaline basalts, such as ocean island basalts (OIB). Furthermore, no negative Nb and Ta relative depletion can be observed in these patterns. In chondrite- normalized REE patterns, the rocks display elevated LREE enrichment with respect to HREE, exemplified by high $(La/Yb)_N$ ratio (15-33). Overall, the REE enrichment of the rock suites is 155- 375 and 8.5- 17 times chondrite value for La and Yb, respectively. Using trace element abundances such as Zr, Y, Nb and Ti contents and also the ratios of Zr/P_2O_5, Nb/Y, Zr/Y, Ti/Y, Th/Yb and Ta/Yb, the basaltic rocks plot in the fields of alkaline and subduction-unrelated OIB-like magmas. Moreover, theoretical modeling using REE ratios e.g. Sm/Yb and La/Yb displays that the parental melt originated from partial melting of deep garnet-bearing enriched mantle with low (<15%) partial melting. Therefore, we conclude that the tectonic environment of melt formation is unrelated to subduction process and mostly corresponds to within-plate magmatism in an extensional setting. This conditions is more probably consistent with hot spot/mantle plume activity and continental rift-related events.

KEYWORDS: Alkaline basalt, Late-Cretaceous, Central Alborz

Geochemistry and petrogenesis of host rocks of hydrothermal springs in Meshkinshahr, northwest of Sabalan volcano

Khatami, M.[1], and Modabberi, S.[1]

[1]School of Geology, College of Science, University of Tehran, Tehran, Iran
E-mail: maryam_khatami@ut.ac.ir

The study area is located northwest of Sabalan Volcano. Sabalan region is located between two structural areas of Alborz-Azerbaijan and Orumiyeh-Dokhtar. Samples from eight hot springs available in the area were sampled. These rocks are in continental and orogenic range with high aluminum oxide and potassium oxide.According to Harker diagrams for the host rocks sample of the hot springs under study, oxides of the major elements, such as Al2O3, CaO, MgO, FeO2, P2O5, TiO2, show a marked decrease with increasing SiO2. These trends are justified by the crystallization of myfic minerals and plagioclase. K2O shows an upward trend with increasing SiO2. This process can be related to the crystallization of potassium feldspars. Na2O shows an almost irregular course, which can be due to the alteration of the specimens, as the Na and K elements are Mobile elements, and their inconsistency in the process can be evidence of the alteration of the specimens. Overall, most of these diagrams show distinct process rock compositions, which may indicate their parent magma kinship. As noted earlier, CaO shows a decreasing trend against SiO2. CaO is a compatible oxide, thus having a high content in the early stages of subtraction and tends to participate in the formation of minerals such as pyroxenes (especially clinopyroxenes) and calcium plagioclases, so it can be concluded that the final stages of differentiate decrease. MgO also declines against SiO2. Since Mg is one of the compatible elements in magma, it tends to separate from magma at high temperatures and at the beginning of the differentiate process. It can enter the structure of refractory minerals such as olivines and pyroxenes in magma. As a result, as the subtraction process progresses and the SiO2 content in the magma increases, the amount of Mg in the magma and the resulting rock decreases. FeO is also a compatible oxide that shows a decreasing trend against SiO2. In addition to being involved in the formation of the first refractory minerals and pyroxene, this oxide is also incorporated into the magnetite structure. TiO2 is also oxide compatible, which results in a downward trend of SiO2. P2O5 does not show a uniformity.

KEYWORDS: Geochemistry, Patrogenesis, hydrothermal springs, Sabalan volcano

Structural evolution of Moghanlu Gneissic mass, NW Iran

Aflaki, M.[1], Honarmand, M.[1], and Zaringol, Z.[1]

[1]Earth Sciences Department, Institute for Advanced Studies in Basic Sciences, Zanjan, Iran
E-mail: (aflaki@iasbs.ac.ir)

Moghanlu gneissic mass, late Ediacaran-Cambrian in age (579-531 Ma), is part of the Takab magmatic–metamorphic assemblage of NW Iran, Zanjan province. It characterized by complex composition and structure inherited from experience of several orogenic events, including metamorphic rocks in central part which are sorounded by plutonic intrusions. They are dominantly overprinted by brittle fault zones. Recent geochemical and isotopic studies investigate tectono-magmatic evolution of the complex and indicate effect of late Oligocene crustal thickening and later extentional events (results in formation of a core-complex structure) on its post collisional evolution. But, the structure of Moghanlu gneissic mass is not well undrestud. To have a better insight from its tectonic evolution, we motivated to search for destribution of ductile deformation within the gneissic part and brittle fault zones, especially around the complex. Our studies reveal a mylonitic fabric for the gneissic rocks, with high strain bands in deeper part of the outcrops. Altough ductile structures are overprinted and rotated by younger brittle events, there is a systematic change in orientation of foliation within the area. Foliation is dominamtly NW-SE striking, but its dip gradually changes from semi-vertical at the western part of the mass to semi-horizontal at cental part and moderatly dipping NE-ward at eastern part of the area. Most measured lineation are NE or SW trending. Shear sence indicators in meso- and micro-scalescale view, including C/C‘-type shear bands and Sheath folds, are compatible with up to the NE shearing through the area. These structural data present evidences of mylonitic gneiss, in central part of the Moghanlu mass, with structure comparable to core-complexes. The ductile mylonitic foliation is overprinted by brittle-ductile structures including gash fractures and minor conjugate shear bands. Orientations of these structures are compatible with direction of maximum compression perpendicular to the orientation of foliation. It suggests their exhumation to upper part of the crust during an extensional event. Satellite images and field observations reveal that present outcrop of the Moghanlu mass is bounded by Precambrian-paleozoic rocks at NE and Cenozoic rocks at SW. It thrusted along its western and southern boundaries over mudstones of Upper Red Formation, Miocene in age. Our structural data present evidence of a core-complex structure which may have been emplaced, later, during late Cenozoic compressional tectonic regimes.

KEYWORDS: Moghanlu; Mylonitic gneiss; Petrophabric; Sanandaj-Sirjan; Structural evolution.

Geology of Bajalia Anticline in Amarah, Al-Teeb, Iraq-Iran Border

Abdulnaby, W.[1], Mahdi, M.[1], Al-Mohammed, R.[1], Darweesh, N.[1], Hashoosh, A.[2]

[1]Department of Geology, College of Science, University of Basrah
[2]Groundwater Authority, Ministry of Water Resources, Maysan Governorate

Bajalia Anticline is located about 60 km northeast the center of Amarah city within the Low Folded Zone of Iraq at Al-Teeb area near Iraq-Iran border. Field and office works were achieved in order to study the topography, geomorphology, stratigraphy, structural geology, and hydrology of Bajalia Anticline. The Anticline has longitudinal shape with about 28 km long and 5 km width, and it has northwest-southeast trend, which is the Zagros trend. Injana, Mukdadiya, and Bai Hassan formations (Upper Miocene-Pleistocene) are the three formations that were recognized in the study area. The topography of the Anticline indicates that the elevations range from about 40 meters at the southwestern limb to 120 meters at the northeastern limb. The geomorphology of the study area shows differential erosion that occurs because of physical properties of rocks. Different huge valleys run through the Anticline perpendicular to the hinge line. The geometrical structural analysis depicts that the Anticline is asymmetrical, non-cylindrical, linear, upright, horizontal, and open fold. Most of the fractures in the Anticline are joints. These joints were classified based on the tectonics axes, which are a, b, and c, into: ac, bc, hol. A major reverse fault is located at the margin of the southwestern limb parallel to the fold axis with about 25 km length. This fault is responsible on the vergency of the Anticline and overturned of part of the southwestern limb. The Anticline was formed as a result of the collision between the Arabian and Iranian plates during the Late Tertiary. The maximum stress axis, which caused by collision, is perpendicular to the hinge line. The geometrical and genetic classification indicates that the Anticline was formed by high folding intensity. Salt tectonics of the Middle Miocene Fat'ah and the Late Jurassic Gotnia evaporite formations may play a role in forming the Anticline. This role can be identify by geophysical studies to the Anticline.

KEYWORDS: Bajalia Anticline, Geology of Iraq, Structural geology of Amarah, Hemrin-Makhul Folded Belt

Tectonic evolution of the Central Alborz: from paleostress investigations to the present state of the stress

Pourbeyranvand, Sh.1, Gholami Dargahi, M.2

[1]International Institute of Earthquake Engineering and Seismology
[2]Kharazmi University
E-mail: beyranvand@iiees.ac.ir

Central Alborz has so far been affected by several strong tectonic stages. In this summary of the paper, it has been attempted to summarize the changes in the direction of maximum compressional stress in the Central Alborz region over time from the Eocene to the present-day. The paleostress direction in this area which is calculated by fault slip data stress inversion has been published in some papers.

Abbasi and Shabiani (2005) used 181 fault slip observations and associated lineaments to determine the paleostress state during the Pliocene to Holocene geological time in the south-central Alborz in geographic range 51 to 52.5 using stress tensor inversion method. Stress directions from the Eocene to the Late Quaternary change clockwise, from NW-SE to NS and finally to NE-SW.

Mehrnaz et al. (2005) used the data related to the shear fault planes and the associated lineation and implemented the stress inversion method in East Tehran at Longitude 51 ° 30 min to 51 ° 45 min and Latitude 35 ° 30 min to 35 ° 45 Min. The obtained the paleostress direction through this study during the Mesozoic and the Cenozoic (Paleogene) is NS.

Finally, Eliassi and Ahmadian (2008) studied a number of mesoscale faults containing slickenside lineations related to the Eocene from latitude 50 degrees 50 minutes to 51 degrees 25 minutes and from latitude 35 degrees 45 minutes to 36 degrees 8 minutes by Multiple Inverse Method. The results of this study were checked by some other geological phenomena such as axial level of folds, and Stylolites. The calculated stress paths have an N-S trend, indicating an increase in stress intensity during fault system activities.

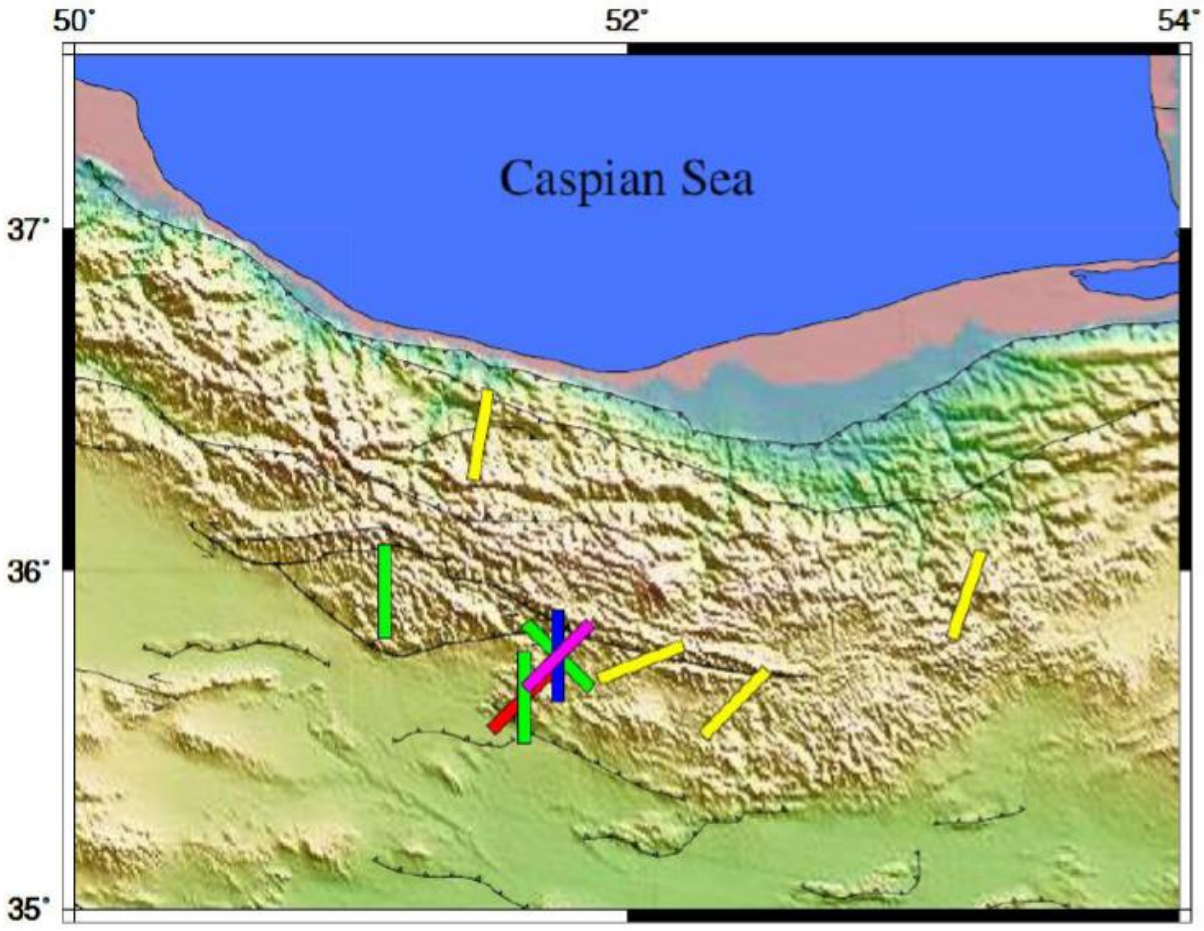

Figure 1. Comparison between paleostress and contemporary stress directions in the central Alborz. Description of the colors can be found in the text.

From many studies, only the above-mentioned ones were employed because the rest could not be used in comparison with the others effectively because of inaccurate information about the location of the paleostress sites under investigation. The other 3 studies were analyzed regarding the geological time. Thus the paleostress main orientation conducted through these studies were classified into 4 phases including the Mesozoic, the Paleogene (the Eocene), the Neogene, and the Quaternary. The main paleostress direction in these phases is illustrated in fig. 1 as red, green, blue and magenta bars.

A recent study on the present state of the stress in the Central Alborz is used seeking a comparison between the paleostress results in the study area with the contemporary stress directions (Pourbeyranvand, 2019). The SHmax from focal mechanism stress tensor inversions is in yellow.

The present-day stress, a trend with a mean NE direction is the dominant trend. The difference between the paleostress directions and the calculated present-day SHmax directions reflects the clockwise rotation of the principal stress orientations over time in most of the cases but the differences in the geological times covered by the studies and also the location of the sites under

investigations causes complexities in the analysis of the data. Hence it seems that a simple rotation model cannot be easily assigned to the tectonic evolution of the study area.

Anyhow, the clockwise rotation which is observed in this study from older geological time up to more recent and finally present time, is supported by some other similar studies comparing the paleostress and contemporary stress directions, carried out in other locations in the country. A paleostress study compared to the present state of the stress in the Azerbaijan NW Iran (Aflaki et al. 2017) and also a similar study in the Western Zagros (Pourbeyranvand, 2003) revealed a comparable clockwise rotation of the principal stress orientations through the geological time. The issue thus worth more investigations and when completed, can lead to an insight to the tectonic evolution of the Alborz range which is very important from a variety of different aspects including seismotectonic, economic, industrial and also oil and gas perspective.

KEYWORDS: Central Alborz; Fault-slip data; Focal mechanism; Tectonic evolution; Stress inversion

Refrences

Abbassi M.R., Shabanian Borujeni, E., (2005). Determination of stress state and direction by inversion of fault-slip data in the southern flank of Central Alborz, Geosciences, Vol. 14, No. 55, 2-17 pp.

Aflaki, M., Shabaniyan, E. and Davoudi, Z., (2017). Deformation evidence from Plio-Quaternary paleostress in Mahneshan Miyaneh basin, Bulletin of Earthquake Science and Engineering, Year 4, V. 4.

Eliasi, M., and Ahmadian, S., (2009). The geometric arrangement of σ1 paths in the Kan-Karaj extension (south-central Alborz) based on multiple inversion method. Earth Science, Spring 1387, Vol. 17, No. 67, 140-149 pp.

Pourbeyranvand, Sh. (2013). Stress variations in the Zagros by inversion of earthquake Focal mechanisms, Ph.D. These, University of Tehran, Tehran, Iran.

Pourbeyranvand, S., 2018. Stress studies in the Central Alborz by inversion of earthquake focal mechanism data. Acta Geophysica, 66(6), 1273–1290. DOI: 10.1007/s11600-018-0207-1

Sa'adat, M., Alavi, A. and Saeedi, A., (2005) Analysis of Fragile Tectonics and PaleoStress pattern in the east of Tehran. 24th Earth Sciences Conference, Tehran, Geological Survey. 24th Earth Sciences Conference, Tehran, Geological Survey.

The effect of dextral Abarkuh Fault on the occurrence of sinistral top-to-the NW deformation in the Zagros Hinterland Fold-and-Thrust Belt, Iran

Ghanbarian, M.A.[1], and Sadeghi Mazidi, M.[1]

[1]Department of Earth Science, College of Science, Shiraz University, Shiraz, Iran
E-mail: maghanbarian@shirazu.ac.ir

The sinistral top-to-the NW deformation in the ductile and brittle-ductile shear zones of the central part of the Zagros Hinterland Fold-and-Thrust Belt (ZHFTB) has already been introduced. In the present study, fault slip data, pressure-solution seams (stylolites), and en-echelon vein arrays were investigated in the rock exposures with different ages, in the northeastern margin of Fars Province (between north of Bavanat to north of Shurjestan as an important part of the ZHFTB), via an intensive field campaign. The results of this study indicate that in the time span of the occurrence of these structures, the maximum principal (σ1) stress axes were horizontal and directed towards NE-SW and ENE-WSW. These directions are compatible with the expected directions of σ1 stress axes responsible for occurrence of the sinistral top-to-the NW ductile and brittle-ductile shear zones of the area. This compatibility indicates a longstanding stable stress condition over a long period and different pressure/temperature conditions. This may suggest the occurrence of a major dextral NW-SE trending fault in the NE of the ZHFTB (i.e. 25 km NE of the Main Deep Fault or Abadeh Fault) which we named it Abarkuh Fault. The dextral activities of the Zagros Thrust System and this newly-recognized fault, which are subparallel, might result in the sinistral top-to-the NW deformation in the area between the Abarkuh Fault and the Main Deep Fault (i.e. ZHFTB). Although the Abarkuh Fault is hidden by Quaternary alluvium of the Abarkuh plain, a significant change in topography between the Abarkuh plain and its southwestern mountains (e.g. the Hambast and the Pouzehsiah Mountains) and great age difference of rock units of the Esteghlal Anticline and its northeastern rock exposures may be evidence of the existence of the Abarkuh Fault.

KEYWORDS: Central Iran, Fault slip inversion, Stress inversion, Stylolite, Tension gash.

Eocene to Quaternary deformation and stress filed in Central Iran "Evidence of an anticlockwise rotation"

Babaee, S.E.[1], Hajiloo, M.[1] and Rezaeian, M.[1]

[1]Department of Earth Sciences, Institute for Advanced Studies in Basic Sciences (IASBS), Zanjan 45137-66731, Iran
E-mail: seyederfanbabaee@gmail.com

Paleostress analysis data in the northern edge of the Urmia-Dokhtar Magmatic Arc (UDMA) in the south of Qazvin is presented. Evolution of stress filed related to the geodynamic events reveals eight different fields since Eocene. Tens of structural outcrop in folds and faults was investigated in the Cenozoic formations. To analyse the fault slip data, we used multiple inversion method (MIM; Yamaji 2006) that has an advantage in separating multiple stress tensors from a heterogenous data set. Four parameters including stress ellipsoid form and stress axes were calculated based on the multiple inversion method that detects temporal change of tectonic stress state. Stress state for eight major deformation phases reveals that the orientation of the maximum horizontal stress axis has an azimuthal change from 165° to 20° during Eocene to present time. That coincide with a 145 degree anticlockwise rotation of maximum horizontal stress in less than 56 million years during Cenozoic.
The geodynamic regime in this area has been governed by several tectonic phases in Eocene to Pliocene which correlated with those in the Iranian Plateau. Three tectonic phases in the Eocene (compression, transtension and transpression), two phases in the Oligocene (compression and transpression) were introduced. Also, in the Oligo-Miocene, Miocene and Pliocene a transpressional, compressional and transpressional tectonic regime were detected, respectively. The anticlockwise rotation of the stress filed was investigated through Iranian Plateau, it can be tentatively supported by hypothesis of an anticlockwise change in the movement direction of the Arabian indenter with respect to the Eurasian plate.

KEYWORDS: Paleostress; Cenozoic; anticlockwise rotation

3rd TRIGGER International Conference
8-10 October 2019, Zanjan, Iran
Institute for Advanced Studies in Basic Sciences
Gava Zang, Zanjan, Iran

Microstructural characteristics of the mylonitic rocks in the TanbourMetamorphic Complex, Sanandaj-Sirjan metamorphic belt, SE Iran

Mansouri, S.M.[1], Keshavarz, S.[1]*, Shahpasandzadeh, M.[1], Faghih, A.[2]

[1]Department of Earth Sciences, Graduate University of Advanced Technology, Kerman, Iran

[2]Department of Earth Sciences, College of Sciences, Shiraz University, Shiraz, Iran

Email: s.keshavarz@kgut.ac.ir

Tanbour Metamorphic Complex is located east of the Sirjan within the Sanandaj-Sirjan metamorphic belt, SE Iran. Deformed and metamorphosed rocks of this complex consist of slates, phyllites, chlorite schists, actinolite schists, marbles, mica schists, garnet schists and amphibolites, gneisses, metasandstone and metabasic rocks. The sedimentary protoliths were turbiditic sandstone, carbonates and politic rocks, which are metamorphosed regionally up to amphibolite facies (Dimitrivic, 1973; Moazzen, 2004; Moradian et al, 2005). While there is no radiometric data for the metamorphism history and rocks, based on microfossil studies, Lower to Upper Permian ages were suggested for phyllites, slates and garnet-mica schist (Mijalkovic and Saric, 1973; Safei et al., 2015). Polyphase deformation is highlighted by occurrence of two generations of foliation in this deformed zone, where the first and dominant phase of deformation produced a penetrative foliation (S1) in mica-garnet schists and actinolite schist. This foliation has a mean attitude of N50°W, 20°NE. The second phase of deformation produced asymmetric crenulation cleavage (S2), which commonly lies at an angle of about ~35° to S1. In addition, two generations of mineral/stretching lineation have been recognized in the amphibolites, schists and gneisses in the study area. Several mesoscopic and microscopic structures including lenticular/subrounded δ- and σ-type K-feldspar porphyroclasts, quartz petrofabrics, veins and drag folds were used to estimate strain (Passchier &Trouw, 2005; Mukherjee, 2017). Kinematic indicators including S-C shear bands, asymmetric mantled porphyroclast, oblique quartz foliation, domino-like structure and mica fish confirm strong dextral sense of ductile shearing. Microscopic evidence in the quartz-rich samples indicate the presence of two type of recrystalization regims, which characterized by deformed ribbon quartz, weak undulatory, oblique grain shape alignments and lobate boundaries microstructures and second type of quartz grains typically have straight grain boundaries and relatively uniform sizes that are similar to adjacent subgrains. These features show intracrystalline deformation accompanied mainly by grain boundary migration (GBM) and subgrain rotation (SGR) recrystallization of quartz, respectively. Deformation of feldspar porphyroclasts in the Tanbour mylonites ranges from fracturing to bulging recrystallization (BLG) and subgrain rotation (SGR). Dynamic recrystallization and dislocation creep regimes, derived from quartz and feldspar microstructures studies provide further constrains on deformation temperature in sheared rocks, although they are also controlled by strain rate, existence of fluid phases and 3D strain-type geometry(Stipp et al., 2002;). The textural features of the quartz and feldspar in the study area indicate temperature of mylonitization range between 450 and 600°C in the amphibolite facies conditions.

KEYWORDS: mylonites, shear zone, Sirjan, Tanbour metamorphic complex, Zagros

Hydrogeological Structure of the southern portion of the Anar fault, Central Iran

Kardoost, A. [1], Shahpasandzadeh, M. [1 *], Keshavarz, S. [1], Abbasnejad, A. [2]

[1]Department of Earth Sciences, Graduate University of Advanced Technology, Kerman, Iran
[2]Department of Geology, ShahidBahonar University, Kerman, Iran
Email: mshahpasandzadeh@kgut.ac.ir

The subsurface flow model of faults, cutting poorly lithified sediment, constitute one of the greatest uncertaintyin many fields of subsurface fluid research due to their wide range of potential hydraulic behaviour. The conduit, barrier or conduit-barrier behaviour of faults can impact groundwater resources (e.g. Caine et al., 1996); For example, compartment of aquifers by fault barriers can limit the extent of accessible groundwater, or prevent the spread of contaminants.In contrast, fault conduits can influence groundwater recharge, or provide pathways for salt water intrusion intofreshwater aquifers. An understanding of theseprocesses is important for protecting groundwater supplies in modern societies (Wada et al. , 2010). Although there is a reasonable understanding of how faults impact fluid flow in crystalline or lithified rock, less is known about how faults in poorly lithified sediment impact groundwater flow. These sediments accommodate major aquifers in Iran.

Located in an arid and semi-arid region, the central Iran is struggling with the recent droughts and a constant drop in groundwater levels due to irregular harvests. This condi_on has made the region vulnerable to social and environmental crises. Hydrogeological structure of faults such as the Anar fault isone of the most ambiguous issue in many groundwater studies (e.g.; Rawling et al., 2001; Caine et al., 1996).This research illustrates the hydraulic behaviour of the southern por_on of the Anar fault and identify the structure and deformation processes of the fault zone in poorly lithified alluvial sediment, which influence fluid-flow. In this research, the outcrop inves_ga_ons of the sediments are used to deduce fault zone hydraulic conduc_vity structure. In fact, the behaviour of the fault in poorly lithified alluvial sediment was determined by the structural and hydrogeological features of the fault. The 200-km-long Anar strike-slip fault is known as aseismically ac_ve fault with a minimum slip rate es_mate of 0.8 ± 0.1 mm/yr in the central Iran (e.g. Le Dortz et al., 2009; Foroutan et al., 2012). In this research, we have focused on the southern portion of the fault, which runs along the Anar salt flat and through the populated city of Anar. The fault affected locally voluminous deposits of poorly lithified alluvial sediment, constituting the aquifer and confining units of the Anar plain. With an averaged net sedimentation rate of ~ 0.47 ± 0.11 mm/yr) Foroutan et al., 2012), the age of the aquifer could be poorly constrained between 240 to 480 ka. The aquifer is characterized dominantly by alluvial deposits, composed of coarse gravel alluvial conglomerates, inter-bedded with sand and clay layers. The fault zone structure was found to be different along the southern portion of the Anar fault.The mixed zone scomprise of variably deformed sediment that accommodate the majority of strain. Specific structural elements in the mixed zones differ according to the lithology, in particular the rheology and stratigraphic relationships. The mixed zones are flanked by damage zones. The damage zones comprise antithetic or synthetic subsidiary faults that cutsometimes disaggregation bands that cut fine-grained sediment. Our findings show the cemented fault zones could reduce fault zone hydraulic conductivity more than primary fault zone processes. Although the most modest method of understanding fault zone hydrogeology is through analysis of hydrogeological data, analysis of the hydraulic head either side of the southern portion of the Anar

fault infer the seal capacity of northern segment of the fault. In addition, the estimated hydraulic conductivity of fault zone in the north and south segments of the southern portion of the Anar fault are 1.38 E-04 and 2.54 E-04, respectively.

The gradient of groundwater at the north of Anar fault is from the west and northwest towards east and southeast, but at its southern part, from the west and southwest toward the east and northeast. Groundwater at the west of Anar fault, which is the recharge area, is much fresher than in the east, so that it abruptly becomes saline at the east. The depth of groundwater at the west of this fault is less that its eastern part, and additionally, there is a sharp difference in groduwater depth between the southern and western sides. Accordingly, this fault behaves as a low permeable barrier, because of chemical precipitation (especially aragonite) in the fault zone, as well as just a position of permeable and non permeable layers against each other. The mother wells or all Qanats near the fault zone lies at the west of fault.

This means that the eastern side has not sufficient groundwater and groundwater is collected in the west. In another words, upon reacharging the west of the fault, where groundwater is accumulated, there is no need to continue excavation of Qanats.

KEY WORDS: Fault zone hydraulic behaviour, hydraulic conduc_vity, Anar Fault, central Iran

References

Caine, S. J., J. P.Evans, C. B.Forster, 1996., Fault zone architecture and permeability structure. Geology 24, 1025-1028.

Le Dortz, B. Meyer, M. Sebrier,H. Nazari, R. Braucher, M. Fattahi,2009., Holocene right-slip rate determined by cosmogenic and OSL dating on the Anar fault, Central Iran. Geophys. J. Int. 179, 700-710.

Foroutan,M., M. Sebrier, H. Nazari, H.Meyer, B. M. Fattahi,A. Rashidi, 2012., New evidence for large earthquakes on the Central Iran plateau:palaeoseismology of the Anar fault , Geophys. J. Int. 189, 6–18.

Wada, Y., L.P.H.Van Beek, C.M. Van Kempen, J.W.T.M. Reckman, S.Vasak, and M.F.P. Bierkens, 2010., Global depletion of groundwater resources.Geophysical Research Letters 37, L20402.

Structural pattern of the Shirinak Cu deposit in the Urumieh-Dokhtar magmatic arc

Ebrahimi, Z.[1], Shahpasandzadeh, M.[1 *], Keshavarz, S.[1], Bani Amerian, J.[1]

[1]Department of Earth Sciences, Graduate University of Advanced Technology, Kerman, Iran
Email: mshahpasandzadeh@kgut.ac.ir

Emplacement of porphyry/vein-type Cu deposits is not only influenced by magmatic and hydrothermal processes, but also by the prevailing regional structures and tectonic regime (Richard et al., 2012; Asadi et al., 2014). The Cu deposits often occur in island arcs, continental magmatic arcs, and collisional tectonic setting. The geological studies (e.g. Shafiei et al., 2009; Zarasvandi et al., 2015; Asadi, 2018) manifest Cu deposits in the Kerman Cenozoic magmatic arc (KCMA), as the southeastern part of the Urumieh-Dokhtar magmatic arc, was associated with a common calc-alkaline magmatism and tectonic regime.

Determining structural pattern and role of structures in emplacement/deformation of the Cu deposits have a great importance in preparing 3D geological models and ore exploration. No structural studies have been carried out in the Shirinak Cu ore deposit yet. The purpose of this research is constraining structural pattern and determining structural controlling of the ore deposit. With detailed field mapping, geometrical/kinematic of the structures and their relationship with Cu mineralization have been constrained.

The Shirinak Cu deposit is mainly composed of Upper Eocene volcanic and pyroclastic rocks of the Razak Complex, which is intruded by sub-volcanic granodioritic-dacitic and latter dioritic-monzodioritic plutons, influenced by hydrothermal alterations. The Cu mineralization occurs mainly in the siliceous vein/veinlet networks.

According to this research, the 3D geological model of the ore deposit is suggested as a granitoid stock, intruded by dibasic dykes. In this model, intrusion of the granodioritic-dacitic plutons, as the first magmatic phase, was associated with ore mineralization. Emplacement of the stock is controlled by nearly parallel NW-SE striking right-lateral with reverse-component faults; similarly, the NE-SW striking left-lateral strike-slip faults restricted the plutonic extrusion. The vein/veinlet Cu mineralization often recorded along these latter faults, which usually intersect the former NW-SE striking faults. Interestingly, field evidences display a network of aforementioned fault system in the ore district. According to the interaction and mechanism of the prevailing fault system, we suggest a rhomboidal horst-graben structure for the Shirinak Cu deposit.

KEY WORDS: Structural style, structural controlling, fault, Shirink Cu deposit, Kerman

Reference:

Asadi, S., Moore, F. and Zarasvandi., A. 2014, Discriminating productive and barren porphyry Cu deposits in the southeastern part of the Central Iranian volcano-plutonic belt, Kerman region, Iran: A review. Earth-Science Reviews 138, 25–46.

Asadi, S., 2018, Triggers for the generation of post–collisional porphyry Cu systems in the Kerman magmatic copper belt, Iran: New constraints from elemental and isotopic (Sr–Nd–Hf–O) data, Gondwana Research, 64, 97-121.

Richards, J. P., Spell, T., Rameh, E., Razique, A. and Fletcher, T., 2012, High Sr/Y magmas reflect arc maturity, high magmatic water content, and porphyry Cu ± Mo ± Au potential: examples from the Tethyan arcs of central and eastern Iran and western Pakistan. Economic Geology 107, 295-332.

Shafiei, B., Haschke, M., and Shahabpour, J., 2009, Recycling of orogenic arc crust triggers porphyry Cu mineralization in Kerman Cenozoic arc rocks, southeastern Iran. Mineralium Deposita, 44, 265.

Zarasvandi, A., Rezaei, M., Sadeghi, M., Lentz, D., Adelpour, M. and Pourkaseb, H., 2015. Rare earth element signatures of economic and sub-economic porphyry Cu systems in Urumieh-Dokhtar magmatic arc (UDMA), Iran. Ore Geology Reviews 7, 407-423.

Kinematics and active tectonics of the NW continuation of the Zagros Main Recent Fault (NW Iran)

Niassarifard, M.[1], Shabanian, E.[2], Solaymani Azad, S.[3], Madanipour, S.[1]

[1]Department of Geology, Tarbiat Modares University, Tehran, Iran.E-mail: mehrdadniasari@gmail.com

[2]Department of Earth Sciences, Institute for Advanced Studies in Basic Sciences (IASBS), Zanjan 45137-66731, Iran

[3]Seismotectonics & Seismology Department of Geological Survey of Iran

The Main Recent Fault (MRF) is a major active strike-slip fault system on the border between the northern Zagros belt and Central Iran. Both the geometry and kinematics of the fault is rather well-known along its central part and at the SE termination of the fault system, while our knowledge on the geometry, structural pattern and kinematics of the continuation of the fault system towards northwest from the Piranshahr fault (NW Iranian Kurdistan) is insufficient. The lack of such kinds of data has hampered any conclusion on the structural and geodynamic roles of the MRF in the accommodation of ongoing deformation in NW Iran and SE Anatolia. Traditionally, the MRF is considered to be turn NW into the Bitlis thrust zone system changing its pure dextral strike-slip character. Nevertheless, possible relationship between this major crustal fault system and other main faults and their related deformation in NW Iran – SE Anatolia is unclear. This study is aimed at (1) characterizing both the geometry and kinematics of faulting, as well as the pattern of Quaternary displacements along the NW continuation of the MRF, and (2) describing its possible structural connection to the nearby main active faults of the region. The geodynamic role of the fault in the accommodation of ongoing convergence in NW Iran is investigated in the light of collected data and deduced results. We have used a combined approach including fault-slip data analysis and tectonic geomorphology to investigate active faulting of the MRF in NW Iran. More than 425 fault-slip data were gathered and analyzed from Quaternary and active fault zone in the region between Khoy and Piranshahr town. Our original results indicate that, to the north of latitude 37°N (NW from Piranshahr town), the main zone of the MRF continues northwards along a branch of the Neotethyan suture up to the sinistral Khoy – Baskale fault zone in SE Anatolia. This almost 200 km long active fault system is transtensional dextral in character and is constituted by several strike-slip and normal fault zones. Another branch of the MRF turns to NW in the north of Oshnavieh town into the Yuksikova-Semdinli fault in the southeast of Lake Van (Turkey). Our results also reveals that the NW continuation of the MRF clearly terminates to a NE-striking sinistral fault zone. In that area, the active dextral shear between Arabia-Central Iran is accommodated by ESE-trending extension localized at the intersection zone of the NNW-SSE dextral and NE-SW sinistral faults. The extensional basins in the west of Lake Urmia and SE Lake Van are resulted from this plate boundary related extension.

KEYWORDS: NW Iran; SE Anatolia; Zagros suture; Fault slip-data analysis; MRF; strike-slip fault

Active deformation in the north of Zagros – Makran transition zone using Quaternary fault kinematics data

Hassanzadeh, M.[1], Shabanian, E.[1], Ghods, A.[1]

[1]Department of Earth Sciences, Institute for Advanced Studies in Basic Sciences (IASBS), Zanjan 45137-66731, Iran
E-mail: a.hassanzadeh@iasbs.ac.ir

The transition between subduction to collision zones mostly are separated with sharp lithospheric fault. These fault zones are similar to transform faults and may capable of seismic activity. There are some regions in the world which have this condition, e.g., west of Greece (Baker et al., 1997) ،Taiwan (Kao et al., 1998) and New Zealand (Anderson et al., 1993). South-Eastern of Iran is the site of a rare case of young transition between the Zagros intra-continental collision and the Makran oceanic subduction. This transition zone is not like the above cases. Some geologists believe that the main structure and deformation of this zone is control by the ZMP (Zendan-Minab-Palami) fault system. There are scattered seismicity in the north and no seismicity in the south of this transition zone (Yamini-Fard et., 2006). Thus the pattern of seismicity in this area does not show a lineament around the ZMP fault system and this may indicate a complex deformation model. Therefore detection of nature, a pattern of active deformation and seismic potential of this transition zone is very important. Also, it would be useful to know more about other similar regions in the world.

In this study, data were used include remote sensing, satellite imagery, digitized geological and papers map, a pattern of active faults with topography and morphotectonic evidence and field observations. After preparing the fault map using remote sensing analysis of satellite images, depicted faults were controlled and validated by field observations. Structural data (mainly including bedding attitudes, strike, dip and rake of fault planes, with well-known senses) were gathered in several outcrops along the main fault zones in 12 days. The active tectonic investigations based on prepared fault maps, field observations, and fault-slip measurements in 15 important outcrops along the main faults, allows proposing a modern kinematic model for the northern part of the study area. This model explains a variety of faults with different kinematics, all compatible with a NE compression. Also, suggesting that active deformation is taken up by a complex fault network comprising differently-oriented faults reactivated in the present-day stress state.

KEYWORDS: Collision, Makran, Subduction, Transition zone, Zagros

References

Byrne, D. E., Sykes, L. R., & Davis, D. A. N. M. (1992). Great Thrust Earthquakes and aseismic slip along the plate boundary of the Makran, 97(91), 449–478.

Gholamzadeh, A., Yamini-Fard, F., Hessami, K., & Tatar, M. (2009). The February 28, 2006 Tiab earthquake, Mw 6.0: Implications for tectonics of the transition between the Zagros continental collision and the Makran subduction zone. Journal of Geodynamics, 47(5), 280–287.

Kao, H., Jian, P. R., Ma, K. F., Huang, B. S., & Liu, C. C. (1998). Moment-tensor inversion for offshore earthquakes east of Taiwan and their implications to regional collision. Geophysical Research Letters, 25(19), 3619-3622.

Niazi, M., (1980). Microearthquakes and crustal structure off the Makran coast of Iran. Geophysical Research Letters, 7(5), 297-300.

Regard, V., et al., (2010). The transition between Makran subduction and the Zagros collision: recent advances in its structure and active deformation. Geological Society of London, Special Publications, 330(1), 43–64.
Yamini-Fard, F., Hatzfeld, D., Farahbod, A. M., Paul, A., & Mokhtari, M. (2007). The diffuse transition between the Zagros continental collision and the Makran oceanic subduction (Iran): Microearthquake seismicity and crustal structure. Geophysical Journal International, 170(1), 182–194.

Seismotectonics of Central Alborz

Banimahdi Dehkordi, M. J.[1], Ghods, A.[1], Mousavi, Z.[1], Shabanian, E.[1], and Abbasi, M.[2]

[1]Institute for Advanced Studies in Basic Sciences
[2]University of Zanjan
E-mail: jdehkordi@iasbs.ac.ir

The tectonic activity in the Alborz mountain range, northern Iran, is due both to the northward convergence of central Iran toward Eurasia, and to the northwestward motion of the South Caspian Basin with respect to Eurasia. The motion is oblique to the belt and involves roughly ~5 mm/y of shortening and ~4 mm/y of left-lateral strike–slip motion. Previous studies have shown Central Alborz has a low rate of strain rate, especially around Tehran city. The low strain rate has been further distributed between several large active faults. The low seismicity, large recurrence time of earthquakes, a large number of active faults and sparse seismic networks are the main obstacles to study the seismotectonics of the region. There are several precise seismotectonic studies in Tehran region but they are for small regions, performed over short periods and does not cover the whole Central Alborz. To overcome some of the mentioned obstacles, we take two approaches. First, we have compiled a new catalog of earthquakes and focal mechanisms for Central Alborz by compiling waveforms of all permanent and temporary seismic networks in the region over the period of 1996-2019. By combining the data from all the networks, we have improved the azimuthal coverage and decreased the possibility of systematic location biases caused by deviations of the assumed travel time model from the true Earth. By expanding the time period of our catalog, we have increased the number of well-located events and focal mechanisms by as much as possible. We first located all events using manually picked Pg and Sg arrival times and then applied a multiple-event relocation analysis to precisely relocate some of the seismic clusters. Figure 1 shows single-event location of 490 events. By visual inspection of waveforms, we made sure that the selected events are not related to explosions. The selected events have Pg azimuthal gap smaller than 180 degrees. Figure 2 shows 60 focal mechanism solutions derived using first polarity method. To obtain the focal mechanism solutions, we face the problem of temporal polarity change of short period stations of IRSC seismic networks. We have overcome this problem by calibrating the polarities using larger events and also using teleseismic events. The seismicity map (Fig. 1) shows that the seismicity is mostly concentrated in the east of Central Alborz along Mosha, Firuzkuh, and Astaneh faults. Our focal mechanism solutions indicate a mostly left-lateral strike-slip mechanism. Unlike Firuzkuh and Astaneh faults, the seismicity along Mosha fault is more disperse, implying the fault is connected to a myriad of subsidiary faults. Seismicity along the so-called Garmsar fault is mostly limited to the segment south of Kavir Kuh and it seems that the eastern part of the Garmsar fault is related to the front of the salt glacier and is not an active fault. We detect a rather disperse and disconnected alignment of seismic events along Hableh Rud valley. The disconnected seismicity along the Hableh Rud is very correlated with the salt extrusions in the region. Events along the lineament have either thrust or strike-slip sense of motion. Second, in order to study the present-day crustal deformation, we use two types of data, first Iranian Permanent GPS Network (IPGN). It's contain 28 stations that data was collected from 2006 to the end of 2018 and second 55 km network stations, it's contain 18 stations. This is the first time such data will be used. Figure 3 indicates that IPGN stations generally scattered near Tehran, where Kahrizak, Mosha, and North Tehran faults located. East of the study

region, there are only one IPGN station and four 55 km stations. The concentration of 55 km network stations in this area helps us to investigate the answer of challenging question on North Alborz and Khazar faults in more details. The distribution of 55 km stations in south and east-south of Garmsar fault can help us to overcome the lack of IPGN stations in this area. In addition, in the west of the interesting area, liniments at the north of the Taleghan fault and south of the Eshtehard fault, have not covered by IPGN stations, while 55 km network covered all around this gap area. By collecting the combination of both GPS networks we can present more precise and valuable results.

KEYWORDS: Iran, Central Alborz, Seismotectonics, Focal mechanism, GPS, Faults

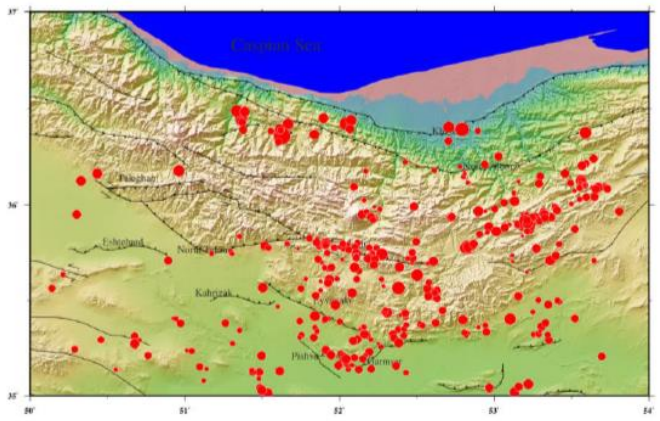

Figure 1. Seismicity around the Tehran by the permanent and temporary network. Red circles are selected earthquakes whose accuracy is estimated better than 5 km with a gap less than 180°.

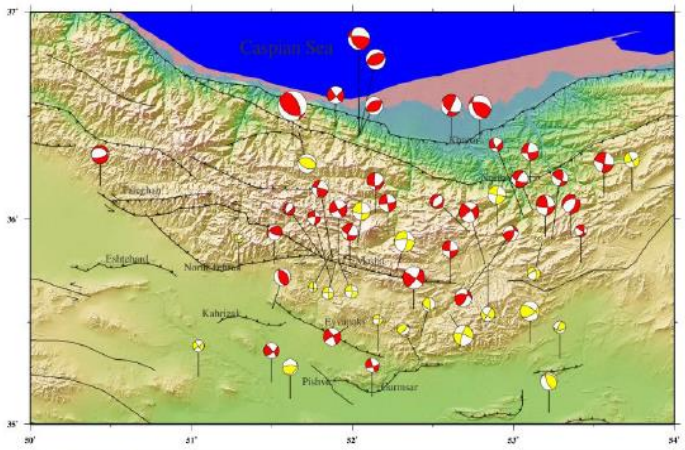

Figure 2. Map of the focal mechanisms. The red balloons are the most reliable mechanisms. Most mechanisms show left-lateral strike–slip and reverse.

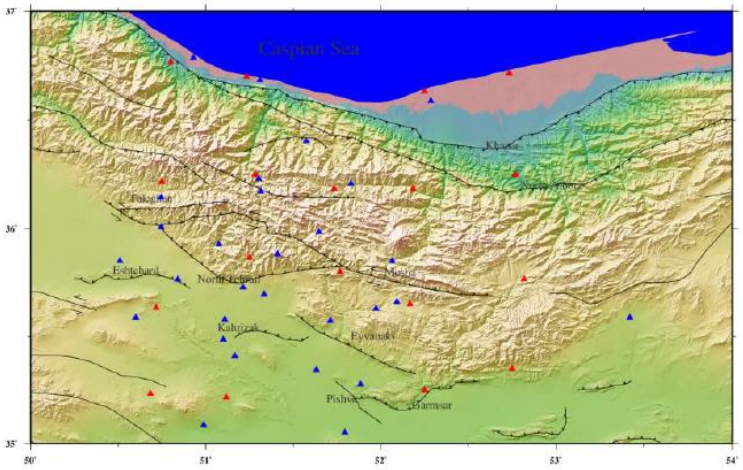

Figure 3. Location of the IPGN stations (blue triangle) and 55km stations (red triangle).

3rd TRIGGER International Conference
8-10 October 2019, Zanjan, Iran

Institute for Advanced Studies in Basic Sciences
Gava Zang, Zanjan, Iran

Fault kinematics and stress history in the Makran accretionary wedge, SE Iran

Aghdamirad, H.[1], and Najafi, M.[1]

[1]Institute for Advanced Studies in Basic Sciences
E-mail: hamidaghdamirad511@gmail.com

The Makran is one of the largest accretionary wedges on Earth, produced from the convergence between the Arabian and Eurasian plates since the Late Cretaceous. It is associated with the active subduction of the Arabian oceanic lithosphere at a present-day rate of about 20 mm/a in an almost northward direction (McQuarrie et al. 2003).

In this study, a combination of remote-sensing mapping and field survey (more than 700 measurements) permit to define the gemetry and mechanism of faulting and the variations of stress field in time and space, across the Makran. The results indicated that, the modern stress field in the north, inner, outer and the north part of the Coastal Makran has an NE-SW compression direction, which is in accordance to earthquake focal mechanisms and GPS vectors. Althoug, the paleostress field show an N-S compression direction, perpendicular to the trend of folds and thrusts. This early E-W fold-and-thrust system is displace by NE-SW sinistral and N-S dextral recent transverse faults. However, the coastal Makran has experienced a different evolution of the stress fields. The area had an NNE-SSW compressional system during Miocene, which was replaced by an extensional regime in Plio-Quaternary. Consequently, the Miocene sedimentary rocks in the north part of the Coastal Makran recorded both compressian and extensional events, although, the Plio-Quaternary sediments only show the extensional fault systems (Fig. 1).

KEYWORDS: Makran Accretionary Wedge, Subduction Zone, Fault Kinematic, Stress Field

سازمان زمین‌شناسی کشور
GEOLOGICAL SURVEY OF IRAN
SORBONNE UNIVERSITÉ
cnrs

The Kharvana Fault System as an active fault system in NW Iran

Mesbahi, F.[1], Bakhti, K.[1]

[1]University of Tabriz, Faculty of Natural Science, Department of Earth Sciences
E-mail: mesbahif@tabrizu.ac.ir

The NW Iran as a part of the Alpine−Himalayan orogenic belt is a dynamic and unstable region from the viewpoint of tectonic and seismicity. Although several articles have already studied active faults of NW Iran, many faults in this region are still remained unknown or not investigated. The Kharvana Fault System is intoducing for the first time in this research.

The Kharvana Fault System with general NW−SE trending folds and right-lateral strike-slip and reverse faults is located in NW Iran, North-West of Tabriz city.

The geological maps, Landsat satellite images, earthquake catalogs and field measurements have been used to verify structural and active tectonic features of the Kharvana Fault System.

The Kharvana Fault System could be considered as the southeastern continuation of the Nakhichevan−Sardarapat fault system in Azerbaijan toward NW Iran. The Nakhichevan−Sardarapat fault system with dextral strike-slip movement, consists of four segments with left-step en-echelon pattern.Toward SE, the Kharvana Fault System reaches to the Qoshadagh active fault.

The WNW-ESE trending Qoshdagh Fault is a dominantly dextral strike-slip fault that is also called South Ahar fault. The Qoshdagh Fault, is one of the most important active faults in NW Iran, from the viewpoint of seismicity. In 2011, the twin earthquakes with the magnitudes of 6.1 and 6.3 in Richter scale have occurred along the Qoshdagh Fault, which led to a lot of destruction and death in the Ahar and Varzeqan towns. The major faults within the Kharvana Fault System from North to South are Kharvana Fault with dextral strike-slip movement, Estarkhan−Komar fault with reverse movement, Nahand fault with dextral strike-slip and reverse movements and Zonouz fault with dextral strikeslip movement.Based on the occurrence of earthquakes up to magnitude of 5 in Richter scale and dextral displacement of the drainage pattern along the major faults within the Kharvana Fault System, it is an active fault system.

KEYWORDS: NW Iran; Kharvana Fault System; dextral strike-slip fault; reverse fault; active fault

Geological arguments for a devastating earthquake in Alborz province

Malekzade, Z.[1]

[1] Department of Geology, Payame Noor University, PO BOX 19395-3697, Tehran, Iran.

This article introduces the Alborz Master Fault Zone (AMFZ) as one of the major active fault systems in Alborz orocline north of Iran. The AMFZ is a left-lateral strike-slip fault system extending over a distance of 500 km from Tazareh syntax to the east to the Rudbar syntaxes in the west and is related to oblique underthrusting of the South Caspian Sea plate beneath central Iran. Therefore, the AMFZ is accommodating the boundary-parallel components of slip along obliquely convergent plate margins. The AMFZ follows the strike of the Alborz orocline with two different N65E in the eastern part and N65W in the western part. Each part of the AMFZ is responsible for the devastating earthquakes. The fatal one was Qumis earthquake that is amongst the five biggest events in the world.

The stress state along the AMFZ changed after the reorganization of Arabian plate convergence in respect of the Eurasia and/or after developing the rectilinear Alborz to the orocline. This event is in connection with the change of the transpressional tectonic regime to the transtensional one. This study decides to show that after the change of stress state, the step overs that have already divided the AMFZ to segments, play the role of the barrier against earthquake rupture and/or the rupture, unless in especial condition, could not jump from one segment to another. This behavior of the faults may suspect the Astaneh as the only causative fault for the Qumis earthquake that is a traditional earthquake in Alborz.

Post-Pliocene Faulting in Polour region, central Alborz

Sharifi, A.[1], and Yassaghi, A.[1]

[1]Department of Geology, Tarbiat Modares University, Tehran, Iran
E-mail: a_sharifi@modares.ac.ir

Structural analysis of Polour region in south and southeast of Damavand Mount in the central part of Alborz demonstrates evidence of recent fault activity in Mesozoic to present deposits. In this region, Quaternary basaltic and trachyandesitic rocks of Damavand Mount are the youngest masses laying on the quaternary alluviums. Detailed structural mapping resulted in identification of two main NW and NE-trending fault zones. The NE-trending faults that cut the quaternary rocks of the Damavand Mount eruption are younger and have also cut the NW-trending one. Study of the fault kinematic indicators such as slickensides and riedel shear fractures shows the faults mechanism from normal to oblique slip (left-slip fault with normal component). Since the faults has cut the Damavand quaternary rocks, they are the youngest faults in the region. It is proposed that the faults, like the NE-trending Karaj-Chaloos Fault, have developed more likely by reactivation of older basement faults during northwest wards movement of the South-Khazar block since Pliocene.

KEYWORDS: Central Alborz, NE-trending, left-slip Fault, Pliocene, South-Khazar block, Recent faulting

Evaluation of Anthropogenic Contribution to Groundwater loss Using by GRACE Satellite Gravity Data

Asaadi, S.[1], and Joodaki, G.[1]

[1]Department of Surveying Engineering, University of Zanjan (ZNU), Zanjan, Iran

E-mail: Shahabasaadi71@znu.ac.ir

In recent years and decades, the issue of drought has become one of the biggest global problems in all arid and semi-arid regions of the world. Undoubtedly, identifying and monitoring drought can be a great step toward struggling this global problem and reducing the resulting damage. The purpose of this thesis is to investigate the feasibility of estimating the amount of groundwater in agriculture uses by using GRACE satellite data. The level-2 GRACE satellite data is used to estimate the monthly changes in groundwater levels in the Central Plateau Basin during the period January 2003 to July 2017. The results show a sharp decline in groundwater level changes trends (a volume decline of about 142 cubic kilometres during this period) in the centre of Iran. By correcting and removing the share of water equivalent to snowfall, rainfall, canopy and soil moisture, and also by using the GLDAS hydrology model, it was shown that how much the groundwater volume has declined, and by removing the amount of groundwaters from the results we find how much of the uses were used in agriculture.

By using piezometric wells data as the correct data, and comparing them with the data obtained from GRACE satellite, we found that these two series of data were in good matching, and it was concluded that by using GRACE satellite data, the amount of groundwater reserves with an acceptable accuracy could be estimated.

KEYWORDS: Drought, Groundwater, Hydrology, Grace Satellite, Piezometric wells

LAND SUBSIDENCE ANALYSIS IN THE ARDABIL PLAIN USING SBAS-INSAR TECHNIQUE

Ghorbani, Z.[1], Joodaki, G[1], and Javadnia, E.[1]

[1]Department of Surveying Engineering, University of Zanjan (ZNU), Zanjan, Iran

E-mail: zahra.gh@znu.ac.ir

Ardabil Plain with an approximate area of 1097/23 km², is an inter-mountain plain in northwestern Iran in the geographical coordinates of 38°5' to 38°27' North latitude and 48°9' to 48°37' East longitude, has been encountered a significant drop in groundwater in recent years. Land subsidence due to the exploitation of groundwater resources, and severe atmospheric changes; is one of the environmental problems that must be investigated in a long-term research. Previous studies in this study area have also generally focused on geotechnical methods of soil layers and geology to use deformation information along with underground numerical simulations to detect land subsidence mechanisms. However, a combination of radar interferometry technology and remote sensing technology to investigate land degradation factors at various scales has rarely been studied. Therefore, Interferometric SAR technique based on Small Baseline Subset (SBAS-InSAR) time series analysis has been used to measure the displacement with the approach of creating a permanent monitoring system and to show an overview of the existing threats posed by the subsidence of Ardabil plain. In this study, two ENVISAT ASAR satellite image datasets were selected for the period 2003 to 2006 related to descending pass orbits for track 235 with 16 images and track 6 with 20 images. By analysing the two descending pass data along the satellite line of sight, we find that both tracks have a high degree of correlation and relatively good temporal overlap. Processing of radar images shows that the southeastern part of Ardabil Plain, which has the largest volume of deep wells utilized for agricultural and drinking purposes in the region, had the highest subsidence behaviour compared to other areas. After reduction of residual topographic, orbit errors and atmospheric phase error with the weather model corrections, the maximum subsidence rate in Ardabil Plain was about 11 to 14 mm/year, which is consonance with geotechnical modelling results. Thus, the feasibility and applicability of SBAS-InSAR technique in monitoring the surface deformation of the study area could be one of the most suitable and effective methods for monitoring local subsidence phenomena at different scales.

KEYWORDS: Ardabil Plain; Subsidence; Groundwater; ENVISAT ASAR; SBAS-InSAR; Time-Series

3rd TRIGGER International Conference
8-10 October 2019, Zanjan, Iran
Institute for Advanced Studies in Basic Sciences
Gava Zang, Zanjan, Iran

Comparison of Different data Processing Strategies for Precise GPS Observations across the Makran accretionary wedge, SE Iran

Kheradmandi, M.[1*], Abbasi, M.[2], Najafi, Z.[1], Mousavi, S.[1], Abbasy, S.[3]

[1]Department of Earth Sciences, Institute for Advanced Studies in Basic Sciences (IASBS), Zanjan, Iran
[2]Department of Surveying Engineering, University of Zanjan, Zanjan, Iran
[3]Department of Surveying Engineering, University of Isfahan, Isfahan, Iran
Email: mohana.kh@iasbs.ac.ir

The Makran accretionary prism is formed in the subduction zone between the Arabian and Eurasian plates. Despite recent studies on the seismicity and structure of Makran, its active deformation is not fully constrained. For this purpose, we installed 6 temporary GPS stations across the Makran onshore accretionary wedge in southeast of Iran, from coastal line to the Jazmuran depression. These stations were measured in two epochs in 2017 and 2018 with two Trimble 5700 receivers in three consecutive sessions.

In this study we investigate the performance of two main GPS data processing strategies, i.e. differential and Precise Point Positioning (PPP) for geodynamics applications. A differential processing software gives the characteristics of the spatial baselines created between stations while the PPP strategy gives directly the position of the station without any connection with other adjacent points. This is why in PPP method one can directly estimate the velocity vector for each station.

In differential processing, two methods have been considered: the first one was to process only the baselines between three pairs of stations giving the baseline of each session, and the second one was to use the International GNSS Service (IGS) stations as reference points. The first method was conducted using an available software and the second method via the online differential processing software AUSPOS.

In PPP method we used two online processing services: CSRS-PPP and APPS. The first service is given by the Natural Resources Canada (NRCAN) and the second one is given by Jet Propulsion laboratory (JPL) of NASA.

The baseline length is the key parameter for geodynamical interpretations. The length obtained from PPP method as well as from the differential processing AUSPOS service is compared by the lengths estimated from differential processing software. The results are presented in Table below.

In Makran GPS profile conducted by Institute for Advanced Studies in Basic Sciences (IASBS) there are six stations AZIZ, RAHM, RAMZ, TKHT, ESPK and SHMS. The measurement duration on each station is at least 48h with 30s interval.

As it can be seen from this Table, the online service CSRS-PPP gives the nearest results to the classical differential processing method. It can be suggested therefore that this free service can be confidentially used for precise GPS data processing. The other advantage of this service is that it gives the geocentric position and the corresponding error ellipse of any point at the end of processing. One can therefore estimate the point velocity as well as its error ellipse for each point separately.

Table. Differences of the baseline lengths estimated from different computation services with the lengths obtained from differential GPS processing software. Measurements have been done in 2017 and 2018.

Baseline	AUSPOS (mm)	CSRS-PPP (mm)	APPS (mm)
AZIZ-RAHM (2017)	0.117	0.053	0.168
AZIZ-RAHM (2018)	1.637	0.572	1.113
RAMZ-TKHT (2017)	0.365	0.493	3.526
RAMZ-TKHT (2018)	0.725	0.032	0.095
ESPK-SHMS (2017)	1.150	1.482	0.967
ESPK-SHMS (2018)	0.898	0.024	0.305

KEYWORDS: APPS; AUSPOS; CSRS-PPP; Geodynamics; GPS; Makran accretionary wedge

An investigation in the location forcasting of large earthquakes and subsequent aftershocks using coulomb stress changes in the oblique collision zone of arabiaeurasia tectonic plates

Rastbood, A.[1], Bulghar, R.[2], Ghanouni, B.[3] and Ghasemzadeh, A.[4]

[1]Assistant Professor, Tabriz University, Tabriz, Iran. E-mail: arastbood@tabrizu.ac.ir
[2]MsC Student, Tabriz University, Tabriz, Iran
[3] MsC Student, Tabriz University, Tabriz, Iran
[4] BsC Student, Tabriz University, Tabriz, Iran

Human being has been faced with destructive natural phenomenon specially earthquake for a long time. It is essential to know the time and place of large earthquakes and their aftershocks in order to warn of them to reduce the physical and financial damage. Maybe these days we can't predict the earthquake occurrence exactly but the study about previous earthquakes can identify the areas with high seismic potential and with this knowledge in building construction we can mitigate the damages due to a large earthquake. Study of stress changes in the Earth's crust is useful for the predicting of earthquakes probability. Analysis of Coulomb Stress Changes has been used in many seismic zones. These studies showed that the area and the magnitude of next earthquake will affect by the static stress changes which are the result of previous earthquakes in the region. In order to investigate the possible location of large earthquakes, we compute cumulative co-seismic Coulomb Stress Changes of 249 historical and instrumental earthquakes with magnitude (M > 5.5) in nine major regions in the oblique collision zone of Arabia – Eurasia tectonic plates, in historical order, using the component of stress associated with the fault orientation and slip direction of the next event. The results of the earthquake interactions, show falling before or after of some next event. Also in order to know about the area with the highest earthquake probability, we compute the cumulative Coulomb Stress Change caused by the co-seismic deformation of historical and instrumental earthquakes on strike-slip and reverse fault planes with optimum geometry. The results show that the hazardous areas that have the potential for large earthquakes, could be the areas in the region of increased co-seismic Coulomb Stress Change due to previous earthquakes and an active fault in the optimum direction of strike-slip and reverse faults. Nine major regions of study area include: 1- NW IRAN, 2- Talesh, 3- Alborz (Central and East Alborz), 4- Kopeh-Dagh, 5- Zagros (north and south sections), 6- Zagros-Makran transition zone, 7- eastern region of IRAN, 8-Makran subduction zone, 9-Central region (east and west sections). Study area is divided into 13 sections for three main reasons: (a) The regional stress directions in different regions of IRAN are different, (b) Performing large-area computing at high resolution will greatly increase processing time and (c) The co-seismic Coulomb Stress Changes on next events at high spatial intervals, will be very low or zero. Also, in order to investigate the possibility of spatial forecasting of aftershocks caused by an earthquake, we estimate the correlation between spatial distribution of aftershocks and Coulomb

Stress Change pattern due to main-shock. The computation of Coulomb Stress Change of mainshock was performed on strike-slip and reverse faults with optimum geometry and also on faults with known geometry in the region. According to our calculations, most of the aftershocks occurred in the areas of increased Columbian *S*tress Changes due to the main-shock.

KEYWORDS: Active Faults; Coulomb Stress Changes; Dislocation; Earthquake.

Multiresolution analysis of geodynamic network in theoblique collision zone of arabia-eurasia tectonic plates using spherical wavelets

Rastbood, A.[1], Bulghar, R.[2], Ghanouni, B.[3] and Ghasemzadeh, A.[4]

[1]Assistant Professor, Tabriz University, Tabriz, Iran
[2]MsC Student, Tabriz University, Tabriz, Iran
[3] MsC Student, Tabriz University, Tabriz, Iran
[4] BsC Student, Tabriz University, Tabriz, Iran
E-mail: arastbood@tabrizu.ac.ir

In this research we present a spherical wavelet-based multiscale approach for estimating a spatial velocity field on the sphere from a set of irregularly spaced geodetic displacement observations.

Because the adopted spherical wavelets are analytically differentiable, spatial gradient tensor quantities such as dilatation rate, strain rate and rotation rate can be directly computed using the same coefficients. In a series of synthetic and real examples, we illustrate the benefit of the multiscale approach, in particular, the inherent ability of the method to localize a given deformation field in space and scale as well as to detect outliers in the set of observations. This approach has the added benefit of being able to locally match the smallest resolved process to the local spatial density of observations, thereby both maximizing the amount of derived information while also allowing the comparison of derived quantities at the same scale but in different regions. We also consider the vertical component of the velocity field in our synthetic examples, showing that in some cases the spatial gradients of the vertical velocity field may constitute a significant part of the deformation. This formulation may be easily applied either regionally or globally and is ideally suited as the spatial parametrization used in any automatic time-dependent geodetic transient detector. We have presented both synthetic and real examples of multiscale estimations of velocity fields on the sphere. This technique is well suited for dense geodetic networks and is straightforward to implement. First, we estimate a two-component velocity field using spherical wavelet frame functions of multiple scales. We then compute gradient quantities directly from the estimated field to identify potential deformation signals. The primary control on the estimation is the spacing among the stations. Where stations are dense, we allow for short-scale spherical wavelets in the estimation; where stations are sparse, we allow only long-scale spherical wavelets in the estimation.

In our multiscale estimation, the residual field between the original field and estimated field may reveal two key features. First, if there are systematic residuals in a particular region, then it is probable that one needs to include shorter-scale wavelets in the estimation. Second, if there is a strong residual at a single station, then the station is ‘anomalous’ and is either malfunctioning or is capturing a signal that is not spatially resolved. The synthetic examples illustrate several basic points. In the example with two dilatational sources, one much larger than the other, we saw the advantage of the separation of scales in identifying subtle signals. This example also suggests that derivative quantities based on observations from multiple sites will perform better in detecting signals than the individual components of the velocity field and that the vertical component, if available, should be used in estimating the velocity field, since deformation may not be predominantly in the horizontal directions. With the real observations, we show the usefulness of separating the three-component velocity field into constituent scales. The vertical velocity field contains spatially coherent features

with length scales typically less than those observed in the horizontal velocity field, which reveal deformation across a broad plate boundary zone. Although some of the vertical velocity observations are certainly influenced by non-tectonic effects, they should still be included—along with proper uncertainty estimates—in the monitoring of signals in dense geodetic networks, especially in areas with larger expected vertical motions, such as subduction zones. Regularization is required to obtain a smooth estimated velocity field from the discrete observations. This is achieved through two possible actions. First, one can cull the set of possible spherical wavelets based on the coverage of observations. If each spherical wavelet has a sufficient number of observations constraining its coefficient, then no regularization is needed.

Second, if all spherical wavelets are used for the inverse problem, then extensive regularization will be needed, since most wavelets will have zero observations constraining their corresponding coefficients. In our approach, we have chosen something in between these two 'end-members,' where we at the outset eliminate many candidate spherical wavelets based on data coverage, but we still require a moderate amount of explicit regularization in the inversion. Our ultimate objective is to monitor time-dependent signals in dense GPS networks. Because our emphasis is on continuously recording GPS networks, our station coverage is not as dense as many published velocity fields, which include campaign GPS measurements. In this study, we have only dealt with the spatial part of the problem, showing that the multiscale representation is well suited to identifying and characterizing geophysical signals of all scales. It also has the potential capability of removing scale-specific noise. This approach is a step towards global multiscale monitoring of time-dependent GPS displacement fields, in hopes of efficient and accurate characterization of Earth's surface deformation and the detection of geophysically important phenomena.

KEYWORDS: GPS Velocity Field; Spherical Wavelet; Multi-Resolution Analysis.

Influence of wavelength radar images in estimation of open-pit mine displacements using radar interferometry technology (case study: Gol Gohar Sirjan mine)

Shami, S.[1], Ghorbani, Z.[2]

[1]Faculty of Geodesy and Geomatics Engineering, K. N. Toosi University of Technology, Tehran, Iran 1st
[2] Department of Surveying Engineering, University of Zanjan (ZNU), Zanjan, Iran 2rd
E-mail: (siavashshami@email.kntu.ac.ir)

The volume of minerals extracted from open-pit mines has always been of interest to mining managers. In investigating displacement from open-pit mines and the dangers of its subsidence, Radar interferometry with extensive ground cover, continuous and suitable temporal and spatial resolution against methods such as alignment Leveling, Global Positioning System and UAV photogrammetry which is generally expensive and time consuming, is an appropriate technique. Because open-pit mines include large-scale displacement, the maximum displacement that can be extracted through Radar interferometry technology is affected by two factors: the wavelength of the radar images and the pixel dimensions of the Radar images. By maximising the wavelength of images or decreasing the pixel dimensions of images, the maximum displacement obtained by Radar interferometry technology can achieve. On the other hand, quick extraction in open-pit mines creates a de-correlation between the images, which reduces the maximum displacement. To eliminate de-correlation between images, selecting images with small spatial and temporal baselines can solve this problem. In this study, the displacements of Gol Gohar Sirjan Mine No. 3 using interferograms obtained from ENVISAT images with a wavelength of 5.5 cm and ALOS-1 images with a wavelength of 23.5 cm and the volume extracted from No. 3 of mine calculated. The results show that although the temporal baselines and pixel dimensions of the ENVISAT images were smaller than the images of ALOS-1, the higher the wavelength of the images of ALOS-1 Radar, and Detection and more extracted volume can be calculated. So that the maximum detectable displacement of the ENVISAT images is 7.5 cm and that for the ALOS-1 images is 26 cm. Therefore, as the Radar images wavelength increases. The amount of displacement is more detectable, and the volume calculated from the mine will also come close to reality.

KEYWORDS: Radar Interferometry; Open-pit Mines; Wavelength Radar Images; Displacement; Large-Scale; Gol Gohar Sirjan Mine

Application of fuzzy logic to identification planation surfaces using Geomorphometric parameters in DEM

Latifi, S.[1]

[1]Payame Noor University of mianeh
E-mail: S_latify@yahoo.com

Planation surfaces characterized by slightly undulating and generally featureless topography can result from long continued erosion and deposition in the absence of active deformation. When such low relief surface are uplifted tectonically and intersected by erosion, they can form prominent markers in the landscape. Since a standard identification method for preserved planation surface of other prominent landforms has not been performed. Therefore, the use of local data and accurate analysis of this data is important for the proper description of the geomorphology of the land surface and has been growing at the level of current research.Therefore, the main purpose of the present study was to identify the planation surfaces in the southern slopes of bozgush mountain range using geomorphometric parameters using fuzzy logic method based on digital elevation model (DEM) in geographic information system (GIS). In order to achieve this goal, four effective parameters including: (1) curvature profile, (2) terrain ruggedness index, (3) slope and (4) surface ratio were prepared. Each of raster layers defined and evaluated using of fuzzy membership function method. After applying the functions, the membership degree was determined over the fuzzy overlay and the final map was executed. The result show that planation surfaces with more then eighty percent of membership degree is corresponds properly with field observations and geological studies. All these indicate that they are remnants of once regionally continuous Planation surfaces which were deformed by both the lower crust flow and the faults in upper crust, and dissected by the network of Shahrchai River.

KEYWORDS: bozgush, DEM, fuzzy logic, geomorphometric, planation surfaces, tectonic.

Investigation of Kermanshah Aftershock Sequence using SAR Interferometry

Jafari, M[1], Mousavi, Z[1], Aflaki, M[1], Motaghi, K[1]

1Institute for Advanced Studies in Basic Sciences
E-mail: mjafari@iasbs.ac.ir

In this study, we have investigated three aftershocks associated with the Mw 7.3 Kermanshah 2017 earthquake. On 25 August 2018, an earthquake with the magnitude of Mw 6.0 occurred in SW of Javanrud in Kermanshah. The second one with the magnitude of Mw 6.3 occurred in SW of Sarpol-e Zahab on 25 November 2018 and the third one occurred in SW of Halabjah (Iraq) with the magnitude of Mw 5.2 on 11 May 2019. Data were acquired on ascending and descending Sentinel-1 satellite passes. We used GMTSAR package to process SAR data. After the interferogram generation, ZTD and planer correction have been applied by data which is provided through Generic Atmospheric Correction Online Service for InSAR (GACOS) website. We estimated the coseismic displacement map related to this aftershock sequence. Then, we evaluated the causative fault plane for the first aftershock, Javanrud, by using Okada [1985].

KEYWORDS: Aftershock, Kermanshah, Sentinel-1, GMTSAR, ZTD

Permanent GNSS Network for Crustal Deformation Monitoring in Iran

Nankali, H.[1], Saadat Y-djamour, A.[1], Walpersdorf A.[2], hossini, S.[1], khorami, F.[1], Tavakoli, P.[1], Tavakoli, F.[1], Mousavi, Z.[3], Sedeghi, M.[1]

[1]National Cartographic Center of Iran- Tehran, Azadi Sq.Meraj Ave. Po.Box:13185-1684

[2]University Grenoble Alpes, CNRS, IRD, IFSTTAR, ISTerre, 38000 Grenoble, France

[3]Department of Earth Sciences, Institute for Advanced Studies in Basic Sciences (IASBS), Zanjan, Iran

Email: nankalihamid@gmail.com

In 2005, National Cartographic Center of Iran (NCC) engaged to establish the Iranian Permanent GNSS Network (IPGN) covering the whole country for continuous measurements.We present the most extensive new unified GPS velocity field and times series, including all newly processed data from the Iranian Permanent GNSS Network (IPGN) collected for 12 years (2006-2018). Finally, we obtain the most comprehensive strain rate map of Iran at large scale. This new processing will bring us more precise information on reference frame realization, crustal deformation, fault slip rate and geophysical phenomena in Iran.

Earthquake Probability investigation by defining high risk areas in Kermanshah and its surroundings by means of Probabilistic Seismic Hazard Assessment

Amirian, F.[1], Dolatabadi, N.[2], Sadidkhouy, A.[3]

[1]M.Sc. student, Institute of Geophysics, University of Tehran, Iran
[2]M.Sc. student, Institute of Geophysics, University of Tehran, Iran
[3]Assistant Professor, Institute of Geophysics, University of Tehran, Tehran, Iran.
E-mail: asadid@ut.ac.ir

Kermanshah province is located in the Zagros seismotectonic province and has witnessed many earthquakes throughout history due to its special position. The Zagros is located on the northern margin of the Arabian Plateau on the Precambrian metamorphic basement. From a structural point of view, the convergent movement of the Arabian Plate in the southwest and the central Iranian ridge in the northeast has produced this strip. Kermanshah province has high seismic activity due to its location in the Zagros area. One-way catalogs and fault maps for the area are needed for hazard analysis. Using geological maps of the study area and using QGIS software, a map of faults was prepared. Then, a catalog of historical and instrumental earthquakes of the area was prepared using earthquake databases (USGS, IRSC, IRIS, ISC). The catalog must be on one magnitude scale to integrate the catalog. Therefore, by using the empirical relationships obtained by drawing graphs, these magnitudes are transformed and all are transformed and ordered in terms of unique magnitude. A-value, b-value, Mc and other seismic parameters calculated using zmap software. Based on the trends of earthquake faults and clusters, seismic maps were selected for the two area source and seismic parameters and zmap diagrams were obtained for each source. The KIJKO software is used to obtain the parameters needed to prepare hazard analysis maps. Using Campbell-Bozorgnia attenuation relationship, CRISIS 2015 software performed hazard analysis and mapping. Given that the buildings in the study area are with the period of the structures is 0.4 (s) and 1(s). Peak ground acceleration and spectral acceleration is calculated for the return period of 50 years and 475 years.

KEYWORDS: Crisis, Hazard map, Kermanshah, QGIS.

Presenting Uniform Hazard Spectra maps for the probabilistic seismic hazard assessment of Zanjan region including the 1990.06.20 Rudbar earthquake

Sirati, E.[1], Dolatabadi, N [2], Sadidkhouy, A.[3]

[1] M.Sc. student, Institute of Geophysics, University of Tehran, Iran, [elaheh.sirati@yahoo.com]
[2] M.Sc. student, Institute of Geophysics, University of Tehran, Iran, [syn_org939@rocketmail.com]
[3] Assistant Professor, Institute of Geophysics, University of Tehran, Tehran, Iran.
E-mail: asadid@ut.ac.ir

Zanjan historical area placed in Alborz-Azerbaijan seismotectonic province has undergone many geological changes due to seismic events and has experienced many casualties and financial losses. The city of Rudbar survived a M=7.3 earthquake in 1990.06.20 which caused faulting and put a lot of focuses in this area as it suffered the loss of 14000 people and many building collapsed duo to usage of material without sufficient resistance. Therefore, a way to reduce risk (hazard) and have a better understanding of the area and alternatively build safely, hazard assessment studies are required. The probabilistic hazard assessment reflects a more realistic result of seismic event by collecting, merging catalogues from Mousavi et al. For historical earthquakes from pre A.D. to 2012 and seismological institutes like ISC (International Seismological Center), IRSC (Iranian Seismological Center) including from 2003 to 2019 and obtaining formulas based on magnitudes. To avoid duplicated data's a Matlab plugin named Zmap was used and the catalogues were declustered by Reasenberg method. At the end two sources were determined based on seismotectonic, fault systems and seismicity of the area and b-value, a-value and Mc for each source was calculated as well. With the help of KIJKO other useful parameters such as Beta, Lambda and M-max was acquired and later on in Crisis these parameters were used plus CampellBozorgnia2008 (Campbell, K. W., and Y. Bozorgnia (2008)) attenuation relation for soil properties compatible with Vs30 and as a result the spectral acceleration (SA) at the period of 0.2 second and peak ground acceleration (PGA) was also calculated. The calculated PGA for the region for return periods (probability of exceedance) of 50, 475, 1000 and 2475 years which the values respectively are 0.4, 0.6, 0.7 and 0.9 g were mapped and Uniform Hazard Spectra (UHS) showed the dangerous zones for the period of 0.2 s as well and the SA for these areas were between 1 to 2 g.

KEYWORDS: Crisis; Kijko; Rudbar; USH; Zanjan

A new method in Probabilistic Seismic Hazard Assessment and Site Effect Exertion using Python Libraries in Kerman Region

Dolatabadi, N.[1], Amirian, F., Rahimi, M.[2], Sadidkhouy, A.[3]

[1] M.Sc. student, Institute of Geophysics, University of Tehran, Iran
[2] M.Sc. student, Institute of Geophysics, University of Tehran, Iran
[3]Assistant Professor, Institute of Geophysics, University of Tehran, Tehran, Iran.
E-mail: asadid@ut.ac.ir

Kerman City has been constructed and expanded on the young Quaternary alluvial deposits. Due to geological conditions, the young and active faults of the region and old faults have been a tremendous history in terms of seismicity. According to researchers, the main reason for the occurrence of earthquakes in Iran is the movement and pressure of Saudi Arabia towards the north due to the opening of the Red Sea. The probabilistic seismic hazard assessment (PSHA) is based on homogeneous earthquake catalogue collected by merging available global catalogues (e.g. International Seismological Center (ISC), USGC, Iranian Seismological Center (IRSC), U.S. Geological Survey (USGS) and Incorporated Research Institutions for Seismology (IRIS)). The catalogue time range goes from Historical Earthquakes to 2019. However, this may result in repetitive data and dependent events, so HMTK Plugin which is implemented within OpenQuake software were used to decluster and calculated seismicity parameters. Nevertheless, due to lack of HMTK in Reasenberg declustering method, a python code written by Kris Vannest was used. Two seismic source zone have been selected due to seismicity, seismotectonic, regional structural geology and fault systems within neotectonic settings of the study area. The b-value stability is reserved regionally and defers less than uncertainty limit. Hazard computations have been done using OpenQuake (version 3.6). The peak ground acceleration (PGA) and spectral acceleration (SA) at periods of 0.2, 0.8, 1.0 and 2.0 s were calculated using a ground motion prediction equations (GMPEs) for active shallow crust, CampbellBozorgnia2008 for soil Properties corresponding to Vs30. calculated SA and PGA for the study area in selected periods were mapped and Uniform Hazard Spectra (UHS) indicates the value of the ground motion parameter vs. the structural periods in a defined probability of exceedance (return period) was calculated as well.

Keyword: Crisis, Kermanshah, GMPE, Openquake, PSHA, UHS.

Evaluation of the effects of cement industries from Health, Safety and Environment (HSE) view

Pourmajidi, P.[1], Tavakoli, A.[2]

[1]Undergraduate Student in Mine Engineering, University of Zanjan
[2]Assistant Professor in Civil and Environmental Engineering, University of Zanjan

The concept of HSE, with a new approach toward health, safety and environment, is a critical subject in the process of development for countries and human societies. HSE include a comprehensive management system which try to consider different aspects of health, environment and safety in a working place or an industry, and predict the potential hazards, accidents and disadvantages in this regard. On the next step, HSE suggest the prevention-based approaches in order to minimize costs, dangers and pollutions. Global development is closely linked with technology, innovation and economic value but, on the other hand cause the pollution and environmental degradation.

Cement industry as one of the fast growing sectors in Iran, is the subject of this research but from the HSE point of view. The current capacity of this industry in country is about 80 million tones and will increase to the 120 million tones for the 1404 horizon. The cement industry is one out of seven strategically selected industries which plays a critical role in country's income, share of added value, employment, market, and so on. The process of cement production is associated with various environmental, biological and social damages. Air pollution, soil degradation, waste production, noise pollution, high rate of energy consumption and GHG emissions are the most important environmental challenges of this activity. In addition, health and safety sectors, different diseases and health problems for workers of this industry and accidents and hazards during the process are considered in this research and suitable solutions are suggested based on international guidelines and successful experiences around the world.

During recent years, the concept of HSE as a mandatory sector must be considered and followed and this attempt could help for better understanding and performance.

Keywords: Health, Safety, Environment, Cement Industry, Development.

Assessment of groundwater quality for drinking and industrial usage in Chenaran plain in North East Iran

Sharafi, N.[1], Mahmudy Gharaie, M.H*[1], Makhdoumi, A.[2], Ahmadzadeh, H.[3]

[1] Department of Geology, Faculty of Science, Ferdowsi University of Mashhad, Mashhad, Iran
[2] Department of Biology, Faculty of Science, Ferdowsi University of Mashhad, Mashhad, Iran
[3] Chemistry Department, Faculty of Science, Ferdowsi University of Mashhad, Mashhad, Iran
E-mail: mhmgharaie@um.ac.ir

Quality investigation of water resources is important for suitable management and environment protection. In this study, quality determination and classification of groundwater in Chenaran arable plain, North East of Iran, Razavi Khorasan Province, were examined for drinking and industrial usages. Eight groundwater samples were collected form the Chenaran plain in September 2018. Temperature, pH and electrical conductivity were measured at the field. Major cations (Ca^{2+}, Mg^{2+}, Na^{+}, K^{+}) and anions (Cl^{-}, SO_4^{2-}, $HCO_3^{-}$and CO_3^{2-}) were analyzed in central chemical laboratory in Ferdowsi University of Mashhad. Electrical conductivity (EC) value was varied from 412 to 5100 µs/cm. Dominant cations and anions were Ca^{2+}, Mg^{2+}, HCO_3^{-} and Cl^{-} in the samples. The Gibbs diagram, which is provided using $Cl/Cl+HCO_3$ and Na/Na+Ca vs. TDS, shows three main controlling processes such as precipitation, water-rock interaction and evaporation. According to the diagram, the groundwater samples were affected by a water-rock interaction and partly evaporation. Also, based on ionic ratios as Na/Na+Cl and Mg/Mg+Ca, Na-bearing silicate minerals dissolution, ionic exchange, limestone and dolomite weathering, and rare halite dissolution has a significant effect on water composition.

Schoeller diagram provides the quality classification based on by total hardness (TH), total solid dissolution (TDS) and major ions. According to this diagram the water samples were classified in good to unsuitable classes for drinking usages. Langelier saturation index was used for corrosive- scale forming of water samples. This parameter indicated that all the water samples were scale forming. Drinking water should not be corrosive or scale forming because it may water could have negative effects on human and animal health, and also industrial constructions.

.

KEYWORD: Chenaran Plain, Human health, Industrial usages, Water quality

Air pollution modeling (PM10 & PM2.5) using time series Sentinel-2 images

Mozafari, S.M [1], Hasanlou, M. [1]

[1] School of Surveying and Geospatial Engineering, College of Engineering, University of Tehran
Email: (s.mohamadmozafari, hasanlou)@ut.ac.ir

Air pollution is one of the major human and environmental health problems in big cities and in developing countries. Accurate monitoring and forecasting of air quality and estimation of the amount of contaminants will reduce the risks to human and environmental health. Particulate matter in the atmosphere is divided into two PM2.5 (particulate materials with a diameter of less than 2.5 μm) and PM10 (particulate materials with a diameter of less than 10 μm), Particulate matter can cause illness, allergies and even death for humans. It can also harm other living things such as animals and food products and damage the natural or artificial environment. Indoor air pollution and poor urban air quality have been cited as two of the world's most important toxic pollution problems in 2008. According to a 2014 World Health Organization (WHO) report, air pollution in 2012 killed about 7 million people worldwide. Due to the availability of Sentinel-2 imagery that offers a spatial resolution of 10 meters and using SNAP and Sen2Cor can calculate atmospheric reflectance. In this study, an empirical relationship is established between the values of PM2.5 and PM10 with satellite images and atmospheric reflectance extraction, and a high-precision air pollution model is produced. Using a 18 months course (from the beginning of 2018 until the end of August 2019 from Tehran) from Sentinel-2 images and receiving in-situ data, at the same time, air pollution rates in different parts of Tehran have been investigated. For this purpose, 23 air quality control stations in Tehran have been used. The study suggests that the atmospheric reflectance study from Sentinel-2, is a good alternative to monitoring air quality on Earth. The feasibility of the proposed algorithms was investigated based on correlation coefficient (r) and RMSE and NRMSE compared to the PM2.5 and PM10 in-situ measurement data. A choice of our proposed multispectral model was based on the highest value r and the lowest value of RMSE and thus the lowest value of NRMSE with PM10 in-situ data. Models produced by Sentinel-2 satellite with PM10 and PM2.5 suspended particles produced by correlation coefficients of 0.83 and 0.84, respectively, confirmed that the use of atmospheric reflectance of satellite images with high spatial resolution is a good alternative to ground air quality monitoring.

KEYWORDS: Air pollution, Particulate matter, Sentinel-2, SNAP, Sen2Cor, high spatial resolution

Seismic Hazard Assessment in Semnan region

Teymouri, E. [1], and Sadidkhouy, A. [1]

[1] Institute of Geophysics, University of Tehran, PO Box 14115-6466, Tehran, Iran
E-mail: Encie.teymouri@ut.ac.ir

Seismic hazard analysis is one of the most useful tool to address uncertainty in regions that are located in an active tectonic zoneand prevent major damage or life loss. In Semnan region, Damghan earthquake is one of the strongest historical earthquakes (M7.9) that happened in 856 AD. In this paper, Deterministic and Probabilistic seismic hazard assessment methods have been used to evaluate the seismic hazard potential along Semnan province, which is located between 34 to 37 N and 52 to 55 E. For this purpose, we extracted the information from seismotectonic map using geological maps, micro-earthquakes catalog and well-known historical earthquakes references. Then, we divided the region in to 7 sources that gained from the same tectonic regime, and we estimated seismicity parameters and seismicity potential, with procedure of faults and with this zoneation. For deterministic hazard assessment, we used an hypothetical site centered in the study area and we specified source zones that may generated a notable ground shaking. Then, we determined the distance from each source zone to the site and Mmax. Finally, we calculated the ground motions (PGA) at the site using a regional attenuation relationship. The result showed that Atari fault is creating the maximum acceleration and is therefore the controlling earthquake of our site. In the probabilistic part of our study, after all the regional information we gathered, suitable attenuation relation for target region were used and peak ground acceleration for sources at Semnan city were obtained and measured for return periods of 50, 100, 200 and 475 year. The results of all sources based on probabilistic approach in return period 50, 100 and 475 years, predicts accelerations respectively, 0.32g, 0.77g, 1.1g and when the return periods increase the acceleration value. Response spectra curves for all sources at defined period has a peak in nearly 0.2 seconds. The obtained seismic hazard maps obviously show more risk for potential seismic sources 1 and 6 and these results are in a good coincidence with the deterministic method.

KEYWORDS: Deterministic method, Hazard assessment, Hazard map, Probabilistic method

Probabilistic Seismic hazard assessment and focal mechanism mapping of Minab fault zone and the Strait of Hormoz

Tavakolizade, N.[1], Sadidkhouy, A.[2]

[1]M.Sc. student, Institute of Geophysics, University of Tehran, Tehran, Iran
[2] Assistant Professor, Institute of Geophysics, University of Tehran, Tehran, Iran
E-mail: nasrintavakoli@ut.ac.ir

This study focuses on probabilistic hazard assessment of Minab transition zone, its accompanied fault zones, and the strait of Hormoz. On the one hand, different tectonic regimes and different convergence angle (confirmed by GPS based velocity measurements), influence Minab fault zone and the strait of Hormoz. On the other hand, this location includes a large population and is one of the main Iranian trading harbors. Seismicity of this region are studied by mapping faults and gathering a precise and complete earthquake data set of historical (based on Ambraseys and Melville (1982) Iran historical earthquake records) and instrumental data based on IRIS, IRSC, ISC, and USGS data sets. Investigated catalogue consist of 8715 earthquakes. Fault map of this area showed plenty of major and thrust faults. The seismotectonic map accompanied by CMT focal mechanisms plotted to demonstrating earthquake mechanisms. Strike-slip, reverse, over-thrusting, and oblique movements are dominating fault mechanisms in the study area. Probabilistic hazard assessment is done based on four sources, elected by fault trends, focal mechanisms, and earthquake accumulation schemes in order to assess seismic hazard potentials. Activity rate (N), b-value, and magnitude of completeness evaluated utilizing Zmap software and Gutenberg-Richter relation. KIJKO implemented to calculating earthquake engineering parameters (lambda and Beta). CRISIS software used for plotting SA (Spectral Acceleration) maps for two recurrence time (RT; 50, 475 years) and two different periods (0.2, 0.8). Maximum evaluated SA for 50 and 475 recurrence time are 0.98(g), 1.65(g) (of 0.2 Time period); and 0.38(g), 0.57(g) (of 0.8 Time period), respectively. Uniform hazard response spectrum (UHRS) for 2, 5, 10, and 64 percent of probability of exceedance plotted. Obtained results are in good agreement with tectonic regimes of the study area and taking them into account while constructing infrastructures and buildings improves location specification.

KEYWORDS: Crisis; Minab; PGA; Seismic hazard assessment; Tectonic regimes; The strait of Hormoz.

Hybrid broadband strong-motion simulation of Malard Earthquake

Teymouri, E. [1], Sadidkhouy, A.[1], Rahimi, H.[1]

[1], Institute of Geophysics, University of Tehran, PO Box 14115-6466, Tehran, Iran
E-mail: Encie.teymouri@ut.ac.ir

In countries located in an active tectonic zone, seismology engineering and earthquake engineering studies, such as seismic hazard analysis and strong motion simulation, contribute to the preparedness to future seismic activities, especially when there's no reliable or proper strong motion records of the past earthquakes. For example, the city of Tehran is built over many faults that have the potential to produce major earthquakes. Realistic estimations of ground motions and time series can lead to PGA and sa calculations that could help with building design and engineering. The most common method of strong motion simulations relies on using either the low frequency or the high frequency, hence hybrid methods are used to calculate synthetics in range of engineering interest (0-10 hz). We referred to 'Hybrid Broadband ground simulation' method by Mai et al (2010) as a basis to simulate the 20th December 2017 earthquake in Malard, Northern Iran, by generating broadband synthetic seismograms. In this case, the low frequency seismograms were combined with high frequency multiple s to s back scattering. To obtain a hybrid broadband simulation, we used compsyn package (Spundich and Zu, 2003) to calculate the low frequency section and then combined it with the generated high frequency by using the broad band toolbox (Mai et al, 2010).

The simulation requires site and source specific parameters. In order to obtain them, we used the main acceleration recorded by 21 stations in less than 100 kilometers radius. The estimated value of high frequency decay (kappa) is 0.49 and the maximum calculated PGA of time series for the closest assumed station is 0.018 m/s^2. That is an adequate compromise with the actual data and for all calculated station. We also compared amplitude spectra of both simulations and observation data and the results, represent a significant coincidence between the simulation and the main event in both of frequency and time domains.

KEYWORDS: Hybrid broadband seismograms, Kappa, Near-source ground motion, Strong motion

Realistic strong ground motion selection based on the conditional mean spectrum in Tabriz, Iran

Bayat, F. [1], Shabani, E.[2]

[1] Institute of Geophysics, University of Tehran, Tehran, Iran

[2] Department of Seismology, Institute of Geophysics, University of Tehran, Tehran, Iran

E-mail: bayaat2014@ut.ac.ir

Earthquake is an inseparable part of human life; the best solution to reduce its damages is to design structures based on the seismotectonic and geotechnical characteristics of the region (Mousavi et al., 2015). In dynamic structural analysis, scientists predict the response of the structures subjected to ground motions having a specified spectral acceleration at a given period and this prediction is generally obtained by selecting strong ground motions matching a target response spectrum (Baker, 2011). The uniform hazard spectrum (UHS), that is a typical response target spectrum, is shown by researchers to be an unsuitable target for this purpose, as it implies that large-amplitude spectral values will occur at all periods within a single ground motion. The conditional mean spectrum (CMS) which is a proposed alternative to the UHS is a response target spectrum that estimates the distribution of the response spectrum, conditioned on the occurrence of a target spectral acceleration value at the period of interest (Lin et al., 2013).

In this study, the peak ground acceleration (PGA) and the spectral acceleration Sa(1.0s) for 5% damping ratio corresponding to 10% and 2% probability of exceedances within 50 years are estimated. The resultant PGAs for the return period of 475 and 2475 years, indicate the maximum value of 0.3g and 1.0 g in Tabriz, respectively. Disaggregation is also calculated in a site in the center of Tabriz on bedrock, then it is used to compute the contributions to the mean annual rate of exceedance (MRE) of PGA corresponding to the mean return period 475 years, 5%-damped Sa(0.2s) and Sa(1.0s) corresponding to different mean return periods (MRPs) of 475 and 2475 years.

Moreover, as expected, the MRE of long-period spectral accelerations is usually controlled by large magnitude earthquakes at long distances while smaller events at shorter distances dominate the PGA and short-period spectral acceleration hazard (Shabani et al., 2013). The CMS at the site specified in Tabriz for PGA corresponding to MRP of 475 years and the resultant 5%-damped Sa (0.2s) and Sa(1.0s) corresponding to different MRPs of 475 and 2475years are calculated, as well. According to the mean disaggregation results of Sa(1.0s) with the MRP of 475 years at a site in the center of Tabriz (Fig. 1), nine response spectra of real ground motions with approximate magnitude 7 and distance 46 km are selected from PEER Ground Motion Database center, we found that the CMS are relatively less than the UHS and a bumpy response spectrum from real ground motions are well captured by the CMS in Fig. 2. It is clear that at high periods, the amplitude of the UHS is higher than the CMS one and according to dynamic structural analysis, it could intensely excite the nonlinear response of a structure. At short periods, the amplitude of the UHS is higher than the CMS as well, and it implies that ground motions matching the UHS will excite higher modes in the

structures to a greater extent.

As a result, the UHS is an undesirable target response spectrum to make an estimate of the expected financial losses due to the damage following an earthquake in Tabriz. As Burks et al., (2012) stated, using the UHS to select ground motions could lead to an over prediction of the response and resulting loss could lead to incorrect decisions regarding insurance pricing or decision-making to retrofit the structure.

KEYWORDS: Conditional mean spectrum; Disaggregation; Seismic hazard; Strong ground motion; Uniform hazard spectrum.

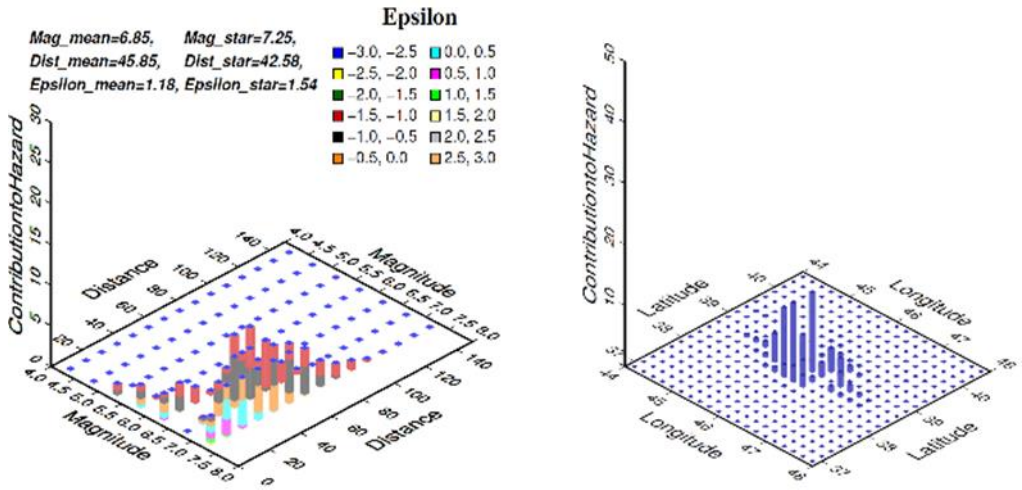

Figure 1. Disaggregated seismic hazard for a site in Tabriz for 10% in 50 years probability of exceedance for Sa(1.0s); bins of width 0.5 in magnitude, 10 km in distance, and 0.5 in ε are used.

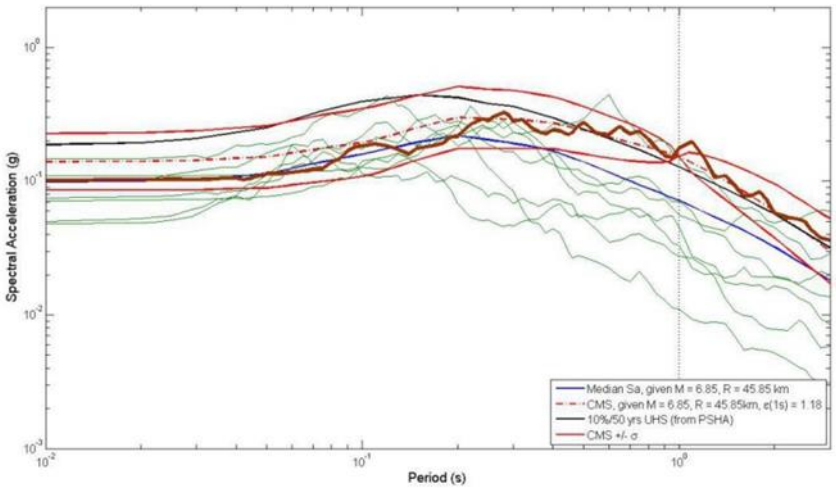

Figure 2. Response spectra from real ground motions having approximately magnitudes of 6.8 and in a distance of 45.8 km, for Tabriz, 10% in 50 years probability of exceedance for Sa(1.0s) after scaling spectra to match the CMS over the entire considered period range. The thick brown colored spectrum is the Loma Pietà recording for the Northridge earthquake.

Anisotropic Velocity Structure beneath the Arabia – Central Iran collision boundary (the Zagros suture zone)

Dashti, F.[1, 2], Lucente, F.[2], Motaghi, K.[1], Najafi, M.[1], Bianchi, I.[3], Shabanian, E.[1] and Ghods,A.[1]

[1] Institute for Advanced Studies in Basic Sciences (IASBS), Zanjan 45137-66731, Iran
[2] Centro Nazionale Terremoti, Rome, Italy
[3] Institut für Meteorologie und Geophysik, Universität Wien, Vienna, Austria
E-mail: fdashti@iasbs.ac.ir

Continental collision along the Zagros suture occurred due to convergence of the Arabian plate and the Eurasia (Fig. 1) initiated at ~35 Ma (e.g., Mouthereau et al., 2012, and references therein) with the main phase at ~27 Ma (e.g., Madanipour et al., 2013; Egan et al., 2009). Here, we study the crustal structure by focusing on both the geometry and the changes in anisotropic properties of the crust.

In this work, our main objective is to recognize dipping interfaces and/or anisotropic layers (subsurface structures) at crustal depth. With that aim, we implement the harmonic decomposition method is based on the derivation of the back azimuthal harmonics of an RF data set as a function of the incoming P- wavefield direction (Girardin and Farra, 1998; Farra and Vinnik, 2000). We used data from CIGSIP (China-Iran Geological Geophysical Survey in the Iranian Plateau) temporary linear array of broadband seismic stations installed in NW Iran (Figure 1). We compute teleseismic receiver functions at 45 stations and then we perform harmonic analysis of the receiver function data set [Bianchi et al., 2008, 2010, 2016] to infer the presence of dipping interfaces and/or anisotropic layers at crustal depth. We then focus on data from seven stations located in the near of the surface expression of the suture zone.

Through harmonic analysis and the subsequent inversion of the receiver function data at these stations, we obtain information on the geometry of the suture zone at depth, deformation induced in the above and below crustal levels by the collision kinematics, and on the S velocity models of the crust across the Zagros suture zone.

Within the receiver functions harmonics, we highlight the seismic signature of the suture zone related to the Zagros Main Recent Fault (MRF), and through modeling we unravel the anisotropic characteristics of the layers surrounding the suture, which is probably due to consistent foliation of the rocky packages involved in the thrusting process.

KEYWORDS: Anisotropic characteristics; Collision boundary; Crustal structures; Harmonic decomposition; Receiver function.

Applying WavDec, F-K and RayDec methods to decompose ambient seismic noise wavefield and retrieving earth model at a site in the south of Tehran

Fotouhimehr, M.[1], Moghadasi, N.S.[1], and Shabani, E.[2]

[1] PhD student, Department of Seismology, Institute of Geophysics, University of Tehran
[2] Assistant Professor, Department of Seismology, Institute of Geophysics, University of Tehran
E-mail: M.fotouhimehr@ut.ac.ir

Seismic ambient noise methods are nowadays widely used in geophysics as easy and non-destructive techniques to study the characteristics of underground structure, which is very important in engineering and hazard assessment purposes. It is presumed that the seismic noise wavefield is mainly composed of surface waves with an unknown relative contribution, so deriving suitable knowledge about noise wavefield composition is crucial in extracting more precise dispersion curves of the carrier surface waves. Furthermore, adding additional information as constraints like Rayleigh wave ellipticity in the inversion process of dispersion curves may improve the accuracy of deduced subsoil structure. In this study, to analyze wavefield composition and to obtain the shear wave velocity model at depth, we benefited the array methods of WaveDec and F-K and also single station techniques of RayDec and H/V. WaveDec technique (Maran`o et al. 2011) as a statistical signal processing technique, is used to decompose ambient noise wavefield and to estimate its parameters. In this method, the measurements from all components of sensors are modeled jointly which leads to substantial improvement in obtaining dispersion curves. Considering both Love and Rayleigh waves' contributions in the wavefield, this method estimates wavefield parameters including amplitude, phase, azimuth, wave number and ellipticity angle (for the Rayleigh wave only) based on the Maximum Likelihood method. In the F-K method (Lacoss et al. 1969), signals from different sensors are delayed and summed up. The delays are computed as a function of the angle of arrival and the velocity of propagation. The principal of H/V spectral ratio technique (Nakamura, 1989) is computing the ratio of the Horizontal to Vertical spectra of ambient vibration recordings of a single seismic sensor to achieve resonance frequency of the site. In the RayDec method (Hobiger, 2009), using the random decrement technique causes to enhance the Rayleigh wave effect and decreases the influence of other wave types in the seismic wavefield.

The array dataset used in this paper is composed of 9 stations which are recorded at a site in the south of Tehran by Haghshenas (2012) which are two hour length records.

In this study, first we compare the ellipticity curves deduced from the above mentioned single station methods and also the WaveDec technique. Results show a good agreement at resonance frequency of 4.1 Hz. Also, the decomposition of the relevant noise wavefield is studied through the WaveDec method (Figure 1). As a next step, the dispersion curves of vertical components are estimated. To deduce the shear wave velocity model, dispersion curves of Rayleigh waves from WaveDec and F-K methods alongside ellipticity information from different mentioned techniques are tested and compared. Our results show that the inversion of dispersion curves deduced via WaveDec and ellipticity from RayDec, could improve the estimation of shear wave velocity model and depth of bedrock in the site.

Keywords: Wavefield decomposition, Ellipticity curves, dispersion curves, Shear wave velocity model, Tehran.

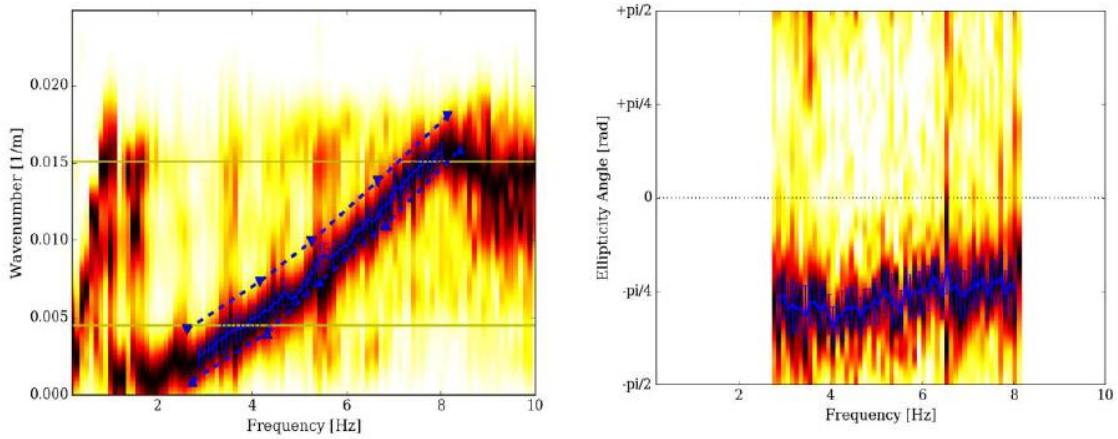

Fig. 1 (Left) Rayleigh wave dispersion curve obtained using WaveDec method (the blue curve with error bars). (Right) Rayleigh wave ellipticity angle curve (the blue curve with error bars), both bounded in array resolution limits presented by light green lines.

Iran strong motion network

Shahvar, M.[1], Farzanegan, E.[1], Eshaghi, A[1], Mirzaei, H. [1]

[1]Assistant Professor, Road, housing and urban development research center (BHRC), Tehran, Iran
E-mail: m.shahvar@bhrc.ac.ir

Strong ground motion records are the main input data to earthquake engineering studies such as dynamic structural analyses and seismic hazard evaluation, helping us to improve our understanding of seismic hazard and risk. This data is used as basic information on the development of earthquake building codes. The Iran strong motion network (ISMN), Road, Housing and Urban Development Research Center (BHRC), is operating a network of about 1115 digital strong motion accelerometer.

Strong motion monitoring of earthquake activity in Iran began at the onset of the 1973, consisting of 270 analog SMA-1 stations. Since then Iran has been at the forefront of strong motion monitoring in Middle East. In the early 1990s, after Manjil destructive earthquake, the National Strong Motion Network was established including dial-up triggered instrumentation replaced the analog sensors. This network, consisting of 1070 SSA-2 sensors, was installed across Iran, 547 free-field stations as well as of 91 dam-related (see Figure 1).

About nearly 13,600 three component strong motions have been recorded from 1973 in earthquakes between 3<Mw<7.8.

This paper describes the current status of network including instrumentation, database and ongoing developments and renovation project for the Iran strong motion network. The renovation project started in late 2016, and will lead to the installation

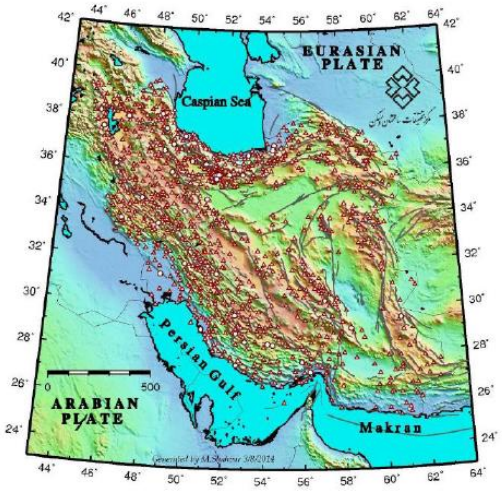

Iranian Strong Motion Network (1972-2015)

KEYWORDS: Strong Motion, Network, Iran, Accelerometer

M_L Shear Wave Velocity Tomography in Turkey Plateau

Gomar, F.[1], Ghods, A.[2], Maheri Peyrov, M.[1]

[1] PhD student, Institute for Advanced Studies in Basic Sciences (IASBS), Zanjan, Iran
[2] Associate Professor of Geophysics, Institute for Advanced Studies in Basic Sciences (IASBS), Zanjan, Iran
E-mail: Fatemehgomar@iasbs.ac.ir

The Turkey plateau is composed by several continentals' terranes in the late tertiary. These terranes were detached by the ocean. Pontides is a north terrane in northern Turkey which shows Laurasia affinities. The Anatolide-Tauride terrane in the south of the Pontides shows Gondwana affinities which was separated from Gondwana in the Triassic. The kirşehir massif is a large complex of metamorphic and plutonic rocks in central Anatolian. The southeast Anatolia forms by north of the Arabian platform. To study the gradient of lateral crustal variations in Turkey and to investigate different crustal blocks, we calculated a 2D ML shear wave velocity tomography map using the waveforms recorded by the KOERI permanent Seismic Network and the European Integrated Data Archive (EIDA). The lateral crustal thickness variation is depended to the ML velocity that vary between the velocity of Lg and Sn phases. If the earthquake occurs in the crust, the maximum amplitude of the shear wave can belong to the Lg wave. According to the Lg group velocity (2.8-3.5 km/s), we can identify the blocks with variable thickness such as blocking and passing region, because the quality of Lg wave propagation is sensitive to crustal thickness lateral variations. The dataset includes 22584 ML velocity readings from 382 earthquakes with a location error of five kilometers or less, a magnitude range of 4-6.5 and happened in the time interval between 2005 and 2017. We calculated the 2D ML tomography map of Turkey, by using a constrained least-squares inversion scheme. Our results exhibit an Lg blocking region (i.e., ML velocity larger than 4 km/s, near to Sn phase) in eastern Turkey (indicated by letter C in Figure. 1) where a thickened crust resulted from the collision of the Arabian Plate and the Anatolian plate. The ML velocity for the Pontides (indicated by letter B in Figure. 1) in the north of the Anatolian fault and south of the Black Sea is in the range of 3.2 to 3.5 km/s, implying an Lg passing region. The Izmir-Ankara-Erzincan suture zone is well resolved by the velocity map, because of the larger average velocity of the Pontides. According to our velocity map, the Tauride area (indicated by letter E in Figure. 1) in the southwest of Turkey is attributed to an Lg blocking region. For the Tauride area, our map shows a region with a strong crustal thinning which is in correlation with the previous studies indicating a tensional regime. The ML velocity for the Menderes Massif (indicated by letter D in Figure. 1) in the western Turkey is in the range of 2.1 to 3.2 km/s, implying an Lg passing region with a distinct pattern correlating with the boundary of the Massif. For the central part of the Anatolian plate and the kirsehir block (indicated by letter A in Figure. 1), the ML velocity is in the range of 2.7 to 3.1 km/s, consistent with an Lg passing region with a small lateral gradient of crustal thickness. The ML velocity for the Arabian plate is about 3.4 km/s slightly larger than the Anatolian plate. The separation of Arabia plate from the Central Anatolian plate in the velocity map is related to the Bitlis suture zone. We were not able to calculate the ML velocity in the north of the Black sea (indicated by letter G in Figure. 1), because of the unavailability of the seismic data in this region. Overall, our results show a boundary of terrane that nearly identical with calculated ML velocity for each continental segment (Figure 1).

2. KEYWORDS: Anatolian plate; Seismic tomography; Shear wave velocity; Turkey; Wave propagation

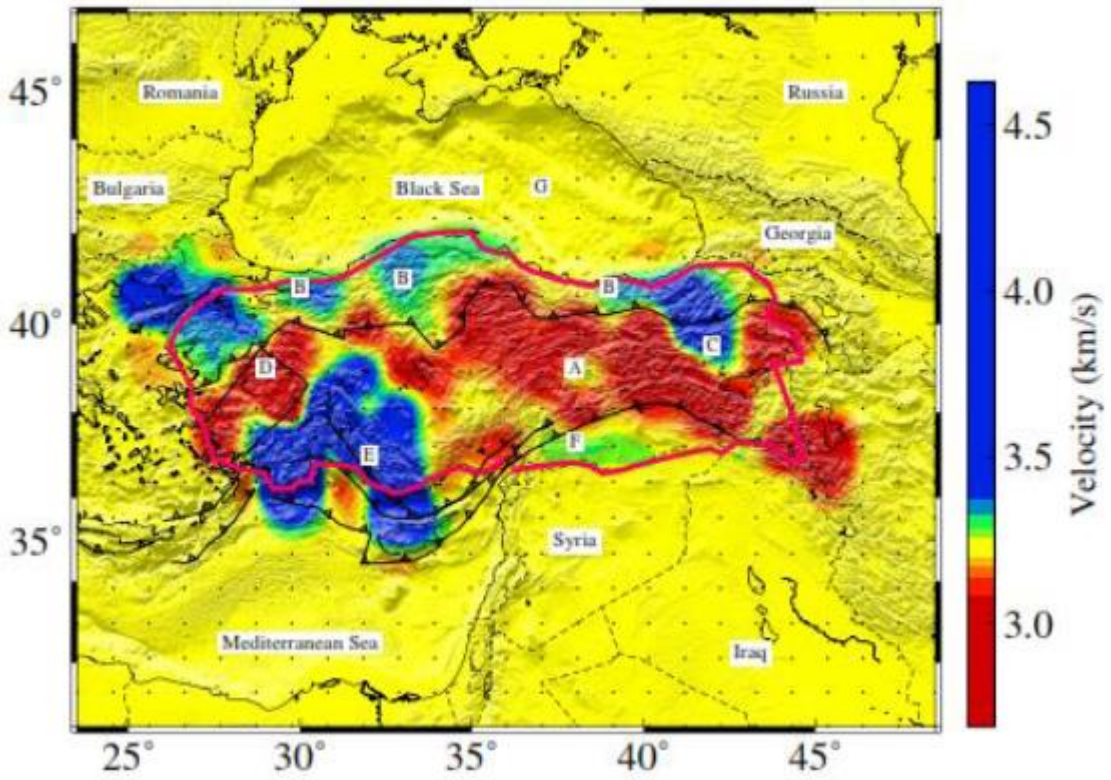

Figure 2. ML shear wave velocity map superimposed on topography of Turkey. The reliable answer is marked by the pink line. Sutures are shown by heavy lines with the polarity of former subduction zones indicated by filled triangles and the dashed lines are political borders. In the regions with high velocity (greater than 3.5km/s), there are a gradient of lateral crustal variations (C and E blocks). In the region with low velocity (less than 3.5 km/s), there aren't lateral crustal variations (B, A, D and F blocks).

3rd TRIGGER International Conference
8-10 October 2019, Zanjan, Iran
Institute for Advanced Studies in Basic Sciences
Gava Zang, Zanjan, Iran

Investigation of the effects of adjacency on seismic response of two dimensional hills

Baba Adam, N.[1], Uromeihy, A.[1], Sohrabi- Bidar, A.[2], Maghami, Sh[2]

[1]Tarbiat Modares University
[2]University of Tehran
E-mail: n.babaadam@modares.ac.ir

It is well known that during an earthquake event, the received motion could be significantly varied in different locations with respect to topographic characteristics of the surface. Although numerous researches have been dedicated to the "site effects", one of its important aspects, which is the adjacency of topographic features, have not been paid enough, whereas a vast number of, populous cities are located near topographic features. The aim of this paper is an investigation of the effects of adjacent hills on the seismic responses on the surface. Previous studies have been focused on the seismic behavior of the single features, mostly, whereas, a realistic look at the surrounding Environment shows a high diversity and the complexity of the ground surface. To study of adjacency, a parametric study has been performed, considering three different cases. First a two-dimensional homogenous hill with different elevations on the half-space is subjected to vertical incident SV riker waves and the responses have been studied at the top of the central hill. Afterward, once again the responses of the same hill have been analyzed by considering another adjacent hill with constant elevation (500 m). Lastly, two same hills (with 500 m elevation) have been defined on both sides and the analysis is repeated. The analysis has been carried out employing the boundary element method in time-domain and the responses have been analyzed in both time and frequency domains, the incident wave has been defined with predominant frequency of 3Hz. The results show that the responses could be greatly under the influence of the adjacent hills according to their characteristics and in specific, the dimensions of the feature.

KEYWORDS: Site effect; seismic response; Tow dimensional; Frequency domain; time domain; topographic features.

Investigation of the Crustal Transition in Western Alborz

Arvin, S.[1], Sobouti, F.[1], Priestley, K.[2], Ghods, A. [1], Motaghi, K.[1]

[1] Department of Earth Sciences, Institute for Advanced Studies in Basic Sciences (IASBS), Zanjan,Iran.

[2]Bullard Laboratories, University of Cambridge, Madingley Road, Cambridge CB30EZ, UK

E-mail: shivarvn@gmail.com

The present day kinematics of Alborz mountain, characterized by the westward extrusion of the South Caspian Basin block, and by the right-lateral shear between the different blocks of Central Iran. The Alborz accommodates the overall motion between the South Caspian Basin and Central Iran (Jackson et al. 2002). The termination of the Alborz Mountain, in the western part, is characterized by a change in strike along the Lahijan fault zone (Left lateral strike slip fault). The South Caspian Basin is a rigid block and remnant piece of oceanic lithosphere structure with unusually thick oceanic like crust, was formed as a remaining back arc basin related to Tethyan subduction beneath the Iranian microcontinent and also is known as one of the thickest sedimentary (~ 20 km) basin in the world (Mangino & Priestley (1998); Brunet et al. (2003); Knapp et al. (2004)). Based on southwestward motion of South Caspian Basin relative to Central Iran, it is believed that the South Caspian Basin is underthrusting beneath the Talesh and Alborz Mountain on its western and southern margins (Jackson et al. 2002). The P tomograms obtained by Motaghi et al. (2018), beneath a dense linear seismic array in west Alborz Mountains, show a sharp velocity contrast in the crust and upper mantle beneath northern flank of the Alborz Mountains from that of the South Caspian Basin and this sharp transition role as the boundary between the lithosphere structure of the South Caspian Basin and Alborz mountain which suggest no underthrusting of the South Caspian Basin beneath the Alborz Mountain.

The aim of this study is investigating the Moho structure and crustal discontinuity in western Alborz in order to find a better understanding of the crustal deformation in the area, especially in two tectonic transition zone, one from oceanic-type crust of South Caspian Basin to continental crust of Alborz, and other transition from actively deforming Alborz to Central Iran crustal blocks.

In order to study the crustal seismic structure across the West Alborz ranges by analysis of P wave receiver functions, we used 250 teleseismic events with magnitude greater than 5.5, located between 30◦ and 90◦ epicentral distances were recorded by 24 seismic stations belong to the temporary seismic network in the NW Iran installed and operated by the Institute for Advanced Studies in Basic Sciences (IASBS). This network was called Deylaman profile, has included with 16 seismic stations along a linear profile extending from The South Caspian Basin, Western Alborz, and Ghazvin region to Boien Zahra region located in Central Iran and there are also 8 seismic stations in surrounding the profile. The average inter-station distance in each profile was 13 km. The stations were repositioned during the deployment (from August 2014 until April 2016) and the recording span at individual

stations varied between 4 and 31 months.

Receiver functions are determined using the iterative deconvolution method of Ligorria and Ammon (1999). The obtained receiver functions were migrated to the depth and the structure and geometry of the Moho boundary beneath the network were well identified (Fig.1). The transition boundary from the oceanic-like crust of the southern Caspian basin to the Alborz continental crust was identified. The thickness of the sediments in central Iran is about 15 km. The thickness of the crust in central Iran is about 40 to 48 km. in Alborz, the thickness of the crust is increased to 50 km. Coming from Alborz to the southern Caspian Basin, there is a sharp variation in crustal thickness, which corresponds to the Lahijan fault zone that faces the thin oceanic crust of the southern Caspian basin to the thick continental crust of Alborz. The scattering in seismicity (Hassanzadeh, 2016) exactly in the region of sharp change of crustal thickness is a confirmation of the location of crustal transition between South Caspian basin and Alborz.

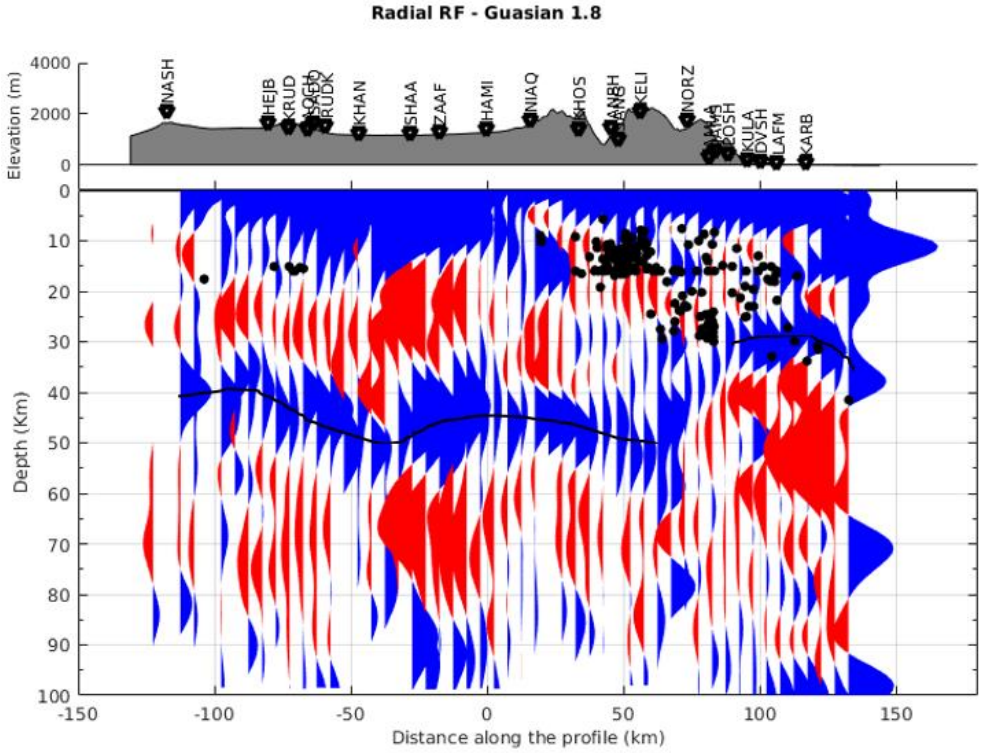

Figure 1. P reciever function along the profile migrated down to the depth of 100 Km. triangles show the projection of the stations onto the profil. The black solid The black solid line refer to the Moho discontinuity along the profil. The black circles are the seismicity of the study area.

KEYWORDS: Crustal deformation, Receiver Function, Western Alborz

Structure of the upper mantle beneath the Zagros collision zone revealed by surface wave tomography

Zarunizadeh, Z.[1], Motaghi, K.[1], Abdulnaby, W.[2], Aoudia, A.[3], Pachhai, S.[4], Ghods, A.[1]

[1]Department of Earth Sciences, Institute for Advanced Studies in Basic Sciences, Zanjan, Iran
[2]Researcher, Department of Geology, University of Basrah, Basrah, Iraq
[3]International Centre for Theoretical Physics, Trieste, Italy.
[4] Institute of Geophysics and Planetary Physics, Scripps Institution of Oceanography, University of California, San Diego, California, USA.
E-mail: Z.zarunizadeh@iasbs.ac.ir

The Zagros collision zone in western Iran is a one of the youngest and most active continentalcontinental collision zones all over the world resulting from collision of a strong lithosphere beneath the Arabian plate with a weak lithosphere along the margin of the Iranian plateau. Previous studies showed great interests in studying deep structures of the Zagros collision zone during the two last decades. Despite these, many questions remained under debate. In order to study the upper mantel structure across the northern part of the Zagros collision zone, we analyzed 1750 teleseismic waveforms recorded from 105 events. The data were gathered by 13 permanent stations of the Iranian National Broadband Seismological Network (INSN), 23 stations from a dense array (CIGSIP) installed by Institute of Geophysics and Geology, Chinese Academy of Sciences in collaboration with the Geophysical survey of Iran and Department of Earth Sciences, Institute for Advanced Studies in Basic Sciences (IASBS), 8 stations from a temporary array operated by IASBS in NW Iran and 6 temporary seismic stations belonging to Basra University (Iraq). We used the twoplane-wave tomography method prepared by Forsyth and Li (2005) to carry out a teleseismic surface wave tomography. The inversion was performed based on 2-D sensitivity kernels (Yang and Forsyth, 2006) at a grid size of 0.5 × 0.5 degrees. Both amplitude and phase of Rayleigh waves were employed to calculated phase velocity tomograms at period range of 33 s - 111 s. A Bayesian Markov chain Monte-Carlo algorithm was performed to invert local dispersion data into 1D S-wave velocity models beneath each grid.. Our 3D shear wave velocity model shows well -resolved image for the lithosphere structure beneath the Zagros collision zone. The Moho depth variations show lateral variations where it is thicker beneath the Zagros Mountains and thinner beneath the east of Iraq and Central Iran. The most interesting deep feature observed in the 3D velocity model is the high velocity anomaly beneath the Zagros Mountains at depth between 70 km and 150 km. The high velocity anomaly extends ~100 km beneath the SSZ, probably due to underthrusting of the Arabian lithosphere beneath SSZ across the MZT suture zone.

KEYWORDS: Surface wave tomography, Bayesian Monte-Carlo, Upper mantel structure, Zagros collision zone.

Moment Magnitude Estimation Based on Displacement Spectral Inversion Method using Iran Strong Motion Data

Eshaghi, A.[1], Shahvar, M.[2], Farzanegan, E.,[3] and Mirzaee, H.[4]

[1] Road, Housing and Urban Development Research Center, Tehran, Iran
E-mail: attieh.eshaghi@gmail.com

Earthquake magnitude scales are related measurements of an earthquake. The most commonly used magnitude scales such as local magnitude or body wave magnitude are dependent on the frequency of the recorded waves and above a certain size will saturate. To overcome the saturation problem, moment magnitude **M** was introduced (Hanks and Kanamori, 1979) that is calculated from the seismic moment, M_0, which can be estimated from spectral methods (Brune, 1970), the moment tensor inversion, or the waveform inversion. The spectral method, which is generally based on the Brune source model, is a simple yet very efficient method. In this study, the source parameters of the earthquake including M_0, **M** and corners frequency (f_c) were estimated using the Displacement Spectral Inversion method based on the Brune source model in the frequency domain. In this study, 4373 three components accelerograms recorded by stations of Iran Strong Motion Network (ISMN) across the country are used. All data were inspected with eye and the P and S-waves arrivals and the S-wave window, were determined. Then the records were filtered using a band-pass filter and their corrected velocity and displacement time histories were estimated (Fig1). Moment magnitude (**M**) is calculated from the following equation (Hanks and Kanamuri, 1979):

$$\mathbf{M} = 2/3\log10\ (M_0) - 6.03, \qquad (1)$$

Where the scalar moment, M_0, is the seismic moment in N.m. M_0 is calculated from the following equation based on the low-frequency plateau in displacement spectra (Ω_0).

$$M_0 = \frac{4\pi\rho\beta^3}{R_{\theta\varphi}FP}G(R)\Omega_o \qquad (2)$$

Where, ρ is the density, β is the shear wave velocity, and F is the free surface magnification correction factor. $R_{\theta\varphi}$ is the mean value of the radiation pattern and G(R) is the geometrical spreading function. In the inversion of the displacement spectra, the inversion is carried out in a frequency range that has a Signal to Noise Ratio≥3 and the three parameters of Ω_0, f_c and the frequency-independent quality factor (Q) are assumed to be unknown, where they are obtained through the nonlinear inversion. In this study, similar to Abercrombie (1995), the following general model for fitting the displacement spectra has been selected:

$$\Omega(f) = \frac{\Omega_0 e^{\frac{-\pi f t}{Q}}}{\left[1+(\frac{f}{f_c})^{\gamma n}\right]^{\frac{1}{\gamma}}}, \qquad (3)$$

Where Ω(f) is the Fourier spectrum of displacement, f is the frequency, n is the high-frequency fall off rate (on a log-log plot), and γ is a constant. Here n = 2 and γ= 1, similar to the Brune spectral shape model and t is the travel time of the considered wave. To determine the best fitting parameters,

we employ a bonded Nelder-Mead (1965) simplex algorithm. After the inversion, unknown parameters Ω_0, f_c and Q are obtained. Using the obtained Ω_0, the seismic moment and, ultimately, the **M** are calculated. The final M_0 of the earthquakes with at least three records was calculated by averaging the values obtained at all stations and using this mean values, the final **M** of the earthquakes were determined. The results show that the mean residuals is close to 0.3 and standard deviations (σ) is about 0.2 (Table 1, Fig 2). The obtained values from the two selected windows do not differ significantly, but the S window yields less mean residual and σ. As it can be seen, this method estimates the final value of **M** slightly more than the real value. Consequently, if we want to calculate the **M** of the earthquakes using this method, we would have to consider applying the corrective relationships, which requires further studies. Using this method, **M** can be estimate rapidly after the earthquake occurrences for earthquake early warning and rapid response systems. Furthermore, just using the available records of earthquakes, the **M** of rather smaller events without reported **M** can be calculated, which is very useful in earthquake catalog homogenization or in forward-modeling studies of records.

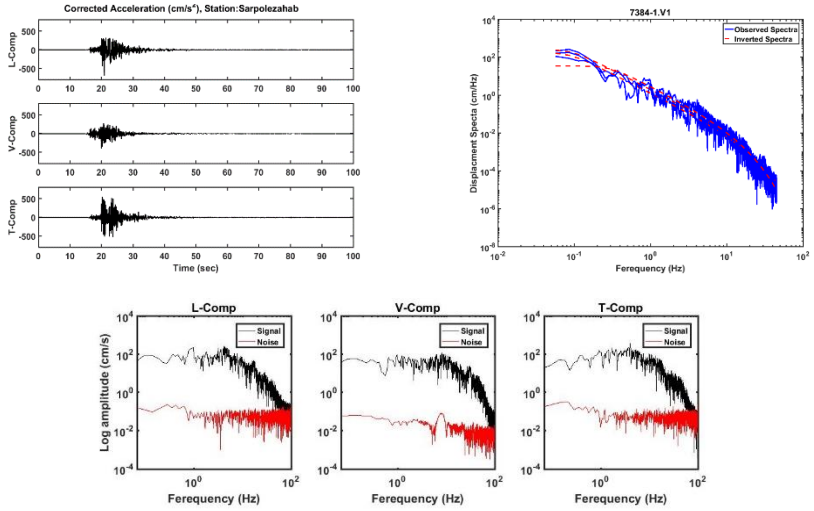

Figure 1. An example of the three components of the corrected acceleration time histories (top, left), observed and inverted spectra of the vertical component (top, right), and the signal and noise spectra (bottom) related to the 2017 Sarpol-e Zahab earthquake, recorded at the Sarpol-e Zahab station.

Table 1. Mean and σ values for earthquakes with reported **M**, with at least three recorded accelerograms, based on S-wave window (S) and whole signal widow (W).

Earthquake with at least 3 records	Mean	σ
M_W	0.31	0.18
M_S	0.27	0.18

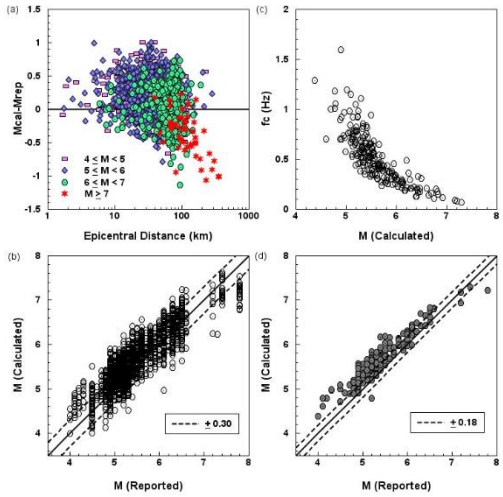

Figure 2. Results based on the S window: a) Residuals for all accelerograms versus distance. b) Calculated magnitude (M(Calculated)) versus the reported magnitudes (M(Reported)) for all accelerograms along with the obtained σ. c) Calculated f_c values for all earthquakes versus the M(Calculated). d) M(Calculated) for each earthquake versus the M(Reported) along with the obtained σ.

KEYWORDS: Accelerograms, Brune Source model, Moment Magnitude, Source Parameters, Spectral model

Green's Function uncertainty estimation for earthquake source inversion: a case study of August 2012 Ahar-Varzaghan

Zeynal Kheiri, H.[1], Moghtased-Azar, K.[2], Sadegh Nojehdeh, P.[1]

[1] University of Tabriz, Tabriz, Iran
[2] Assistant Professor, University of Tabriz, Tabriz, Iran
E-mail: h.kheiri96@ms.tabrizu.ac.ir

Estimation of moment tensor parameters is one of the important tasks in seismology. In addition, the uncertainty analysis of the estimated parameters is crucial for evaluating the quality of the solution. In the waveform-based earthquake source inversions, two major origins of uncertainty can be recognized. The first one is associated with the data error, which may be owing to instrumental or ambient noise effects. The second source of uncertainty, which is almost always neglected, is related to the uncertainty of Green's functions (GFs) due to the inaccuracy in the crustal model considered. The aim of this paper is the calculation of the GF uncertainty in order to improve the estimation of the moment tensor parameters and their uncertainty.

Recent strategies in Bayesian waveform inversions rely on statistical description of the GF uncertainty by means of a Gaussian distribution characterized by a covariance matrix. Hence, a fast and simple method for evaluation of the covariance matrix of GFs can be introduced. In order to estimate the GF covariance matrix, we use the method of Hallo and GalloviČ (2016). They proposed a simplified approach to obtain approximate covariance, bypassing the numerically expensive Monte-Carlo simulations. They derived closed-form formulae for approximate auto-covariance and cross-covariance functions to simplify the evaluation of the GF uncertainty avoiding any demanding computations. We use approximate auto-covariance functions (ACF) and approximate cross-covariance functions (AXCF) for computing the GF covariance matrix of seismic waveforms $f(t)$ and $g(t)$:

$$\widetilde{cov}(t.\tau) = \frac{1}{L_1}\int_{-\frac{L_1}{2}}^{\frac{L_1}{2}} f(t-l_1)f(t+\tau-l_1)\,dl_1 - \frac{1}{L_1}\int_{-\frac{L_1}{2}}^{\frac{L_1}{2}} f(t-l_1)\,dl_1 \;\frac{1}{L_1}\int_{-\frac{L_1}{2}}^{\frac{L_1}{2}} f(t+\tau-l_1)\,dl_1 \quad (1)$$

$$\widetilde{xcov}(t.\tau) = \frac{1}{L_1 L_{12}}\int_{\frac{L_1}{2}}^{\frac{L_1}{2}}\int_{-\frac{L_{12}}{2}}^{\frac{L_{12}}{2}} f(t-l_1)g(t+\tau-l_1-l_{12})\,dl_{12}dl_1$$

$$-\frac{1}{L_1}\int_{-\frac{L_1}{2}}^{\frac{L_1}{2}} f(t-l_1)\,dl_1 \;\frac{1}{L_1 L_{12}}\int_{\frac{L_1}{2}}^{\frac{L_1}{2}}\int_{-\frac{L_{12}}{2}}^{\frac{L_{12}}{2}} g(t+\tau-l_1-l_{12})\,dl_{12}dl_1 \quad (2)$$

Where t is time, τ is time lag between samples, l_1 is time shift, l_{12} is time shift between the waveforms and L_1 and L_{12} is the width of the uniform time shift distribution.

This approximate approach requires a 'mother' GF and a statistical description of the random time shifts of the signal as an input. The 'mother' GF is calculated using a mean velocity model by the discrete wavenumber method (Bouchon 1981). It is assumed that the only effect of the velocity model perturbations on the covariance matrix is the time shift of the signal. Moreover, it is presumed that such representative of the true uncertainty for each time lag τ is just the covariance function's (CF) average over time, $\frac{1}{T}\int_{-\infty}^{\infty}\widetilde{cov}(t.\tau)dt$, where T is the duration of the dominant part of the signal.

By calculating the mean of the CF over time we obtain covariance dependent only on the time lag. If this covariance function is evaluated from the ACF or AXCF, it is called stationarized approximate covariance function (SACF or SAXCF).

We perform proposed methods on an MT inversion using waveforms recorded by a real earthquake in Iran. The test event from 11 August 2012 (12:23 UTC) with moment magnitude 6.4 was located in the East Azerbaijan Province at depth 14 km. Fig. 1 shows the ensemble of the solutions displayed in terms of double couple (DC) mechanism nodal planes and histograms of DC component. The reference solution obtained with ISOLA software (strike 83°, dip 83° and rake 169° (in red)). It is worth noting that we applied four covariance matrices in the inversion. The simplest case can be derived when we consider covariance matrices with off-diagonal components obtained using ACF and SACF. Indeed, the approximate cross-covariances between components of the same receiver are taken into account using the AXCF and SAXCF. According to the obtained results, it can be concluded that the most reliable estimate of the uncertainty of the MT parameters will be revealed when employing the SACF covariance matrix. The AXCF and ACF (Fig. 1a, c) provide a good estimate of focal mechanism uncertainty, but the uncertainty is still underestimated as it does not fully cover the reference solution. Inversion with the SAXCF (Fig. 1g) provides the largest MT uncertainty estimate, since receivers are usually in the far distance from the source in this case study, and they are also placed on different soils.

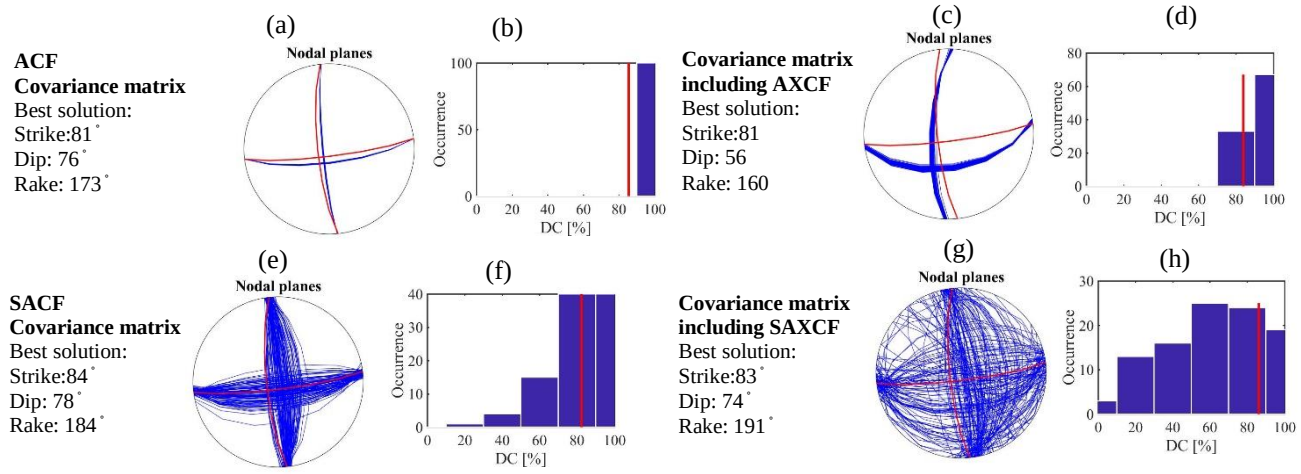

Figure 1. Statistical analysis of best-fitting solutions from MT. Panels show histograms of DC mechanism nodal planes (a, c, e, g), DC component (b, f, d, h). The reference solution is plotted in red lines.

KEYWORDS: Moment Tensor Inversion, Focal Mechanism, Uncertainty Estimation, Green's Function, Velocity Model

References

Hallo, M. & Gallovič, F. (2016) Fast and cheap approximation of Green function uncertainty for waveform-based earthquake source inversions. *Geophys. J. Int*., 207(2), 1012-1029

Duputel, Z., Rivera, L., Fukahata, Y., & Kanamori, H. (2012) Uncertainty estimations for seismic source inversions. *Geophys. J. Int*., 190(2), 1243–1256

Shearer, P. M. (2009). *Introduction to Seismology*. Cambridge University Press (2nd edn)

Spatial distribution of slip for the 2010 August 27 Mw 5.8 Kuh-Zar earthquake

Bazargan, S.[1], Asaadi, N.[1], Shomali, Z.H.[2,3] , and Rezapour, M.[2]

[1]University of Zanjan, Department of Physics

[2]University of Tehran, Institute of Geophysics

[3]Uppsala University, Department of Earth Science

E-mail: bazargan.s@alumni.ut.ac.ir

The slip distribution of a moderate earthquake of Iran, the 2010 August 27 M_w 5.8 Kuh-Zar earthquake, was estimated from regional broadband seismic data using constrained non-negative least squares linear slip inversion method. A great many inversions were carried out to determine the optimal parameters used in the process such as rupture velocity and rise time. A rupture velocity of 2.55 km/s and rise time of 1.8 s were utilized for the event. Results show a rupture with peak slip of 15.0 cm and total seismic moment release of 2×10^{25} dyne-cm. The effect of the stations with different epicentral distances was also analyzed using a sensitivity test. Due to the non-uniqueness of the inversion problem, a set of solutions is presented for the Kuh-Zar earthquake. To the best of our knowledge, this is the first time to consider constrained non-negative least squares linear finite-fault inversion procedure to the Kuh-Zar earthquake.

KEYWORDS: seismic data, slip inversion, the 2010 Kuh-Zar earthquake

Introduction

This study is focused on acquiring spatial slip distribution of the 2010 August 27 M_w 5.8 Kuh-Zar earthquake which occurred in Kuh-Zar, a village in Damghan county, Semnan Province. Based on the seismic zoning of Iran by Mirzaei et al. (1998), there are five major seismotectonic provinces in the country, that is Zagros in the southwest, Alborz-Azerbaijan in the north and northwest, Central East Iran, Kopeh Dagh in the northeast and Makran in the southeast of Iran. The Kuh-Zar earthquake is almost situated on the border of Alborz-Azerbaijan and Central East Iran seismotectonic provinces which is in the proximity of the southern border of Alborz region. The epicenter of this event is located north of the Torud fault which is the causative fault for the 1953 Torud earthquake, one of the remarkable events of this area. The study aimed to obtain finite-fault modeling of the broadband three-component displacement waveforms of the Kuh-Zar earthquake through a least squares inversion method for the spatial slip distribution.

Data

The data used in this study is obtained from national broadband seismic network operated by the International Institute of Earthquake Engineering and Seismology of Iran (IIEES,). These data consist of 26 waveforms for the 2010 August 27 M_w 5.8 Kuh-Zar earthquake. The aftershocks of the corresponding earthquakes were taken from the catalog of Iranian Seismological Center (IRSC). The

observed waveforms were filtered and decimated from the original 50 to 10 samples per second. The instrument responses were removed, and the data were then converted to displacement. A band-pass filter of 0.025-0.07 Hz was applied to the displacement waveforms.

Model Parameterization

Green's functions were computed using the frequency-wavenumber integration code (FKRPROG) developed by Saikia (1994). Also, the inversion algorithm applied to the observed data is based on a stabilized constrained non-negative least-squares method introduced by Hartzell and Heaton (1983).

Non-uniqueness of the inversion problem led us to prepare a set of solutions. Therefore, we used different hypocentral parameters and focal mechanisms. Different hypocenters reported by various seismological agencies, i.e., ISC, GCMT, USGS, and EMSC (Table 1) were tested. Since the nodal plane with a better fit to the data can be construed as the main fault plane (Abercrombie et al. 2001), the focal mechanism (strike, dip, and rake) of the fault reported by GCMT and NEIC (Table 2) were tested to find the nodal plane with the best fit. And, the resulting models helped us to determine the fault plane from the auxiliary plane. The measure to choose the optimal result in all runs has been total variance reduction—demonstrating the fit between observed and synthetic data—and the final variance of the data misfit. As a result, the inversion found better fits with strike equals to 212˚nodal plane of GCMT (Table 2); thus, this plane is the fault plane, and we used it for the rest of the investigation.

Table 1. The hypocentral parameters recorded by different agencies for Kuh-Zar earthqauke.

Agencies*	Lat. (˚)	Lon. (˚)	Depth (km)	Time
ISC	35.48	54.50	11.0	$19^{h}\,23^{m}\,48^{s}.87$
GCMT	35.53	54.49	14.9	$19^{h}\,23^{m}\,52^{s}.40$
USGS	35.49	54.47	7.0	$19^{h}\,23^{m}\,49^{s}.00$
EMSC	35.49	54.55	10.0	$19^{h}\,23^{m}\,48^{s}.30$

* Isc (http://www.isc.ac.uk), International Seismological Center; GCMT (http://www.globalcmt.org), Global Centroid Moment Tensor; USGS (https://earthquake.usgs.gov), United States Geological Survey; EMSC (https://www.emsc-csem.org), European-Mediterranean Seismological Center.

Table 2. The focal mechanisms reported by GCMT and NEIC.

2010 Kuh-Zar	Nodal Plane 1			Nodal Plane 2		
	Strike(˚)	Dip(˚)	Rake(˚)	Strike(˚)	Dip(˚)	Rake(˚)
GCMT	212	78	-2	302	88	-168
NEIC*	20	85	-10	111	80	-175

*The National Earthquake Information Center

The result of the 2010 Kuh-Zar Earthquake

The velocity model based on the study of Ashtari et al. (2005) was used for this event. We determined several spatial slip distributions for the Kuh-Zar earthquake using different hypocentral parameters. According to these models (not shown here), the distribution of slip is critically sensitive to the depth of hypocenter. GCMT and USGS hypocenters (Table 1) were found to provide the best fit to the observed data with maximum total variance reduction of about 44 % for spatial distribution, but the variance of the data misfit obtained by GCMT is the least. Moreover, USGS hypocenter gave a slip pattern with surface fault rupture which has not been corroborated by Shahvar and Zare (2013). Furthermore, all of the hypocenters except GCMT provided models which are not covering all of the slip distribution inside the given fault plane because of their lower depths (EMSC hypocenter has the least variance reduction and its peak slip is 6 cm). Therefore, the slip pattern acquired by GCMT hypocenter is chosen as the preferred spatial slip model of Kuh-Zar earthquake (Figure 2). Based on the preferred model, the peak slip is almost 15 cm, and the total seismic moment release is about 2.0×10^{25} dyne-cm.

The rupture velocity of 2.55 km/s provided the best fit to the data. It indicates that the rupture front propagated with a rupture velocity as 70 percent as the shear wave velocity in the source area. Based on lots of inversion trials, rupture velocities higher than 2.55 km/s failed to explain the rupturing well. In accord with different inversion runs, optimum rise time was also chosen to be 1.8 sec.

Figure 1 demonstrates the observed data and synthetics. East-west component of DAMV, CHTH, and THKV stations, and Z component of BJRD, KHMZ, SHRT, and GRMI stations were omitted because we could not acceptably fit the waveforms due to the presence of noise.

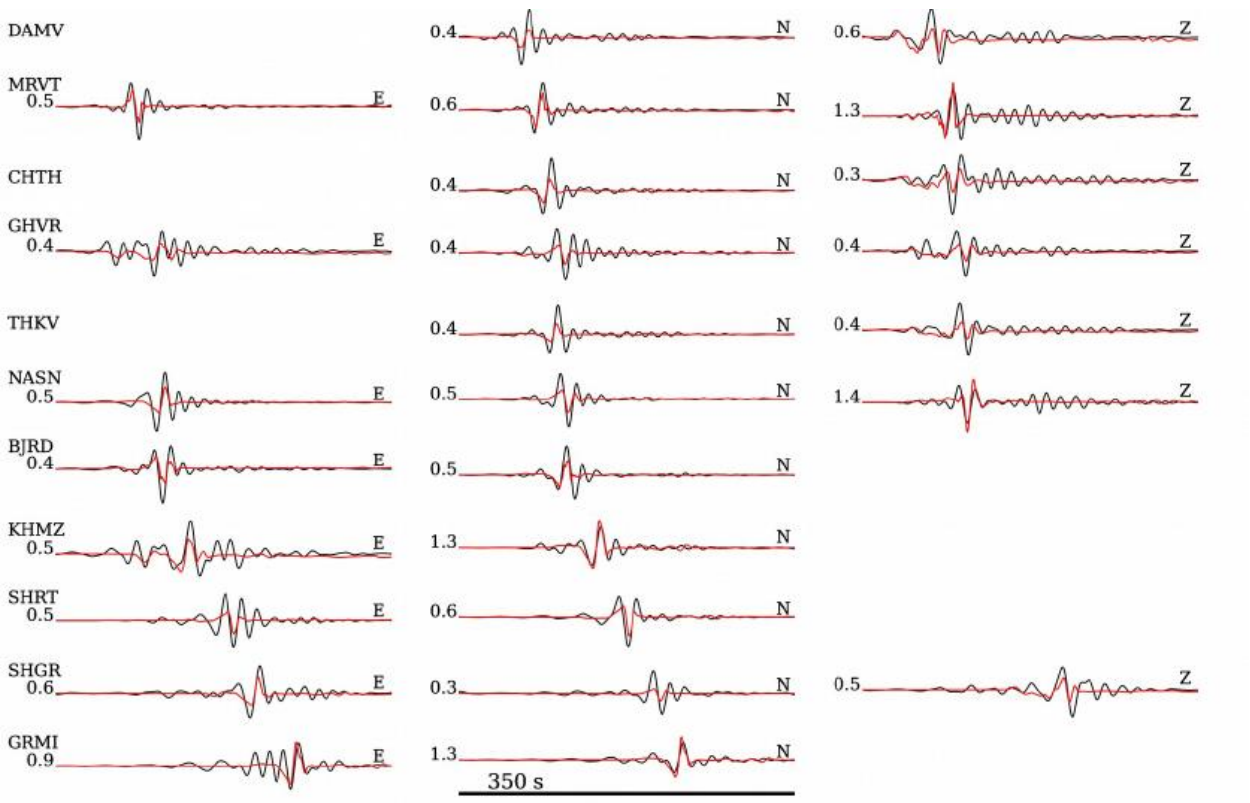

Figure 1. Observed data (black) and synthetics (red) for the spatial slip distribution of the Kuh-Zar

earthquake with respect to our preferred model with total variance reduction of 44%, rupture velocity of 2.55 km/s and rise time of 1.8 s obtained from GCMT hypocenter and focal mechanism. E component of DAMV, CHTH, and THKV, and Z component of BJRD, KHMZ, SHRT, and GRMI were omitted because we could not satisfactorily fit the signals due to the presence of noise. Numbers on the left of each signal pair show the synthetic to observed amplitude ratio. Signals are displayed in order of increasing the distance from the epicenter.

Figure 2 (right) shows analogies between the projected final spatial distributions on the Earth surface with the aftershock distribution (one month after the main shock). The dashed square depicts the

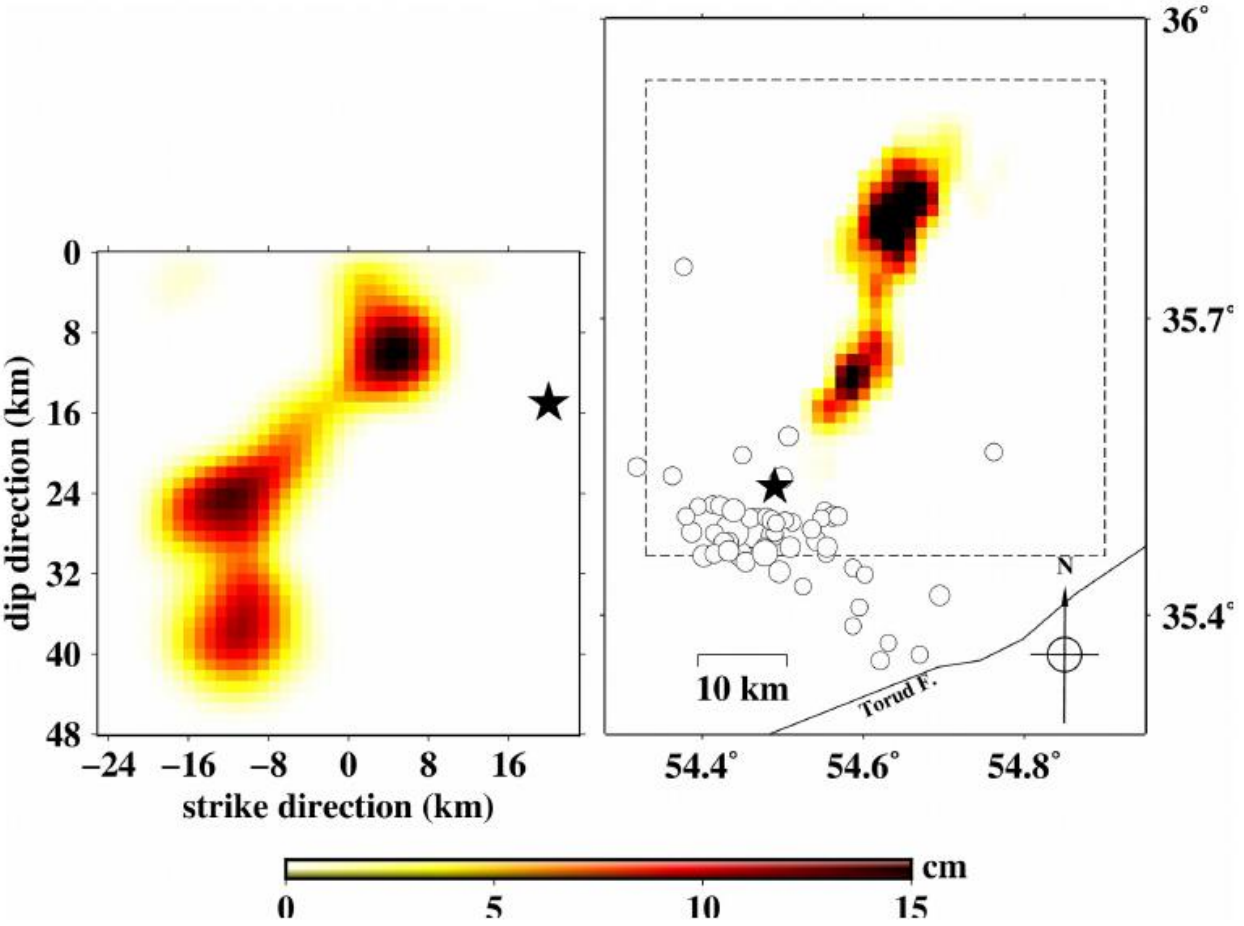

whole region of the fault plane. Aftershocks are a phase of relaxing stress concentrations followed by a mainshock (Scholz, 1990) and occurred southwsest of the slip distribution for the Kuh-Zar earthquake. It is shown that the aftershocks distribute mostly outside of the asperity zone.

Figure 2. Slip distribution for the preferred finite-fault models for the Kuh-Zar earthquake in the latitude-longitude coordinate (right) and along strike-dip directions (left). The dashed square (right) presents the fault plane (with the strike of 212˚) on the earth. Black stars show GCMT hypocenters in both figures. The white circles refer to the aftershocks which occurred during a month after the main shock and were taken from the catalog of Iranian Seismological Center (IRSC). The aftershocks distribute outside of the asperity zone. The peak slip value of the event is 15.0 cm. Also, the Torude fault has been shown in a black line (right) situated south of the slip distribution.

References

Abercrombie, R.E., Bannister, S., Pancha, A., Webb, T.H. and Mori, J.J. [2001] Determination of fault planes in a complex aftershock sequence using two-dimensional slip inversion. Geophysical Journal International, 146, 134-142.

Ashtari, M., Hatzfeld, D. and Kamalian, N. [2005] Microseismicity in the region of Tehran.

Tectonophysics, 395, 193-208.

Hartzell, S.H. and Heaton, T.H. [1983] Inversion of strong ground motion and teleseismic waveform data for the fault rupture history of the 1979 Imperial Valley, California, earthquake. Bulletin of the Seismological Society of America, 73, 1553-1583.

Mirzaei, N., Mengtan, G., and Yuntai, C. [1998] Seismic source regionalization for seismic zoning of Iran: major seismotectonic provinces. Journal of Earthquake Prediction Research, 7, 465-495.

Saikia, C.K. [1994] Modified frequency-wave-number algorithm for regional seismograms using

Filon's quadrature–modeling of L(g) waves in eastern North America. Geophysical Journal

International, 118, 142–158.

Shahvar M.P., Zaré M. [2013] The 27 August 2010 Mw 5.7 Kuh-Zar earthquake (Iran): field investigation and strong-motion evidence. Natural hazards, 66(2), pp.689-706.

Scholz, C.H. [1990] The mechanics of earthquakes and faulting. Cambridge University Press,

Cambridge.

S-wave quality factor tomography in NW Iran

Andayeshgar, S. [1], Motaghi, K. [2], Rezaeian, M. [3]

[1]PhD student in seismology, Department of Earth Sciences, Institute for Advanced Studies in Basic Sciences, Zanjan, Iran

[2,3]Assistant Professor, Department of Earth Sciences, Institute for Advanced Studies in Basic Sciences, Zanjan, Iran

E-mail: s.andayeshgar@iasbs.ac.ir

Northwest Iran is one of the active tectonic regions in the Alpine Himalayan belt. This area includes important geological structures including the North Tabriz Fault, the south Caspian basin, Sahand and Sabalan volcanoes, Talesh Mountains and Lake Urumieh. Existence of active fault zones, the effects of volcano magnetism and sedimentary basins affects strongly on earthquake wave attenuation. This inspired us to investigate systematic amplitude residuals (observed amplitude – predicted amplitude by available attenuation relations) to carry out a tomography for upper crust in the study region in order to detect quality factor variations due to the heterogenic geological structures. Here, we analyze 2901 seismograms from 302 small and moderate events (Mw < 5.2), recorded by 11 permanent stations of Tabriz network (governing by Institute of Geophysics, University of Tehran), one permanent stations of International Institute of Seismology and Earthquake Engineering (IIEES) network and 23 temporary stations installed by Institute for Advanced Studies in Basic Sciences (IASBS), Zanjan. We prepare a data set composed of spectral amplitudes for different magnitudes and hypocentral distances. The difference between the logarithm of observed amplitude and the logarithm of predicted amplitude (i.e., residual) at a frequency of 1 Hz was considered as input data for a 2D quality factor tomography. The predicted amplitude is calculated by spectral ground-motion equations for the NW Iran calculated by Motaghi et al. (2016). The residuals show systematic pattern which inspire the idea that 2D attenuation coefficient variations might be observed in the region. We assume that the 2D variations are caused by lateral variations of quality factor and thus we perform a shear wave quality factor tomography using the weighted damped least-squares method. Our results (figure 1) show a low (lower than average) quality factor anomaly (marked by A) north of the NTF and low quality factor anomaly south of Marand (marked by D). According to geological map (1:2,500,000), these are covered by thick Neogene and Quaternary sediments. Therefore, we attribute these anomalies to sedimentary basins. East of Marand, a high quality factor area (marked by B) is observed trending NW-SE which might be attributed to Cretaceous volcanic rocks with an age of about 100 ±40 million years. Another anomaly is observed with a high-quality factor in the southern mountains of Marand (marked by C). According to the geological map, this anomaly is attributed to the Precambrian metamorphic rocks with an age of ~540 million years. Under the Talesh Mountains (marked by E) and in east of the Sabalan (marked by F), we observed two anomalous features with high and low quality factors, respectively. These features are not consistent with the observable surface structures in mentioned geology map. Instead, we found out that the features are deep (depth > 15 km) because they are disappeared after removing rays generated by deep events (deeper than 15 km) beneath the Talesh mountains. These anomalies are observed in gravity maps and previous seismic velocity tomography studies (e.g., Bavali et al., 2016). We interpret the deep low quality anomaly in east of the Sabalan

(marked by F) as a hot structure remained from the Sabalan young eruption. The deep high quality anomaly under the Talesh Mountains (marked by E) might be interpreted as a cold dense crust probably related to an oceanic-like crust beneath the Southern Caspian basin (figure 2).

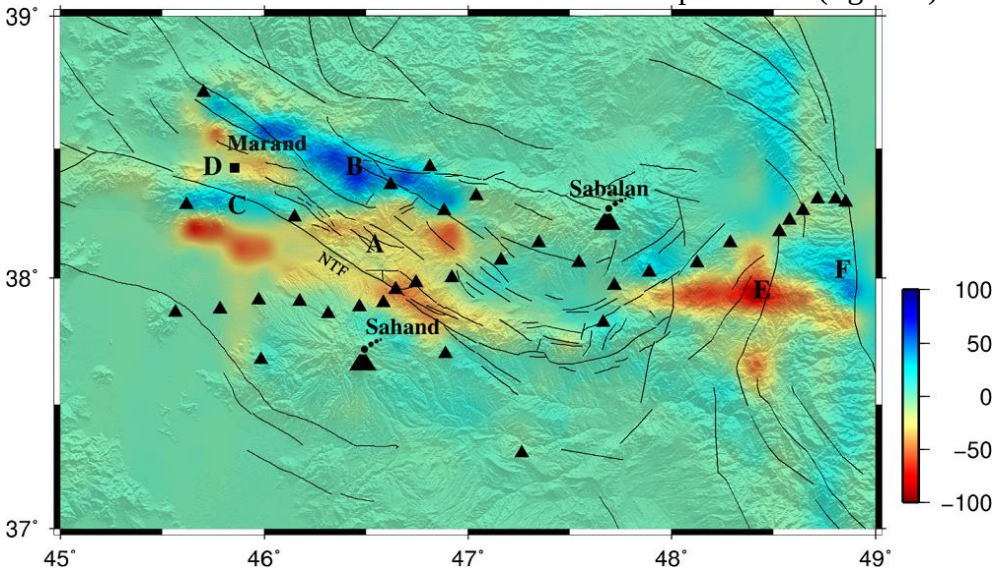

Figure 1. Quality factor tomogram for northwest Iran. Seismic stations are marked by black triangles. Black lines show main faults (Taghipour et al., 2018). NTF: North Tabriz Fault. A–F are anomalous features discussed in the text.

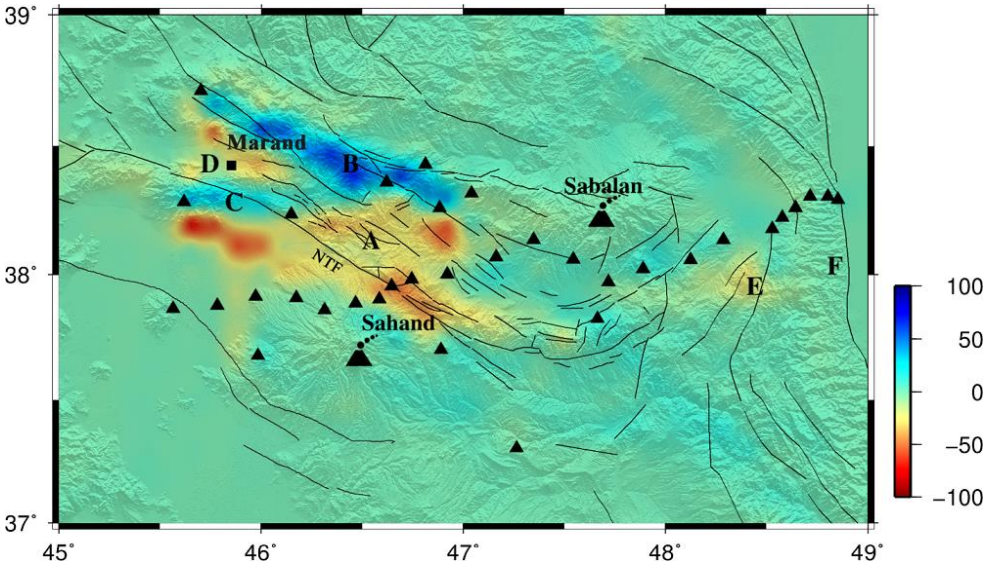

Figure 2. Quality factor tomogram for northwest Iran after deleting deep events (>15 km). Anomaly F disappears while anomaly E weakens considerably.

KEYWORDS: Quality factor, Tomography, Attenuation, NW Iran.

A Fuzzy approach to kinematic source inversion

Kheirdast, N[1], Ansari, A.[1], Custodio, S.[2]

[1]International Institute of earthquake engineering and seismology (IIEES), Tehran, Iran

[2]Instituto Dom Luiz, Faculdade de Ciencias, Universidade de Lisboa, Lisbon, Portugal

Kinematic source inversion is to infer the spatial-temporal source function over a given fault from seismic data. The forward formulation that comes from the representation theory of seismology (Aki & Richards 2002) is a Fredholm integral of the first kind and the inverse problem based on which, is inherently ill-posed. Ill-posedness refers to either no solution exists or there is not a unique solution available. One way to control the ill-posedness is to decrease the number of parameters involving in the inversion which comes from the model approximation method we use. One way to decrease the number of parameters is to use adaptive methods from those we used the fuzzy function approximation method. Fuzzy function approximation is a uniformly convergent approximation method that can estimate every function to any degree of accuracy. The method is nowadays used in machine learning approaches. Based on fuzzy function approximation we developed an inversion method that can map seismic data into the slip in a stable way using the Adaptive neuro-fuzzy inference system (ANFIS).This method controls the amount of small singular which is responsible for ill-posedness. The method has been tested for the SIV1-benchmark problem and a comparison between inferred source function as well as synthetic data shows proper conformity in both model and dataspace.

3rd TRIGGER International Conference
8-10 October 2019, Zanjan, Iran
Institute for Advanced Studies in Basic Sciences
Gava Zang, Zanjan, Iran

Constrained magnetostratigraphic dating and tectono-stratigraphic evolution of the Tarom Intermontane Basin, Northern Iranian Plateau

Paknia, M. [1], Ballato, P.[1], Mattei, M.[1], Heidarzadeh, G.[2], Cifelli, F. [1], Hassanzadeh, J. [3], Vezzoli, G .[4], Mirzaie Ataabadi, M. [5]*, and Ghassemi, M .[6]

[1] Department of Science, University of Roma Tre, Rome, Italy
[2] Institute of Earth and Environmental Sciences, University of Potsdam, Potsdam, Germany
[3] Division of Geological & Planetary Sciences, California Institute of Technology Pasadena, USA
[4] Department of Earth and Environmental Sciences, University of Milano-Bicocca, Milan, Italy
[5] Department of Geology, Faculty of Science, Univesity of Zanjan, Zanjan, Iran
[6] Research Institute for Earth Sciences, Geological Survey of Iran, Tehran, Iran
E-mail: majid.mirzaie@znu.ac.ir

The Tarom Basin is an elongated, NW-SE-striking, intermontane basin in northwest Iran. It is located at the transition of the Iranian Plateau and the South Caspian Basin. Currently, the basin is drained by the Qezel-Owzan River, however, the existence of deformed post Eocene red beds and Quaternary terrace conglomerates suggests that it experienced several episodes of internal drainage and limited connectivity with the Caspian foreland.

In order to decipher the origin and constrain the tectono-stratigraphic evolution of this basin, we carried out an integrated magnetostratigraphic, geochronologic and sedimentologic study along three stratigraphic sections. A total of 539 oriented, fine-grained (mudstone and sandstone) samples were collected from paleomagnetic sampling sites consisting of fluvio-lacustrine, playalake and alluvial-fan deposits. Stepwise thermal and alternating field demagnetization allowed isolating a linear magnetization component that decays toward the origin and represents the primary magnetization carried mostly by magnetite. Our results indicate that a first episode of uplift and deformation along the basin margins took place after ca. 35 Ma. This was followed by a period of erosion and non-sedimentation until ca. 16.3 Ma. By that time, basin development occurred in association with the establishment of internal drainage conditions and uplift of the northern (Alborz Mountains) and southern (Tarom Range) basin margins. This configuration led to the accumulation of a > 1.5-km-thick sequence of red beds at least until ca. 7.5 Ma, implying that intrabasinal deformation and incision must be younger than that. Sedimentation occurred at nearly uniform rates with a sharp increase at ca.

12.3 Ma and few episodes of acceleration that may reflect thrust loading during enhanced shortening phases along the basin margins.

KEYWORDS: Tarom basin, magnetostratigraphy, sediment accumulation rates, uplift and subsidence.